NDOT Research Report

Report No. 361-16-803

Characterization of Unbound Materials (Soils/Aggregates) Mechanistic-Empirical Pavement Design Guide (MEPDG)

January 2018

Nevada Department of Transportation
1263 South Stewart Street
Carson City, NV 89712

Disclaimer

This work was sponsored by the Nevada Department of Transportation. The contents of this report reflect the views of the authors, who are responsible for the facts and the accuracy of the data presented herein. The contents do not necessarily reflect the official views or policies of the State of Nevada at the time of publication. This report does not constitute a standard, specification, or regulation.

TECHNICAL REPORT DOCUMENTATION PAGE

1. Report No. P361-16-803	2. Government Accession No. N/A	3. Recipient's Catalog No. N/A
4. Title and Subtitle Characterization of Unbound Materials (Soils/Aggregates) for Mechanistic-Empirical Pavement Design Guide (MEPDG)		5. Report Date January 2018
		6. Performing Organization Code NONE
7. Author(s) Peter E. Sebaaly, Jeyakaran Thavathurairaja, and Elie Y. Hajj,		8. Performing Organization Report No. WRSC-UNR-20180101
9. Performing Organization Name and Address Pavement Engineering & Science Program Department of Civil & Environmental Engineering University of Nevada, Reno, Nevada 89557		10. Work Unit No.
		11. Contract or Grant No.
12. Sponsoring Agency Name and Address Nevada Department of Transportation Research Division 1263 South Stewart Street Carson City, NV 89712		13. Type of Report and Period Covered Final Report
		14. Sponsoring Agency Code
15. Supplementary Notes Charlie Pan, Project Manager, Materials Division, Nevada Department of Transportation		

16. Abstract

The resilient modulus is a critical engineering property used to characterize the unbound and subgrade materials in the AASHTO Mechanistic Empirical Pavement Design Guide (MEPDG) where a hierarchical approach is followed. Three levels of input are specified in the AASHTOWare® Pavement ME design software. This includes direct measurement from the laboratory testing offering the highest level of accuracy (i.e., Level 1), estimated values using correlations with materials properties (i.e., Level 2), and typical values offering the lowest level of accuracy (i.e., Level 3). The major objective of this study is to develop resilient modulus models for new design and rehabilitation projects for NDOT District 1 to be used in the MEPDG.

Unbound and subgrade materials were sampled from District 1 and various testing were conducted to determine numerous properties and characteristics including; materials classification (AASHTO and USCS), R-value, moisture-density relations, unconfined compressive strength, and resilient modulus. The resilient modulus test was conducted according to AASHTO T 307 procedure. The stress dependent resilient modulus models were developed for the unbound and subgrade materials. In summary, the stress dependent behavior of the resilient modulus for base and borrow materials in NDOT District I was found to fit very well the theta model. Meanwhile, the stress dependent behavior of the resilient modulus for the subgrade materials fitted very well both the universal model and Uzan model. The MEPDG procedure was used to determine the design resilient modulus for the new design projects. On the other hand, for the rehabilitation projects, a new approach based on the simulation of FWD testing was developed in this research and implemented to determine the design resilient modulus. It was observed that the design resilient modulus of the subgrade layer is independent of the pavement structure while the design resilient modulus of the borrow and base layers are dependent on the pavement structure.

Based on the analyses of the data generated from this research, two different resilient modulus models were developed; a) for new pavement design and b) for rehabilitation pavement design. The statistical analyses of the generated data indicated that the design resilient modulus of the subgrade layer for new and rehabilitation projects can be estimated based on the R-value or the unconfined compressive strength properties. However, the design resilient modulus of the borrow and base layers for new and rehabilitation projects can only be estimated based on the R-value. This leads to the conclusion that the unconfined compressive strength is not a good indicator of the strength properties of the borrow and base layers and a confined compressive strength must be measured.

17. Key Words Mechanistic-Empirical Pavement Design, Unbound Materials, Soils, Resilient Modulus, flexible Pavement	18. Distribution Statement No restrictions.		
19. Security Classif. (of this report) Unclassified	20. Security Classif. (of this page) Unclassified	21. No. of Pages 128	22. Price Free

Form DOT F 1700.7 (8-72) Reproduction of completed page authorized

SI* (MODERN METRIC) CONVERSION FACTORS

APPROXIMATE CONVERSIONS TO SI UNITS

Symbol	When You Know	Multiply By	To Find	Symbol
		LENGTH		
in	inches	25.4	millimeters	mm
ft	feet	0.305	meters	m
yd	yards	0.914	meters	m
mi	miles	1.61	kilometers	km
		AREA		
in^2	square inches	645.2	square millimeters	mm^2
ft^2	square feet	0.093	square meters	m^2
yd^2	square yard	0.836	square meters	m^2
ac	acres	0.405	hectares	ha
mi^2	square miles	2.59	square kilometers	km^2
		VOLUME		
fl oz	fluid ounces	29.57	milliliters	mL
gal	gallons	3.785	liters	L
ft^3	cubic feet	0.028	cubic meters	m^3
yd^3	cubic yards	0.765	cubic meters	m^3
	NOTE: volumes greater than 1000 L shall be shown in m^3			
		MASS		
oz	ounces	28.35	grams	g
lb	pounds	0.454	kilograms	kg
T	short tons (2000 lb)	0.907	megagrams (or "metric ton")	Mg (or "t")
		TEMPERATURE (exact degrees)		
^oF	Fahrenheit	5 (F-32)/9 or (F-32)/1.8	Celsius	^oC
		ILLUMINATION		
fc	foot-candles	10.76	lux	lx
fl	foot-Lamberts	3.426	$candela/m^2$	cd/m^2
		FORCE and PRESSURE or STRESS		
lbf	poundforce	4.45	newtons	N
lbf/in^2	poundforce per square inch	6.89	kilopascals	kPa

APPROXIMATE CONVERSIONS FROM SI UNITS

Symbol	When You Know	Multiply By	To Find	Symbol
		LENGTH		
mm	millimeters	0.039	inches	in
m	meters	3.28	feet	ft
m	meters	1.09	yards	yd
km	kilometers	0.621	miles	mi
		AREA		
mm^2	square millimeters	0.0016	square inches	in^2
m^2	square meters	10.764	square feet	ft^2
m^2	square meters	1.195	square yards	yd^2
ha	hectares	2.47	acres	ac
km^2	square kilometers	0.386	square miles	mi^2
		VOLUME		
mL	milliliters	0.034	fluid ounces	fl oz
L	liters	0.264	gallons	gal
m^3	cubic meters	35.314	cubic feet	ft^3
m^3	cubic meters	1.307	cubic yards	yd^3
		MASS		
g	grams	0.035	ounces	oz
kg	kilograms	2.202	pounds	lb
Mg (or "t")	megagrams (or "metric ton")	1.103	short tons (2000 lb)	T
		TEMPERATURE (exact degrees)		
^oC	Celsius	1.8C+32	Fahrenheit	^oF
		ILLUMINATION		
lx	lux	0.0929	foot-candles	fc
cd/m^2	$candela/m^2$	0.2919	foot-Lamberts	fl
		FORCE and PRESSURE or STRESS		
N	newtons	0.225	poundforce	lbf
kPa	kilopascals	0.145	poundforce per square inch	lbf/in^2

*SI is the symbol for the International System of Units. Appropriate rounding should be made to comply with Section 4 of ASTM E380.
(Revised March 2003)

TABLE OF CONTENTS

TECHNICAL REPORT DOCUMENTATION PAGE iii
Table Of Contents v
List Of Tables vi
List of Figures x
Chapter 1. Introduction 13
1.1. Objective and Scope 14
Chapter 2. Literature Review 15
2.1. Hierarchical Input Levels of the MEPDG 16
2.2. Overview of Resilient Modulus Test 20
2.3. Correlations for Estimating Resilient Modulus 24
2.4. Implementation and Use of Resilient Modulus 27
Chapter 3. Material Collection 35
Chapter 4. Laboratory Testing 40
4.1. Soil Classification Testing 40
4.2. Moisture-Density Relationship (T 108B) 48
4.3. Resilient Modulus Testing 50
4.4. Unconfined Compressive Strength 62
4.5. R-value Test (T 115D) 65
Chapter 5. Design Resilient Modulus for New Projects 71
5.1. Procedure for Identification of Resilient Modulus Design Value 71
5.2. Identification of Resilient Modulus Design Value for Typical NDOT Pavements 72
Chapter 6. Design Resilient Modulus for Rehabilitation Projects 82
6.1. Procedure for Identification of Design Resilient Modulus for Rehabilitation Designs 82
6.2. Identification of Resilient Modulus for Rehabilitation Design 83
Chapter 7. Resilient Modulus Prediction Model Development 91
7.1. Statistical Analysis 92
7.2. Comparison of Resilient Modulus Prediction Models 96
7.3. AASHTOWare® Pavement ME Comparison 100
Chapter 8. Conclusions and Recommendations 101
Chapter 9. References 103
Appendix A 106

LIST OF TABLES

Table 2.1. Unbound Aggregate Base, Subbase, Embankment, and Subgrade Soil Input Parameters and Test Protocols for New and Existing Materials..... 18

Table 2.2. Models Relating Material Index and Strength Properties to Mr (5). 19

Table 2.3. Chronology of AASHTO Test Procedures for Mr Measurements (6)..... 22

Table 2.4. State DOT/Other Laboratories Conducting Resilient Modulus Testing..... 23

Table 2.5. Methods used to Estimate Design Resilient Modulus for Selected Agencies. 28

Table 3.1. Summary of Collected Base and Borrow Materials from NDOT District 1. .. 36

Table 3.2. Summary of Soil Types in the Selected Locations. 38

Table 3.3. Collected Subgrade Materials. 39

Table 4.1. Summary of Sieve Analysis for Base Materials. 41

Table 4.2. Summary of Sieve Analysis for Borrow Materials. 42

Table 4.3. Summary of Sieve Analysis for Subgrade Materials. 43

Table 4.4. Summary of Atterberg Limits for Borrow Materials. 45

Table 4.5. Summary of Atterberg Limits for Subgrade Materials. 45

Table 4.6. AASHTO Soil Classification Method. 46

Table 4.7. Classification of Subgrade Materials with AASHTO and UCS Methods. 46

Table 4.8. Unified Soil Classification Method. 47

Table 4.9. Summary of Moisture-Density Test Results for Base Materials. 50

Table 4.10 Summary of Moisture-Density Test Results for Borrow Materials. 50

Table 4.11. Sumarry of Moisture-Density Test Results for Subgrade Materials..... 50

Table 4.12. Testing Sequence for Base and Subbase Materials. 51

Table 4.13. Testing Sequence for Subgrade Materials. 51

Table 4.14. Summary of Resilient Modulus Test Results for Base Material (Contract 3546). 56

Table 4.15. Regression Coefficients of Mr Model for Base Materials. 59

Table 4.16. Table 16. Regression Coefficients of Mr Model for Borrow Materials. 59

Table 4.17 Regression Coefficients of Mr Model for Subgrade Materials..... 59

Table 4.18. Summary of Unconfined Compressive Strength Test Results..... 65

Table 4.19. Summary of R-value Test Results. 70

Table 5.1. Major Inputs for Pavexpress Software..... 73

Table 5.2. Pavement Structures for Different Traffic Levels. 73

Table 5.3. Pavement Structure with Borrow Materials..... 73

Table 5.4. Mean Dynamic Modulus Values for District 1 PG76-22NV Mixture (2). 74

Table 5.5. Summary of Sublayers for a 5-inch AC Layer. 76

Table 5.6. Sate of Stress from Load-Induced Stress and Overburden Stress. 78

Table 5.7. Predicted Resilient Modulus from the State of Stress. 78

Table 5.8. Summary of Resilient Modulus for Pavement Structure on Strong Subgrade. 79

Table 5.9. Summary of Resilient Modulus for Pavement Structure on Weak Subgrade.. 80

Table 5.10. Summary of Resilient Moduli values for Pavement Structures with Borrow Layer. 81

Table 6.1. Representative Mean Dynamic Shear Modulus and Phase angle for PG 76-22 NV..... 84

Table 6.2. Damaged Dynamic Modulus Input Values at Different Temperatures and Frequencies. 84

Table 6.3. Cohesion and Friction Angle from the Laboratory Testing..... 85

Table 6.4. Deflections at various Radial Distances generated by the ILLIPAVE Model. 86

Table 6.5. Deflection at Various Distances Backcalculated by the Modulus 6.1 Model. 86

Table 6.6. Backcalculated Modulus for Each Layer..... 87

Table 6.7. Summary of Backcalculated Moduli values for Pavement Structures with Borrow Layer. 88

Table 6.8. Summary of Backcalculated Moduli for Pavement Structures on Strong Subgrade. 89

Table 6.9. Summary of Backcalculated Moduli for Pavement Structures on Weak Subgrade. 90

Table 7.1. Range of Variables for the Design Mr Models Development. 92

Table 7.2. Summary of Design Resilient Modulus Models with UCS. 94

Table 7.3. Summary of Design Resilient Modulus Models with R-value. 94

Table 7.4. Resilient Modulus of Unbound materials (without Borrow Material). 100

Table 7.5. Design Flexible Pavement Structure. 100

Table 7.6. Resilient Modulus of Unbound materials (with Borrow Material). 100

Table 7.7. Design Pavement Structure (With Borrow Material). 100

Table A.1. Summary of Resilient Modulus Test Results for Base Material (Contract 3546). 114

Table A.2. Summary of Resilient Modulus Test Results for Base Material (Contract 3583). 115

Table A.3. Summary of Resilient Modulus Test Results for Base Material (Contract 3597). 116

Table A.4. Summary of Resilient Modulus Test Results for Base Material (Contract 3605). 117

Table A.5. Summary of Resilient Modulus Test Results for Base Material (Contract 3607). 118

Table A.6. Summary of Resilient Modulus Test Results for Base Material (Contract 3613). 119

Table A.7. Summary of Resilient Modulus Test Results for Borrow Material (Contract 3546). 120

Table A.8. Summary of Resilient Modulus Test Results for Borrow Material (Contract 3583). 121

Table A.9. Summary of Resilient Modulus Test Results for Borrow Material (Contract 3597). 122

Table A.10. Summary of Resilient Modulus Test Results for Borrow Material (Contract 3613). 123

Table A.11. Summary of Resilient Modulus Test Results for Subgrade Material (I-15/Goodsprings). 124

Table A.12. Summary of Resilient Modulus Test Results for Subgrade Material (US-95/Searchlight). 125

Table A.13. Summary of Resilient Modulus Test Results for Subgrade Material (NV-375/Rachel). 126

Table A.14. Summary of Resilient Modulus Test Results for Subgrade Material (US-93/Crystal Spring MP62). 127

Table A.15. Summary of Resilient Modulus Test Results for Subgrade Material (US-93/Crystal Spring MP67). 128

LIST OF FIGURES

Figure 2.1. Definition of resilient modulus (6). 21

Figure 3.1. NDOT districts boundaries. 35

Figure 3.2. Locations considered to identify the subgrade materials. 37

Figure 3.3. Subgrade sample locations. 39

Figure 4.1. Gradation curves for base materials. 41

Figure 4.2. Gradation curves for borrow materials. 42

Figure 4.3. Gradation curves for subgrade materials. 43

Figure 4.4. Atterberg limits test apparatus and tools. 44

Figure 4.5. Liquid limit test results for subgrade (I-15/Goodsprings). 45

Figure 4.6. Moisture-density curve for base material (contract 3583). 48

Figure 4.7. Moisture-density curve for borrow materials (contract 3597). 49

Figure 4.8. Moisture-density curve for subgrade materials (US-93/Bonnie Claire)..... 49

Figure 4.9. Vibratory compactor and sample mold. 52

Figure 4.10. Extruded compacted sample. 52

Figure 4.11. Compacted sample with membrane, porous stones and O-rings. 53

Figure 4.12. Sample inside the triaxial chamber. 54

Figure 4.13. LVDT's connected on the outside of the triaxial chamber. 54

Figure 4.14. Theta model for base material (contract 3546). 57

Figure 4.15. Theta model for borrow material (contract 3546). 57

Figure 4.16. Uzan model for subgrade (US-93/Crystal Spring MP62). 58

Figure 4.17. Universal model for subgrade (US-93/Crystal Spring MP62). 58

Figure 4.18. Variation of resilient modulus of base materials with bulk stress. 60

Figure 4.19. Variation of resilient modulus of borrow materials with bulk stress. 60

Figure 4.20. Variation of resilient modulus of subgrade materials with bulk stress. 61

Figure 4.21. Extruded UCS sample. 62

Figure 4.22. Sample after the UCS test..... 63

Figure 4.23. UCS stress-strain curve for base materials (contract 3583). 63

Figure 4.24. UCS stress-strain curve for borrow material (contract 3613). 64

Figure 4.25. UCS stress-strain curve for subgrade material (I-15/Goodsprings). 64

Figure 4.26. Kneading compactor..... 66

Figure 4.27. Exudation-indicator device..... 66

Figure 4.28. Expansion pressure device. 67

Figure 4.29. R-value testing equipment..... 67

Figure 4.30. R-value test results for base material (contract 3546). 69

Figure 5.1. Sublayer thicknesses for the AC layer..... 74

Figure 5.2. Dynamic modulus master curve for mixtures used in District 1. 75

Figure 5.3. Equivalent thickness transformation using MET. 75

Figure 5.4, Effective length computation for single axle load configuration. 76

Figure 6.1. Damaged and undamaged dynamic modulus master curve. 85

Figure 6.2. Forward calculated and backcalculated deflections. 87

Figure 7.1. Residual error plot for the prediction model. 93

Figure 7.2. Normality plot for the prediction model..... 93

Figure 7.3. Correlation between H_{eq} and D for new design. 95

Figure 7.4. Variation of design resilient modulus versus predicted resilient modulus of subgrade (using UCS) for new design. 96

Figure 7.5. Variation of design resilient modulus versus predicted resilient modulus of subgrade (using UCS) for rehabilitation design..... 97

Figure 7.6. Variation of design resilient modulus with predicted resilient modulus (using R-value) for new design..... 97

Figure 7.7. Variation of rehabilitation design resilient modulus with predicted resilient modulus (using R-value) for rehabilitation design. 98

Figure 7.8. Comparison of predicted rehabilitation and new design Mr (R-value). 99

Figure 7.9. Variation of NDOT predicted Mr and predicted Mr for new and rehabilitation design (R-value). 99

Figure A.1. Moisture-density curve for base material (contract 3546). 106

Figure A.2. Moisture-density curve for base material (contract 3583). 107

Figure A.3. Moisture-density curve for base material (contract 3597). 107

Figure A.4. Moisture-density curve for base material (contract 3605). 107

Figure A.5. Moisture-density curve for base material (contract 3607). 108

Figure A.6. Moisture-density curve for base material (contract 3613). 108

Figure A.7. Moisture-density curve for borrow material (contract 3546). 109

Figure A.8. Moisture-density curve for borrow material (contract 3583). 109

Figure A.9. Moisture-density curve for borrow material (contract 3597). 110

Figure A.10. Moisture-density curve for borrow material (contract 3607). 110

Figure A.11. Moisture-density curve for borrow material (contract 3613). 111

Figure A.12. Moisture-density curve for subgrade material (US-95/Searchlight). 111

Figure A.13. Moisture-density curve for subgrade material (US-95/Bonnie Claire). 112

Figure A.14. Moisture-density curve for subgrade material US-93/Crystal Spring MP67). 112

Figure A.15. Moisture-density curve for subgrade material (US-93/Crystal Spring MP62). 113

Chapter 1. INTRODUCTION

The American Association of State Highway and Transportation Officials (AASHTO) adopted the Mechanistic-Empirical Pavement Design Guide (MEPDG) as an interim pavement design standard in 2008 (1). The MEPDG is currently being implemented in the AASHTOWare®Pavement ME design software. The Nevada Department of Transportation (NDOT) already started the implementation of the MEPDG for the structural design of flexible pavements (2). The MEPDG conducts advanced mechanistic analysis of the pavement structure while taking into consideration the combined contributions of; traffic, climate, and materials properties. Currently, NDOT has a draft MEPDG Design Guide that covers the various parts of the design process including an extensive database on the properties and performance of asphalt concrete mixtures. The next logical step in the NDOT implementation process for MEPDG is to develop a database on the properties of unbound materials in the base, subbase (borrow), and subgrade layers.

The MEPDG follows a hierarchical approach in defining the required engineering properties of the pavement structure. Three levels of input are specified: 1, 2, and 3. Level 1 offers the highest level of accuracy while level 3 offers the lowest level of accuracy. In the case of unbound materials in base, subbase, and subgrade layers, the required engineering properties include the resilient modulus (Mr) and Poisson's ratio (μ). Additional unbound materials properties include Atterberg limits, gradation, conductivity, and coefficient of lateral pressure.

Since the impact of Poisson's ratio on the response of the pavement structure to climate and traffic loads is insignificant, this property is typically assumed with a reasonable accuracy. However, the impact of Mr on the response of the pavement structure to the combined actions of climate and traffic loads is highly significant, therefore, the Mr value of each pavement layer must be accurately specified. Level 1 requires the Mr property to be measured in the laboratory under repeated load triaxial (RLT) conditions, level 2 allows the determination of Mr through correlations with other empirical properties of the unbound materials such as the Resistance value (R-value) or the California Bearing Ratio (CBR), and basic properties of the unbound materials such as Atterberg limits, gradation, etc…, and level 3 allows the use of Mr default values.

While the RLT provides a fundamental approach to characterize the nonlinear stress-dependent behavior of unbound materials, the test itself is time-consuming and costly. In light of these issues, most state highway agencies have elected to implement level 2 input for unbound materials. Therefore, a well-defined fundamental approach must be followed to establish a highly reliable relationship to determine the Mr property of unbound materials encountered throughout Nevada from other properties that can be practically and reliably measured.

The Mr input parameter for unbound materials plays a major role in pavement designs and has a significant influence on the projected pavement performance. Hence, a proper estimation of the Mr value for locally available unbound materials used in base, subbase, and subgrade layers becomes critical for designing long-lasting flexible and rigid pavements in Nevada. Currently, NDOT estimates Mr from the R-value (Equation 1) using a correlation that was established for a specific group of soils obtained from specific geographic areas that might not be applicable for the type of unbound materials typically used in Nevada.

$$Mr = 145 * 10^{(0.0147R+1.23)} \quad (1)$$

Where;

Mr: resilient modulus, psi
R: R-value

1.1. Objective and Scope

The objective of this research study is to develop a prediction model for the resilient modulus of the unbound materials to be used for new design and rehabilitation projects in NDOT District 1. In order to achieve this objective, the following tasks have been conducted:

- Collect base, subbase (borrow), and subgrade representative materials commonly used in NDOT District 1.
- Conduct laboratory testing of the collected materials to evaluate the following properties; sieve analysis, Atterberg limit, moisture density relationship, R-value, unconfined compressive strength, and resilient modulus.
- Develop models for the stress-dependent resilient modulus of unbound materials.
- Identify the design resilient modulus for new design and rehabilitation projects.
- Develop prediction models for estimating resilient modulus of unbound materials in Nevada for new design and rehabilitation projects.

Chapter 2. LITERATURE REVIEW

Since the publication of the MEPDG Guide in 2008, some agencies have transitioned to this new method (for example: Arizona, Colorado, Georgia, Indiana, Missouri, Utah, Virginia, and Wyoming). Many other agencies are in the process of evaluating the procedure, creating input libraries to tailor the AASHTO MEPDG procedure to their local conditions, soils, and materials. NDOT is within the latter category of agencies and has started the implementation of the MEPDG for the structural design of flexible and rigid pavements.

NDOT's goal is to implement the MEPDG through a phased approach, similar to many other agencies. This phased approach includes building material libraries and tying some of the inputs to their day-to-day practices to minimize deviations from current practice and maximize the use of historical information and data. One of the input categories to the MEPDG is the characterization of all unbound layers and subgrades. The input parameters for the unbound layers include: resilient modulus, Poisson's ratio, dry density, water content, gradation, Atterberg limits, etc. The resilient modulus is considered a key input parameter that has a significant impact on the structural responses of a pavement structure, and thus affects its performance and design.

Multiple sensitivity analyses have been completed to identify input parameters that significantly affect the calculation or prediction of different pavement distresses. Results from these sensitivity analyses are used to determine where the agency should focus its resources to facilitate the implementation process; in other words, "getting the biggest outcome for the funds invested." The review of published papers and reports indicate the resilient modulus of unbound materials and soils has an impact on pavement performance. The following is a general summary of the impact levels of the subgrade resilient modulus on pavement performance indicators (3):

- Flexible Pavements
    - Fatigue Longitudinal Cracking – Moderate to High Impact
    - Fatigue Alligator Cracking – Low to Moderate Impact
    - Transverse Cracking – None to Low Impact
    - Rutting – Low to Moderate Impact
    - IRI – Variable
- Rigid Pavements
    - Faulting – Low Impact
    - Transverse Cracking – Moderate to High Impact
    - IRI – None to Low Impact

Recognizing the role of M_r of unbound materials on the design and performance of flexible and rigid pavements, some questions that are typically asked by an agency prior to the full implementation of the MEPDG include: a) what test method should be used to measure resilient modulus, b) how is the design resilient modulus determined, and c) what is the "best" correlation (form and accuracy) between M_r and other unbound materials properties or test results?

The literature review, conducted in this research, compiled information in specific areas related to the inputs to the MEPDG, including: a) the latest development and implementation of the MEPDG around the country, and b) summarize existing correlation equations to estimate the M_r from other physical properties of the unbound materials for base and subgrade layers. A similar literature

review and summary was prepared by members of the research team for the FHWA under a project recently completed (under publication) entitled; "Precision and Bias of the Resilient Modulus Test" (4). In addition, selected agencies actively running the resilient modulus test were contacted to obtain any results from recently completed and/or on-going studies relating the resilient modulus to other soil properties for use in design and in building the agency's materials library.

The literature review is divided into several sections, including: 1) the hierarchical input structure of the MEPDG as related to unbound layers to facilitate implementation, 2) a review of laboratory Mr test methods, 3) reviewing Mr test data, 4) summarizing available correlations between Mr and other physical properties or tests, and 5) a brief overview of other agencies practices in establishing unbound materials libraries.

2.1. Hierarchical Input Levels of the MEPDG

Table 2.1 summarizes the input parameters and how they are determined as recommended in the MEPDG Manual of Practice. Most of the input parameters are well defined and commonly measured by the agency on a day-to-day basis for various reasons. Performing the repeated load resilient modulus test, however, is expensive and time consuming. In addition, the process of determining the design resilient modulus has been widely debated. As such, many agencies have expended resources to determine an appropriate procedure to estimate the design Mr for specific site features and design strategy.

The M_r is a required input for all unbound granular materials and subgrades. The M_r values are used in the structural response computation models and have a significant effect on the pavement responses and modulus of subgrade reaction (k-value) computed internally. The M_r can be measured directly from laboratory testing, or obtained through correlations with other material strength properties. There are three different levels of inputs for M_r and consist of the following:

- *Input Level 1 – Project Specific Measured Values:*

  The level 1 resilient modulus for unbound granular materials and subgrade are determined from repeated load triaxial tests. The test standards recommended for use are: AASHTO T 307 and NCHRP 1-28A. The M_r is estimated using a generalized constitutive model (Equation 2). The *k* coefficients are determined by using linear or nonlinear regression analyses to fit the model to the laboratory test results. The input level 1 procedure is applicable to new design, reconstruction and rehabilitation design (5).

$$M_r = k_1 p_a \left(\frac{\theta}{P_a}\right)^{k_2} \left(\frac{\tau_{oct}}{P_a} + 1\right)^{k_3} \qquad (2)$$

  Where;

  M_r: resilient modulus, psi
  θ: bulk stress, psi
  σ_1: major principal stress, psi
  σ_2: intermediate principal stress, psi
  σ_3: minor principal stress/confining pressure, psi
  τ_{oct}: octahedral shear stress, psi
  P_a: normalizing stress (atmospheric pressure), psi
  k_1, k_2, k_3: regression constants (obtained by fitting resilient modulus test data to equation)

In earlier versions of Pavement ME Design, the regression coefficients (k_1, k_2, k_3) could be entered directly into the software. The program used a finite element model for calculating pavement responses within the various unbound layers based on the nonlinear regression coefficient to determine the stress dependent resilient modulus appropriate for the in-place stress condition. Version 1.0 excluded the finite element model and a user could no longer enter the regression coefficients from a repeated load triaxial resilient modulus test. Thus, the design resilient modulus is entered directly in the program which is determined external to the software and only the linear response is considered in calculating the critical pavement responses. The in-place stress condition is determined by the user which should represent the value at the critical condition – higher damage rate.

- *Input Level 2 – Correlations with Other Material Properties or Tests*

  While the repeated load triaxial resilient modulus test provides a fundamental approach to characterize the nonlinear stress dependent behavior of unbound materials, the test itself is time-consuming and costly. In light of these issues, most state highway agencies have elected to implement level 2 input for unbound materials. Many existing correlations can be used to estimate the resilient modulus, and the correlations can be direct or indirect. Table 2.2 summarizes the correlations included in the Pavement ME design software. For input level 2 design, the user can input a representative Mr or use the enhance integrated climatic model to adjust the Mr for seasonal effects or input an Mr for each month of the year.

- *Input Level 3 – Typical Values based on Soil Classification or Local Experience*

  In level 3, typical M_r values are specified for different types of unbound materials or soils. These typical values can represent the global defaults or represent local experience. The global values are built into the software, are dependent on soil classification, and represent the Mr at the optimum water content and maximum dry unit weight. These values should be used with caution as they represent approximate values. Levels 1 and 2 input are recommended to achieve more representative materials behavior (5).

Table 2.1. Unbound Aggregate Base, Subbase, Embankment, and Subgrade Soil Input Parameters and Test Protocols for New and Existing Materials.

Design Type	Measured Property	Source of Data		Recommended Test Protocol and/or Data Source
		Test	Estimate	
New (lab samples) and existing (extracted materials)	Determine the average design resilient modulus for the expected in-place stress state from laboratory resilient modulus tests.	X		The generalized model used in MEPDG design procedure – see equation 1; AASHTO T 307 or NCHRP 1-28A
	At-Rest earth pressure coefficient		X	No national test standard; value used external to the software.
	Poisson's ratio		X	No national test standard, use default values included in the MEPDG.
	Maximum dry density	X		AASHTO T 180
	Optimum moisture content	X		AASHTO T 180
	Gradation	X		Gradation of the unbound aggregate or embankment soil measured in accordance with AASHTO T 88
	Atterberg Limits	X		Liquid limit measured in accordance with AASHTO T 89, and plastic limit and plasticity index determined in accordance with AASHTO T 90.
	Specific gravity	X		AASHTO T 100
	Saturated hydraulic conductivity	X		AASHTO T 215
	Soil water characteristic curve parameters	X		Pressure plate (AASHTO T 99), OR Filter paper (AASHTO T 180), OR Tempe cell (AASHTO T 100)
Existing material to be left in place	FWD backcalculated modulus	X		AASHTO T 256 and ASTM D 5858
	Poisson's ratio		X	No national test standard, use default values included in the MEPDG.

Table 2.2. Models Relating Material Index and Strength Properties to Mr (5).

Strength/Index Property	Model	Comments	Test Standard
CBR	$M_r = 2555(CBR)^{0.64}$ (TRL) Mr, psi	CBR = California Bearing Ratio, percent	AASHTO T193, "The California Bearing Ratio"
R-value	$M_r = 1155 + 555R$ (*20*) Mr, psi	R = R-value	AASHTO T190, "Resistance R-Value and Expansion Pressure of Compacted Soils"
AASHTO layer coefficient	$M_r = 30000\left(\frac{a_i}{0.14}\right)$ (*20*) Mr, psi	a_i = AASHTO layer coefficient	AASHTO Guide for the Design of Pavement Structures
PI and gradation*	$CBR = \frac{75}{1+0.728(wPI)}$ (see Appendix CC)	wPI = P200*PI P200= percent passing No. 200 sieve size PI = plasticity index, percent	AASHTO T27. "Sieve Analysis of Coarse and Fine Aggregates" AASHTO T90, "Determining the Plastic Limit and Plasticity Index of Soils"
DCP*	$CBR = \frac{292}{DCP^{1.12}}$	CBR = California Bearing Ratio, percent DCP =DCP index, mm/blow	ASTM D 6951, "Standard Test Method for Use of the Dynamic Cone Penetrometer in Shallow Pavement Applications"

*Estimates of CBR are used to estimate M_r.

The following summarizes the values and data sources for characterizing the unbound layers or materials used by most agencies that have completed or are in the process of implementing the Pavement M-E software. The default values used become important when completing the calibration and validation of the distress transfer functions to ensure consistency of use.

- Design Resilient Modulus: Many agencies have generated resilient modulus databases for the aggregate base materials commonly specified by the agency and soils that are predominantly encountered within the agency's jurisdictions. Other agencies use correlations to CBR, R-value, materials physical properties, and dynamic cone penetrometer test results.
- Dry Density and Water Content: The software asks for the maximum dry unit weight and optimum water content but the values depend on how the test specimens were prepared and/or the condition of the test specimens for the correlations that the agency is using to estimate the Mr. For example, some agencies use the CBR to estimate the design Mr. A few of these agencies have run soaked CBR tests and measured the resilient modulus at the dry density and water content from the soaked CBR test, while other agencies have measured the resilient modulus at the dry density and water content before the specimen is subjected to water soaking during the CBR test. How the correlation was developed defines the input values. It is important that the dry density and water content entered into the software to be consistent with the method used to define the correlation regardless of what other test is used.
- Poisson's Ratio: Poisson's ratio is identified as an insignificant input parameter in terms of the predicted cracking and distortion type distresses, and is generally estimated. However, Poisson's ratio does have an impact on the selection of the design resilient modulus of any unbound layer because it affects the vertical and horizontal stresses – this is called the Poisson's ratio effect. Therefore, a reliable estimate of the Poisson's ratio based on experience is desired.
- At-Rest Lateral Earth Pressure Coefficient: This input parameter is no longer needed since

the selection of the design resilient modulus is not part of the input level 1 in the current version of the Pavement ME Design software. However, the at-rest earth pressure coefficient is important in defining the design resilient modulus. At-rest earth pressure coefficients can vary from 0.50 to well over 1.0 depending on the condition of the soil or aggregate base layers. The coefficient has an impact on the lateral stress condition, which in turn affects the design resilient modulus.

- Gradation and Atterberg Limits: Most agencies define the average gradation, plasticity limit, and liquid limit for the commonly used aggregate base layers and predominant soils found within the agency's jurisdictions. The local default values are typically compared to the global default values included in the Pavement ME Design software to determine the difference between the two sets of values. Sometimes differences in the physical properties will explain some of the differences between the global and local design resilient moduli.
- Soil-Water Characteristic Curve Parameters: Just about all agencies have used the global default values which are soil classification dependent.
- Specific Gravity: All agencies have simply used the global default value of 2.7 included in the current version of the Pavement ME Design software for all soil classifications.
- Saturated Hydraulic Conductivity: All agencies have used the global default value in their implementation and local calibration studies, which are soil classification dependent.

2.2. Overview of Resilient Modulus Test

The resilient modulus is similar to the elastic modulus of a material and is defined as a ratio of deviatoric stress to resilient or elastic strain experienced under repeated loading conditions that aims to simulate traffic loading. Figure 2.1 shows a representation of the resilient modulus. The main reason for using the resilient modulus as the parameter for unbound bases and subgrades is that it represents a basic material property and can be used in mechanistic analyses to calculate pavement responses used to predict different distresses (i.e. rutting, cracking, and roughness).

Prior to 1980, an attempt was made to standardize the testing procedure. A standard test was not reached due to different philosophies on specimen preparation, on versus off specimen deformation measurements, stress states (vertical stress and confinement), as well as type of load application (haversine versus square load pulses). Several studies were performed in the process in attempts to standardize testing methods. Many of these studies are summarized in the precision and bias report (4). Some other factors that were studied include, drained versus undrained conditions, load cell location, and the number of conditioning cycles required for stable results.

The NCHRP Synthesis 382 summarized Mr testing procedures and results from various sources. The summary is presented based on testing performed prior to 1986, between 1986 and 1996, and after 1996 (6). In summary, the research performed prior to 1986 mostly focused on three different criteria namely: (a) the development of test procedures and equipment modifications to test cohesive subgrades and granular base materials, (b) the development of appropriate models to represent the resilient behavior, and (c) the introduction of few correlations based on soil properties to predict resilient properties (6).

The Mr research performed between 1986 and 1996 focused on the use of various laboratory and field equipment to determine the properties of both unbound bases and subgrades. Some studies were performed to develop a database of resilient properties which were then used to develop

models to predict resilient properties of subgrades and aggregate bases. Considerable advances were made after 1996 which led to the development of a large Mr database for better interpretation of resilient properties for mechanistic pavement design. One of these studies tested the Mr values for LTPP sections across the United States (6).

In other advancements, various studies determined parameters which affect the measurement of Mr. One such study determined that soil suction was an important factor in measuring the Mr. Soil suction is not measured as part of the AASHTO T 307 or NCHRP 1-28A testing procedures. Another study suggested that modifications should be made to the stress state conditions when measuring Mr on unsaturated unbound materials (4).

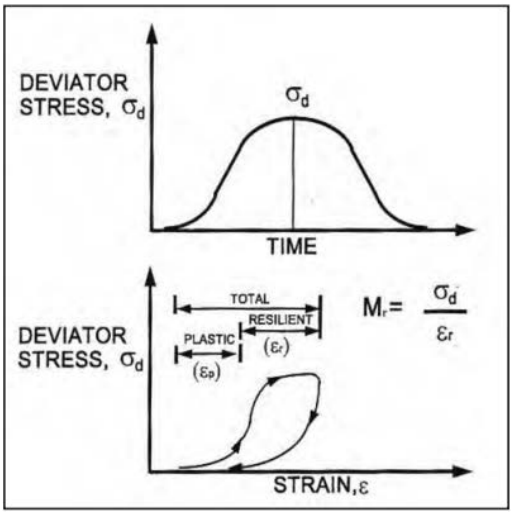

Figure 2.1. Definition of resilient modulus (6).

The resilient modulus test using the repeated load triaxial test simulates traffic wheel loading on in-situ soils by applying repeated or cyclic loads on compacted soil specimens. The stress levels applied to the soil specimens are dependent on the location of the material within the pavement structure. A confining pressure is also applied to the specimen that represents the overburden lateral pressure at a specific location in the subgrade. The axial deviatoric stress consists of two components, the cyclic stress, and a constant stress. The constant stress is typically equivalent to 10% of the total axial deviatoric stress.

The test procedure requires a compacted soil specimen using impact compaction methods. The specimen is then transferred into the triaxial chamber and the confining pressure is applied. The test is initiated by applying various levels of deviatoric stresses. Multiple confining pressures and deviatoric stresses are used during the testing process. The resilient modulus values are determined at each combination of confining pressure and deviatoric stress. The design resilient modulus value is established by determining the Mr value at the appropriate confining pressure and deviatoric stress level corresponding to the location of the materials within the pavement structure.

Various versions of the repeated load triaxial test have been used to measure the resilient modulus for mechanistic-empirical (ME) based pavement design procedures, including: AASHTO T 274, T 292, T 294, and T 307. All of these test methods differ from each other in one or more of the following aspects: specimen preparation, conditioning, seating stress, testing sequences, and deformation measurements inside/outside of the triaxial cell.

Table 2.3 summarizes the chronology of the AASHTO resilient modulus test procedures. AASHTO adopted test procedure T307 which is similar to the test procedure used in the Long Term Pavement Performance (LTPP) program.

Table 2.3. Chronology of AASHTO Test Procedures for Mr Measurements (6).

Test Procedure	Details
AASHTO T 274-1982	Earliest AASHTO test procedure; No details on the sensitivities of displacement measurement devices were given; Criticisms on test procedure, test duration (5 hours long test) and probable failures of soil sample during conditioning phase; testing stresses are too severe.
AASHTO T 292-1991	AASHTO procedure introduced in 1991; Internal measurement systems are recommended; Testing sequence is criticized owing to the possibility of stiffening effects of cohesive soils.
AASHTO T 294-1992	AASHTO modified the T 292 procedure with different sets of confining and deviatoric stresses and their sequence; Internal measurement system is followed; 2-parameter regression models (bulk stress for granular and deviatoric stress model for cohesive soils) to analyze test results; Criticism on the analyses models.
Strategic Highway Research Program P-46-1996	Procedural steps of P-46 are similar to T 294 procedure of 1992; External measurement system was allowed for displacement measurement; Soil specimen preparation methods are different from those used in T 292.
AASHTO T 307-1999	T 307-1999 was evolved from P-46 procedure; recommends the use of external displacement measurement system. Different procedures are followed for both cohesive and granular soil specimen preparation.
NCHRP 1-28 A: Harmonized Method-2004 (RRD 285)	This recent method recommends a different set of stresses for testing. Also, a new 3-parameter model is recommended for analyzing the resilient properties. The use of internal measurement system is recommended in this method.

A recent review of 30 state DOTs and other agencies specifications indicated that 22 out the 30 are currently using AASHTO T 307 test method for measuring the Mr of unbound materials (4). Table 2.4 lists the resilient modulus test procedures being used by different agencies (4). The overall satisfaction of those agencies regarding the use of resilient modulus for ME-based pavement design was found to be low due to constant modifications of the test procedures, measurement difficulties, and design-related issues.

The resilient modulus test data generated from the triaxial test should undergo data anomaly checks to identify if issues with the data exist. It is essential to ensure that the good quality data without errors are used before making any assessment on the M_r results. Possible problems that could affect the M_r test data are listed below (7):

- Different condition sequences or different stress application sequences used in the test program
- Leaks occurring in the membrane during the test
- Different stress states used in the test program than required by the test protocol
- Test specimens that begin to fail or exhibit disturbance at the higher stress states
- LVDT clamps that begin to move or move suddenly because of vibrations during the loading sequence

- LVDTs that begin to drift during the testing sequence or become restricted due to friction in the measurement system
- Measured deformations that begin to exceed the linear ranges of the LVDTs

Table 2.4. State DOT/Other Laboratories Conducting Resilient Modulus Testing.

State DOT/Other Laboratories	Test Protocol Followed
Alaska DOT	AASHTO T 307-99
Alabama DOT	AASHTO T 307-99
Arizona DOT/ASU Geotechnical Laboratory	NCHRP 1-28A
Cold Regions Research & Engineering Laboratory (CRREL)	AASHTO T 307-99
Colorado DOT	AASHTO T 307-99
Florida DOT	AASHTO T 307-99
Georgia DOT	AASHTO T 307-99
Iowa DOT	NCHRP 1-28A/AASHTO T307-99
Idaho Transportation Department Laboratory	AASHTO T 307-99
Indiana DOT	AASHTO T 307-99
Kansas DOT	AASHTO T 307-99
Kentucky DOT/University of Kentucky Transportation Center	AASHTO T 307-99
Louisiana DOT/Louisiana Transportation Research Center (LTRC) Laboratory	AASHTO T 307-99
Manitoba Provence, Canada	NCHRP 1-28A
Michigan DOT	AASHTO T 307-99
Minnesota DOT	NCHRP 1-28A
Missouri DOT	AASHTO T 307-99
Mississippi DOT	AASHTO T 307-99
Montana DOT	AASHTO T 307-99
Nebraska DOT/University of Nebraska-Lincoln (UNL) Geomaterials Laboratory	AASHTO T 307-99
North Dakota DOT	NCHRP 1-28A
New Hampshire DOT	AASHTO TP46-94
New Jersey DOT/Rutgers University Asphalt/Pavement Laboratory (RAPL)	AASHTO TP46-94
OH DOT/ORITE Pavement Material Test Laboratory	AASHTO T 274
Oklahoma DOT	AASHTO T 307-99
Rhode Island DOT	AASHTO T 307-99
Tennessee DOT	AASHTO T 307-99
Texas DOT	AASHTO T 307-99
Virginia DOT	AASHTO T 307-99
Wisconsin DOT	AASHTO T 307-99

The following provides a summary of the more important findings relative to determining the precision and bias of the resilient modulus test methods. These findings were extracted from the FHWA report on the precision and bias of the resilient modulus test (4).

- There are several test systems available on the market today. The so-called high-end equipment (MTS, Interlaken and Instron) is about double the cost of the lower-end equipment (GCTS, GeoComp and IBC). This statement does not imply the high-end equipment is twice as accurate as the lower-end equipment. Few studies have focused on determining if there is a bias between these different systems, as well as defining the precision of the test system.
- The end effects for off-specimen LVDTs were obvious and significantly increased the variability in the test results of triplicate samples, in comparison to on-specimen LVDTs. Different studies, however, have reported opposite results in comparing the resilient modulus values between on-specimen and off-specimen displacement measurements for calculating resilient modulus.
- It was found that all soils exhibited a decrease in resilient modulus with an increase in saturation, but the magnitude of the decrease in resilient modulus was found to depend on the soil type. It was observed and reported a 3 to 5 percent increase in moisture content from optimum conditions can result in a 50 to 70 percent reduction in resilient modulus. The drying of the test specimens can also result in a significant increase in resilient modulus, in some cases ten-fold. Thus, moisture content and dry density are important in measuring the resilient modulus.
- The studies reviewed indicated that the resilient modulus values were impacted by moisture content, soil suction, Atterberg limits, gradation, source lithology, stress-strain levels, degree of saturation, seasonal variation, aggregate angularity, and surface texture.

2.3. Correlations for Estimating Resilient Modulus

Numerous M_r correlation equations have been developed over the years (8). Most of these correlations are regression-based equations developed by comparing the M_r test results from the repeated load triaxial (RLT) to the less expensive and more routine test results such as R-value (R), CBR, unconfined compressive (UC) strength, dynamic cone penetrometer test, physical properties, etc. An extensive literature review was conducted and showed that most of the correlation equations were developed from relatively small sample sets and often for region-specific material types (9). Accordingly, it was recommended to further assess and verify the suitability and reliability of the regression analysis before the use of any of the correlation equations. Two different types of correlations have been developed: direct and indirect.

- Direct correlations consist of developing a relationship between the resilient modulus and various soil properties and in-situ related parameters. These correlations are usually developed by using some type of statistical regression between the test data and resilient modulus. Two types of direct correlations are typically developed. The first method develops a direct correlation between the resilient modulus and various soil properties. The second correlates the moduli with in-situ parameters.
- The indirect method develops correlations by formulating an equation that accounts for confining or deviatoric or both stress forms. Usually these correlations contain model constant parameters. Some of these models can have two, three, or four parameter correlations that account for the different stress states.

Puppala presented a detailed summary of the different types of correlations that have been developed (6). The summary details various correlation equations developed for both direct and indirect correlations. The following lists some of the correlations that have been developed.

Yau and Von Quintus, 2001; Crushed Stone Materials, LTPP Material Code 303:

$$M_r = \left[0.7632 + 0.0084\left(P_{3/8}\right) + 0.0088\left(LL\right) - 0.0371\left(W_{opt}\right) - 0.0001\left(\gamma_{opt}\right)\right] p_a * \left[\frac{\theta}{p_a}\right]^{\left(2.2159 - 0.0016P_{3/8} + 0.0008LL - 0.038W_{opt} - 0.0006\gamma_{opt} + 2.4x10^{-7}\left[\frac{\gamma_{opt}^2}{P_{40}}\right]\right)} * \left[\frac{\tau_{oct}}{p_a} + 1\right]^{\left(-1.1720 - 0.00822LL - 0.0014W_{opt} + 0.0005\gamma_{opt}\right)} \quad (3)$$

Where;

LL: liquid Limit
W_{opt}: optimum water content
γ_{opt}: maximum dry unit weight at optimum water content
$P_{3/8}$: percent passing the 3/8 inch sieve, percent
P_{40}: percent passing the #40 sieve, percent
Number of points: 853
Mean squared error: 1699.6 psi
S_e = 41.23; S_y = 87.42; S_e/S_y = 0.4716

Yau and Von Quintus, 2001; Sand, LTPP Material Code 306:

$$M_r = \left[-0.2786 + 0.0097\left(P_{3/8}\right) + 0.0219\left(LL\right) - 0.0737\left(PI\right) + 1.8x10^{-7}\left(\frac{\gamma_{opt}^2}{P_{40}}\right)\right] p_a * \left[\frac{\theta}{p_a}\right]^{\left(1.1148 - 0.0053P_{3/8} - 0.0095LL + 0.0325PI + 7.2x10^{-7}\left[\frac{\gamma_{opt}^2}{P_{40}}\right]\right)} * \left[\frac{\tau_{oct}}{p_a} + 1\right]^{\left(-0.4508 + 0.0029P_{3/8} - 0.0185LL + 0.0798PI\right)} \quad (4)$$

Where;

PI: plasticity Index
Number of Points: 2,323
Mean squared error: 1883.9
S_e = 43.40; S_y = 80.19; S_e/S_y = 0.5413

Yau and Von Quintus, 2001; Coarse-Grained Gravelly Soils:

$$M_r = \left[1.3429 - 0.0051\left(P_{3/8}\right) + 0.0124\left(\%Clay\right) + 0.0053\left(LL\right) - 0.0231\left(W_s\right)\right] p_a * \left[\frac{\theta}{p_a}\right]^{\left(0.3311+0.0010P_{3/8}-0.0019\left(\%Clay\right)-0.0050LL-0.0072PI+0.0093W_s\right)} * \left[\frac{\tau_{oct}}{p_a}+1\right]^{\left(1.5167-0.0302P_{3/8}+0.0435\left(\%Clay\right)+0.0626LL-0.2353W_s\right)} \quad (5)$$

Where;

Ws: water content of test specimen
%Clay: percentage clay or material passing the 0.0075 sieve
Number of Points: 957
Mean squared error: 301.3
S_e = 17.36; S_y = 26.81; S_e/S_y = 0.6474

Yau and Von Quintus, 2001; Fine-Grained Silty Soils:

$$M_r = \left[1.0480 + 0.0177\left(\%Clay\right) + 0.0279\left(PI\right) - 0.37\left(W_s\right)\right] p_a * \left[\frac{\theta}{p_a}\right]^{\left(0.5097-0.0286PI\right)} * \left[\frac{\tau_{oct}}{p_a}+1\right]^{\left(-0.2218+0.0047\left(\%Silt\right)+0.0849PI-0.1399W_s\right)} \quad (6)$$

Where;

%Silt: percentage of silt fines
Number of Points: 464
Mean squared error: 193.0
S_e = 13.89; S_y = 24.71; S_e/S_y = 0.5622

Yau and Von Quintus, 2001; Fine-Grained Clayey Soils:

$$M_r = \left[1.3577 + 0.0106\left(\%Clay\right) - 0.0437\left(W_s\right)\right] p_a * \left[\frac{\theta}{p_a}\right]^{\left(0.5193-0.0073P_4+0.0095P_{40}-0.0027P_{200}-0.0030LL-0.0049W_{opt}\right)} * \left[\frac{\tau_{oct}}{p_a}+1\right]^{\left(1.4258-0.0288P_4+0.0303P_{200}+0.0251\left(\%Silt\right)+0.0535LL-0.0672W_{opt}-0.0026\gamma_{opt}+0.0025\gamma_s-0.6055\left(\frac{W_s}{W_{opt}}\right)\right)} \quad (7)$$

Where;

P_4: percentage of material passing the #4 sieve.
P_{200}: percentage of material passing the #200 sieve.
γ_s: dry unit weight of test specimen.
Number of Points: 1,484
Mean squared error: 557.9
S_e = 23.62; S_y = 29.22; S_e/S_y = 0.8082

Drum, et al., 2008:

$$M_r = 45.8 + 0.00052\left(\frac{1}{a}\right) + 0.188(UC) + 0.45(PI) + 0.216(\gamma_s) - 0.25(S) - 0.15(P_{200}) \quad (8)$$

Where;

A: initial tangent modulus, psi
UC: unconfined compressive strength, psi
S: degree of saturation, percent
Coefficient of Determination, $R^2 = 0.83$.

Lee, et al., 1997:

$$M_r = 695.4(S_{@1\%}) - 5.93(S_{@1\%})^2 \quad (9)$$

Where;

$S_{@1\%}$: stress at 1.0 percent strain in the unconfined compressive strength test.
Coefficient of Determination, $R^2 = 0.97$.

Hossain and Kim, 2014, Static Compaction:

$$M_r = 6082 + 142(UC) \quad (10)$$

Coefficient of Determination, $R^2 = 0.64$.

$$M_r = 7884.2 + 99.7(UC) + 193.1(PI) - 47.9((P_{200}) \quad (11)$$

Coefficient of Determination, $R^2 = 0.86$.

Hossain and Kim, 2014, Impact Compaction (Proctor Hammer):

$$M_r = 4283 + 143(UC) \quad (12)$$

Coefficient of Determination, $R^2 = 0.73$.

$$M_r = 6113 + 95.1(UC) + 173.7(PI) - 27.8((P_{200}) \quad (13)$$

Coefficient of Determination, $R^2 = 0.91$.

$$M_r = 657(S_{@1\%}) - 6.75(S_{@1\%})^2 \quad (14)$$

Coefficient of Determination, $R^2 = 0.97$.

2.4. Implementation and Use of Resilient Modulus

Several State Agencies have implemented or are in the process of implementing the MEPDG. This section presents the efforts related to developing M_r input databases for each State. Table 2.5 summarizes the outcome from selected agencies regarding resilient modulus and other properties of unbound layers. The important observation from Table 2.5 and from the design manual of selected agencies is that almost no agency performs repeated load triaxial resilient modulus tests for measuring Mr. The Mr is predominantly estimated using a library of values and/or through a regression equation related to other properties or test results.

Most agencies east of the Mississippi River use CBR for estimating the design Mr, while agencies west of the Mississippi use R-value. The regression equations for estimating Mr from the R-value vary by agency, but only two regression equations are typically used for estimating Mr from CBR. The R-value regression equations are listed by agency in the following section, while the two regression equations based on CBR are; Mr =1500*CBR and Mr = $2555(CBR)^{0.64}$.

Table 2.5. Methods used to Estimate Design Resilient Modulus for Selected Agencies.

State DOT	Test Procedure	Mr Correlated with and/or Determined
Arizona	NCHRP 1-28A	R-value and a library of Mr values.
Colorado	AASHTO T 307-99	R-value and a library of Mr values.
Florida	AASHTO T 307-99	LBR-value, backcalculated from deflection basins, and a library of Mr Values.
Georgia	AASHTO T 307-99	Soil Support, Physical properties, and a library of Mr values.
Idaho	AASHTO T 307-99	R-value and a library of Mr values.
Michigan	AASHTO T 307-99	Library of Mr values and backcalculated from deflection basins.
Missouri	AASHTO T 307-99	Regression equations to calculate k_1, k_2, and k_3 from soil physical properties; similar to FHWA regression equations.
Mississippi	AASHTO T 307-99	CBR and a library of Mr values.
Montana	AASHTO T 307-99	Library of Mr values and backcalculated from deflection basins.
Pennsylvania	AASHTO T 307-99	Unconfined compressive strength and a library of values
Tennessee	AASHTO T 307-99	Index of soil properties.
Texas	AASHTO T 307-99	Texas Triaxial Classification Value
Virginia	AASHTO T 307-99	Unconfined compressive strength
Wisconsin	AASHTO T 307-99	Regression equations to calculate k_1, k_2, and k_3 from soil physical properties; similar to FHWA regression equations.
Wyoming	AASHTO T 307-99	R-value and a library of Mr values.

2.4.1. Federal Highway Administration (FHWA)

Two FHWA sponsored studies were reviewed as part of this literature review and both are briefly discussed in the following paragraphs.

1. FHWA sponsored a study in 2001 to investigate the resilient modulus test results stored in the LTPP database. This study had two major goals: evaluate the accuracy of the test data and identify any anomalies and their possible causes, and to develop correlations between the regression coefficients of equation 2 and the materials physical properties that are stored in the LTPP database. A regression equation was derived for each major soil classification and the different aggregate base classification defined in the LTPP database (7). Equation 3 through equation 7 in the previous section are examples of the relationships generated from that study. An important observation made by Yau and Von Quintus from this work was that the standard error of the regression equations was high for many of the

materials, so they recommended that laboratory repeated load triaxial resilient modulus tests be performed to actually measure the regression coefficients.

2. FHWA sponsored a more recent study related to resilient modulus and its use in the MEPDG procedure. This second study was focused on defining the precision and accuracy of the resilient modulus tests (4). One of the important outcomes from the second study was to recommend procedures to be used in accordance with the MEPDG to derive the design resilient modulus for a quasi-input level 1 value. The report documented the precision of the test and made recommendations for a specific test method to be followed. In addition, the procedure documented in the report for determining the design resilient modulus for aggregate base layers, as well as for subgrade soils will be addressed in Chapter 5.

2.4.2. Asphalt Institute

The Asphalt Institute derived an equation to estimate M_r from the R-value test. The test data used in the derivation was from road tests conducted in San Diego, California (10). Equation 15 shows the original equation generated from that confined data set.

$$M_r = 772 + 369(\text{R-value}) \quad (15)$$

The Asphalt Institute used the same from of the regression equation but modified the coefficients from a larger data set, which is included in Table 2.2. That equation was included in as the regression equation based on R-value for input level 2.

2.4.3. Correlations Developed by State DOTs

Colorado DOT

The MEPDG implementation was completed in Colorado in 2013. The process included characterizing in service pavements and the needed properties in the MEPDG as well as the local calibration of the performance models. The unbound and subgrade M_r values were needed to characterize the in service pavements in the MEPDG. The Colorado DOT made a decision early on to use a strength test to estimate the resilient modulus in accordance with the MEPDG input level 2 approach. The strength test was the R-value for which the Colorado DOT had extensive experience and a historical database.

The correlation developed by Colorado DOT for coarse and fine grained materials is shown below in Equation 16. Details of laboratory procedures for resilient modulus and R-values were not reported for this study (11).

$$Mr = 10^{[((R-5)/11.29)+21.72]/6.24} \quad (16)$$

Yeh and Su (12) developed the following relationship for Colorado soils using resilient modulus data from testing conducted at confining pressure of 3 psi and deviator stress of 6 psi, as shown in equation 17. Analysis of the study results showed that the relationship needed to be further calibrated for soils having R values greater than 60.

$$M_r = 3500 + 125\ (R) \quad (17)$$

FWD testing was performed to backcalculate layer moduli at in-situ moisture conditions. The backcalculated moduli was then transformed to an equivalent lab M_r at the optimum moisture content. The moduli at the optimum moisture content was determined using a multi-step process. The field measured M_r at in-situ moisture content was converted to a laboratory M_r at in-situ

moisture conditions using C-factors. The in-situ laboratory M_r was then converted to a laboratory M_r at optimum moisture content using an iterative process (13). For flexible pavements, the equivalent lab M_r was determined using the following equation:

$$M_{requivalent} = E_{SG} \text{ x } C \text{ x } M_r/M_{r\text{-}opt} \quad (18)$$

In addition to the equivalent laboratory M_r, the backcalculated moduli, c-value, $M_r/M_{r\text{-}opt}$ ratio, corrected lab $M_{r\text{-}opt}$ and mean M_r by soil type was summarized.

A similar iterative process was used for concrete pavements with a comparison to the modulus of subgrade reaction. The backcalculated modulus of subgrade reaction, elastic modulus and mean M_r at optimum moisture content was summarized for all pavement sections. The optimum M_r was determined using the following equation:

$$M_{r\text{-}opt} = 60.754 \times k\text{-}value \quad (19)$$

Resilient modulus testing using the repeated load triaxial test was not performed in Colorado during their implementation of the MEPDG because of their historical database.

Georgia DOT

Field testing was performed in Georgia as part of their MEPDG implementation project. FWD, DCP and cores were taken at various pavement sites. The pavement sections included both local sites and LTPP sites.

The DCP testing was only performed at Georgia pavement sections. The DCP penetration rates were used to determine an estimate of in-place resilient modulus. These values were compared to the backcalculated M_r from the FWD deflection basin. It was found that there're is a correlation between the backcalculated and DCP M_r values. The backcalculated M_r showed greater resilient modulus values compared to the DCP values except for sections with coarser particles or rock fragments.

AASHTO T 307 or NCHRP 1-28A resilient modulus tests were not performed for any of the pavement sites. Resilient modulus tests were available from the LTPP database and used to develop GDOT's material library. In addition, GDOT had Georgia Tech perform resilient modulus tests on a range of soils. The c-factors were determined to correct for the difference between laboratory and field-derived M_r values. A large difference was exhibited between the default c-factors reported in the MEPDG Manual of Practice and the ones developed based on the Georgia pavement sites. The laboratory resilient modulus, backcalculated resilient modulus, c-factor, water content and dry density were presented for all LTPP and Georgia specific sites (14).

Idaho DOT

As part of the MEPDG implementation process, Idaho is using input level 2 to determine the M_r for their design procedures. The laboratory resilient modulus test procedure was not an option due to its complexity, time requirements and expensive equipment. Two models were developed for input level 2 in accordance with the MEPDG. The first model consisted of developing a multiple regression to predict the R-value as a function of soil plasticity index and percent passing of the #200 sieve. The second model was a M_r model based on the estimated R-value.

The R-value prediction model was developed using 8,233 data records ranging from 1953-2008 and represents all 25 soil classes in the USC system. The model form developed is presented in

equation 19. This model is recommended when direct measurements of the R-value for unbound granular materials and subgrade soils is unavailable.

$$\text{R-value} = 10^{(1.893-0.00159xp200-0.022xPI)} \quad (20)$$

The second model was developed to determine the resilient modulus based on the R-value. First, the current Asphalt Institute (AI) method for determining M_r from the R-value was validated. The R-value prediction model presented above was used. The AI method values were verified using laboratory measured M_r from Indiana, Mississippi, Louisiana, Arizona and Ohio and consisted mostly of fine grained soils. Verification results showed a significant over-prediction of M_r for the data used in this study. A new model was developed to reduce the bias of the AI method. The model forms for both the AI method and the new Idaho method is presented below:

- AI Method (current MEPDG Default; refer to Table 2.2)

$$Mr = 1155 + 555(R) \quad (21)$$

- Idaho

$$Mr = 1004.4(R)^{0.6412} \quad (22)$$

It is recommended that this model should only be used for similar soil types used in the study which consisted mostly of fine grained soils. In addition to the input level 2 model development, typical input level 3 R-values were summarized for each soil type as well as liquid and plastic limit values (15).

Michigan DOT

Two studies to characterize unbound material in Michigan were performed. The first study outlined the importance of the M_r of the roadbed soil and how it affects pavement systems, while the second study focused on the backcalculation of Mr for unbound base and subbase materials. Both studies focused on developing reliable methods to determine the M_r of the roadbed soil for inputs in the Pavement-ME.

The state of Michigan was divided into fifteen clusters based on the similar soil characteristics. Laboratory tests were performed to determine moisture content, grain size distribution, and Atterberg limits. Another aspect of the study was to determine the differences between laboratory tested M_r values and back-calculated M_r. Based on the analysis, it was concluded that the values between laboratory M_r and back-calculated M_r are almost equal if the stress boundaries used in the laboratory matched those of the FWD tests (16). This observation conflicts with the results from other studies regarding the c-factor defined by AASHO: the ratio of the laboratory-derived and field-derived moduli.

Mississippi DOT

Mississippi DOT has developed several predictive models to estimate resilient modulus of typical Mississippi soils from their soil index properties (17). The study compared various prediction models from other State agencies to Mississippi soils from the LTPP database. A similar study investigated the viability of using FWD data for deriving resilient modulus through empirical correlations (18).

Mississippi DOT tested 34 subgrade soils, 13 granular base/subbase materials, and 16 stabilized soils for developing their pavement materials library for the MEPDG. The NCHRP 1-28A test

method was used for all M_r testing. The report documents the valuable practical experience, lessons and observations that were gained during the testing and review of the data (19).

Missouri DOT

Missouri DOT performed resilient modulus testing in conjunction with the MEPDG implementation process. The focus of the study was to perform M_r testing on common Missouri subgrade soils and typical unbound material using the AASHTO T307 test method. A library of resilient modulus values were developed for granular base materials and subgrade soils. The experimental plan included 27 subgrade soils and five granular base materials commonly found in Missouri. This study also developed regression models to estimate k_1, k_2 and k_3 coefficients using basic soil properties (20).

Montana DOT

Montana DOT compared over thirty different resilient modulus prediction models available in the literature and evaluated those with laboratory data for two soils sampled in Montana (9). This study discouraged the general use of such models without prior testing and verifying the reliability of the model estimates until additional studies suggest otherwise.

Pennsylvania DOT

The implementation process is currently ongoing in Pennsylvania. The unbound and subgrade layers M_r values were evaluated for various pavement sections across the state using the AASHTO T 307 testing procedure. The optimum moisture content and maximum dry density measurements were determined using the Pennsylvania Test Method (PTM) 106-Method B, Modified Proctor compaction effort.

Unconfined compressive strength tests are also being performed but have yet to be completed. PennDOT intends to complete a regression analysis between the design resilient modulus and unconfined compressive strength so that the unconfined compressive strength can be used to determine the design M_r value. The regression equation has yet to be completed.

PennDOT also uses the dynamic cone penetrometer (DCP) for pavement evaluations and in estimating the M_r of the unbound materials and soils. Equation 22 is used to calculate the M_r from the penetration rate measured with the DCP.

$$M_r = 17.6\left[\frac{292}{(DPI)^{1.12}}\right]^{0.64}(C_{DCP}) \tag{23}$$

Where;

DPI: penetration rate or index, mm/blow

C_{DCP}: adjustment factor for converting the elastic modulus to a laboratory resilient modulus which is soil type and water content dependent.

Utah DOT

The implementation of the MEPDG in Utah was performed in 2009. The resilient modulus values were not directly available for most of the pavement sites selected for local calibration. The LTPP database was used to populate the necessary fields without performing additional laboratory testing. No lab test data were available for the UDOT pavement sites.

The subgrade type and other soil parameters were established using the Natural Resource Conservation Survey Soil Survey Geographic database. These inputs were used to characterize the subgrade layers as Level 3 inputs (21).

In addition to the implementation study, another study was performed to investigate the correlations between lab measured resilient modulus and the California Bearing Ratio (CBR) test for aggregate base materials. The AASHTO T307 test was used to determine the M_r of two aggregate base materials. Based on the result, the author concluded that the existing models do not satisfactorily predict M_r for the two aggregates tested and attributes these differences to the variations in properties between the materials used to develop the model and the materials used in Utah. The author also concluded that there is no correlation between the M_r and the CBR for the materials tested in this study (22).

Wisconsin DOT

Wisconsin DOT (WisDOT) funded a laboratory testing program to evaluate the physical and compaction properties of commonly found subgrade soils (23). The resilient modulus was measured using the AASHTO T307 test procedure.

Initially, the results were not good when using the NCHRP 1-37A constitutive model. The results were split between fine and coarse-grained soil, which improved the model accuracy. Statistical correlations were developed to estimate k_1, k_2 and k_3 coefficients from basic soil properties such as; percent passing of the #4, 40, 200 sieves, moisture content, optimum moisture content, dry unit weight, and maximum dry unit weight.

Another WisDOT study conducted an experimental program to develop a resilient modulus predictive model for typical crushed aggregate base materials encountered in Wisconsin (24). The plan included 37 aggregate sources and a wide range of influencing variables, such as physical characteristics, material type, source lithilogy and regional factors, were evaluated for their effect on resilient modulus. WisDOT developed the relationship shown in Equation 24 based on lab testing data conducted on soils ranging from coarse aggregates (A-1) to clays (A-7-6).

$$M_r = 0.72\ (e^{0.0521 \times R} - 1) \qquad (24)$$

Wyoming DOT

A study was performed to characterize representative local materials for unbound base and subgrade layers in Wyoming. Local Wyoming pavement sections and LTPP sections were used to develop a materials database for use in the implementation of the MEPDG. The tests which were performed include:

- FWD testing to backcalculate pavement layer moduli
- Dynamic cone penetrometer testing for subgrade M_r value, and
- Field measured data

The FWD testing was performed to backcalculate in-situ pavement layer moduli using two different backcalculation programs. The DCP test was performed to estimate the California Bearing Ratio (CBR) and the elastic modulus of the soil. For each selected pavement section, the following data were determined: moisture density relationship, Atterberg limits, in-situ moisture content and density, R-Value, lab and backcalculated Mr, and C-factor.

The results were also summarized by soil type to determine Level 3 inputs which can be used if field and lab testing cannot be performed. Some additional findings from the study include (11):

- There was a consistent relationship between optimum water content and maximum dry unit weight.
- There is a significant bias between the M_r for LTTP and Wyoming pavement sections.
- C-factor was only calculated for the Wyoming pavement sections.
- The R-values were also different between the Wyoming and LTPP pavement sections.
- Two relationships between R-value and M_r were derived, as shown in Equation 25 and Equation 26. Both regression equations had similar statistics and the standard error of the estimate. Wyoming DOT made a preliminary decision to select the simpler of the two – Equation 25.

$$M_r = 9713.9 + 61.56(R\text{-}value) \quad (25)$$

$$M_r = 6644(R - value)^{0.1748} \quad (26)$$

Chapter 3. MATERIAL COLLECTION

This research evaluated different types of base, borrow, and subgrade materials from NDOT District 1 shown in Figure 3.1. The most common base material used by NDOT is Type 1 Class B. Six base materials were collected from different projects in District 1. Samples of the borrow materials used on the same contracts were also collected. Table 3.1 summarizes the information on the collected base and borrow materials.

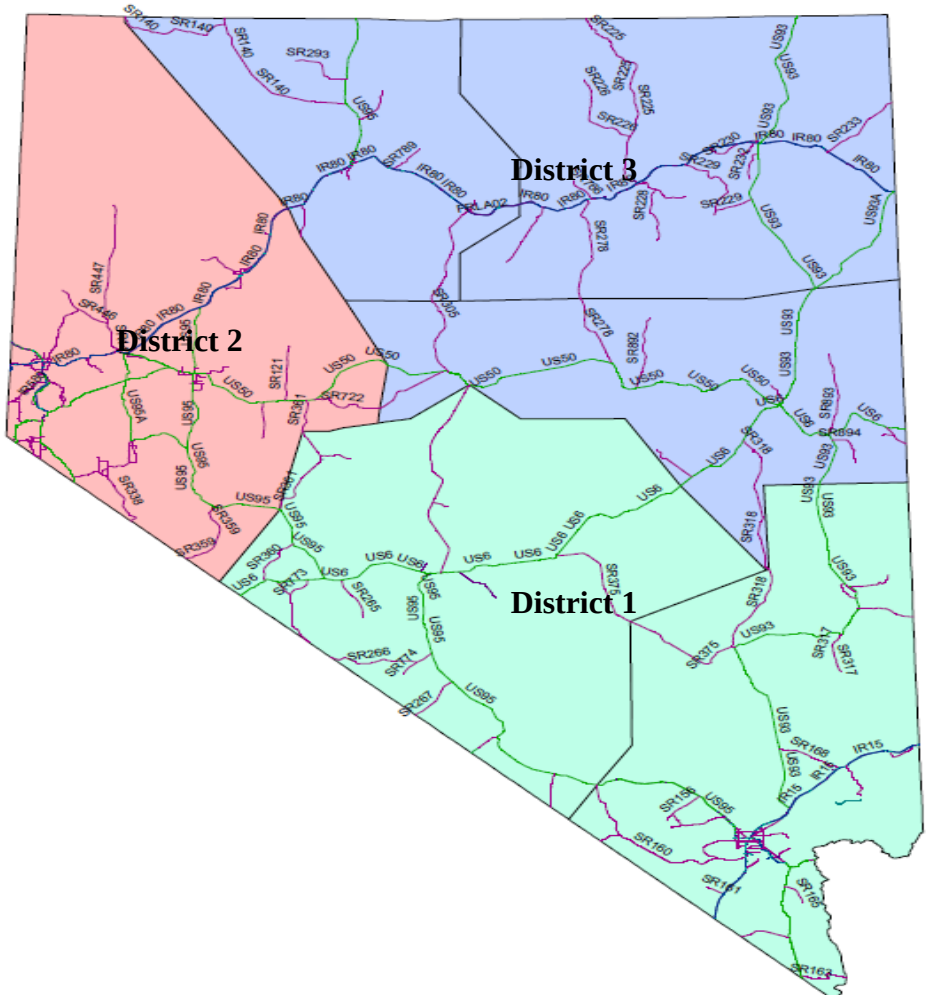

Figure 3.1. NDOT districts boundaries.

Table 3.1. Summary of Collected Base and Borrow Materials from NDOT District 1.

Contract	County	Pit Location	Borrow (bags)	Base (Type 1B) (bags)
3605	CLARK	Sloan Commercial Pit	-	20
3607	Esmeralda	Pit ES 03-08	10	20
3546	CLARK	Apex Pit	10	20
3597	CLARK	Lhoist Pit	10	20
3613	CLARK	Material Pit 69-01	10	20
3583	CLARK	LVP Lone Mountain Pit	10	20

Soils map developed by researchers at Arizona State University was used in to identify the various types of subgrade materials throughout District 1. The types of subgrade materials available under the most mileage of roads in District 1 were identified. Based on this approach, 12 locations were identified as shown in Figure 3.2. The type of existing subgrade with depth was identified at each location as summarized in Table 3.2. Based on the ASU map, the majority of possible subgrade types in NDOT District 1 are; A-1-a, A-1-b, A-2-4 and A-4. In order to cover all four subgrade types, six different locations were selected for sampling at the locations summarized in Table 3.2 and shown in Figure 3.3. The subgrade materials were labeled by the sample number as shown in Table 3.3 along with the amount of materials obtained from each location.

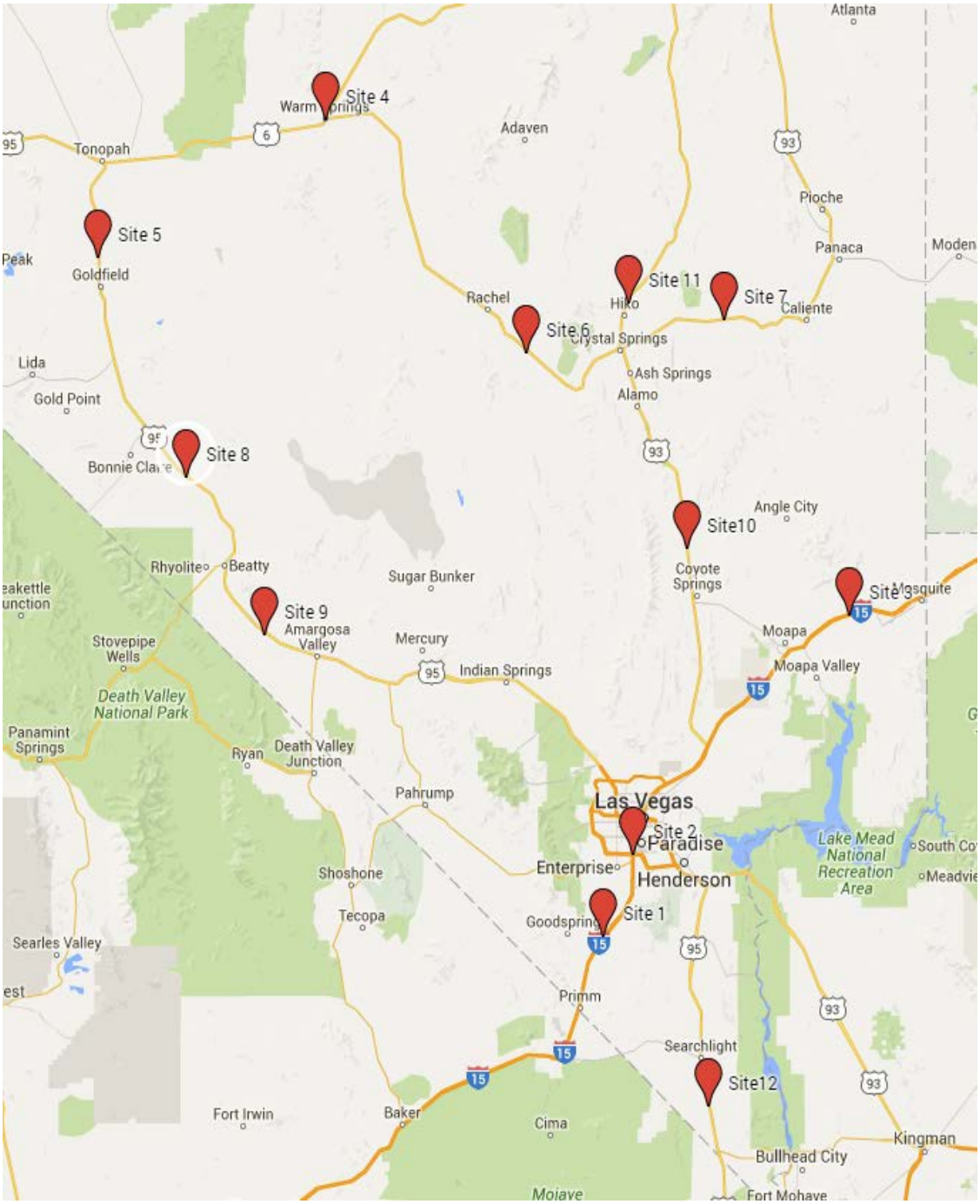

Figure 3.2. Locations considered to identify the subgrade materials.

Table 3.2. Summary of Soil Types in the Selected Locations.

Site	Thickness (inch)	Soil Classification	Latitude (°)	Longitude (°)
1	2.0	A-4	35.8256	115.2970
	5.9	A-4		
2	9.1	A-2-4	36.0657	115.1806
3	2.0	A-2-4	36.7653	114.3457
	16.1	A-4		
	7.9	A-2-4		
4	1.2	A-4	38.1917	116.3685
	19.7	A-6		
	20.1	A-2-6		
	18.9	A-1-a		
5	5.1	A-1-a	37.7967	117.2461
	54.7	A-1-a		
6	9.1	A-2-4	37.4604	115.5078
7	2.0	A-4	37.6185	114.8291
	18.1	A-4		
8	5.9	A-1-b	37.1625	116.9055
	53.9	A-1-b		
9	7.9	A-1-a	36.7103	116.6061
	52.0	A-1-a		
10	2.0	A-4	36.9587	114.9719
	5.1	A-2-4		
11	3.9	A-1-b	37.6653	115.1998
	7.1	A-1-b		
	26.8	A-1-b		
12	7.9	A-5	35.3294	114.8962
	18.1	A-2-4		
	33.9	A-1-b		

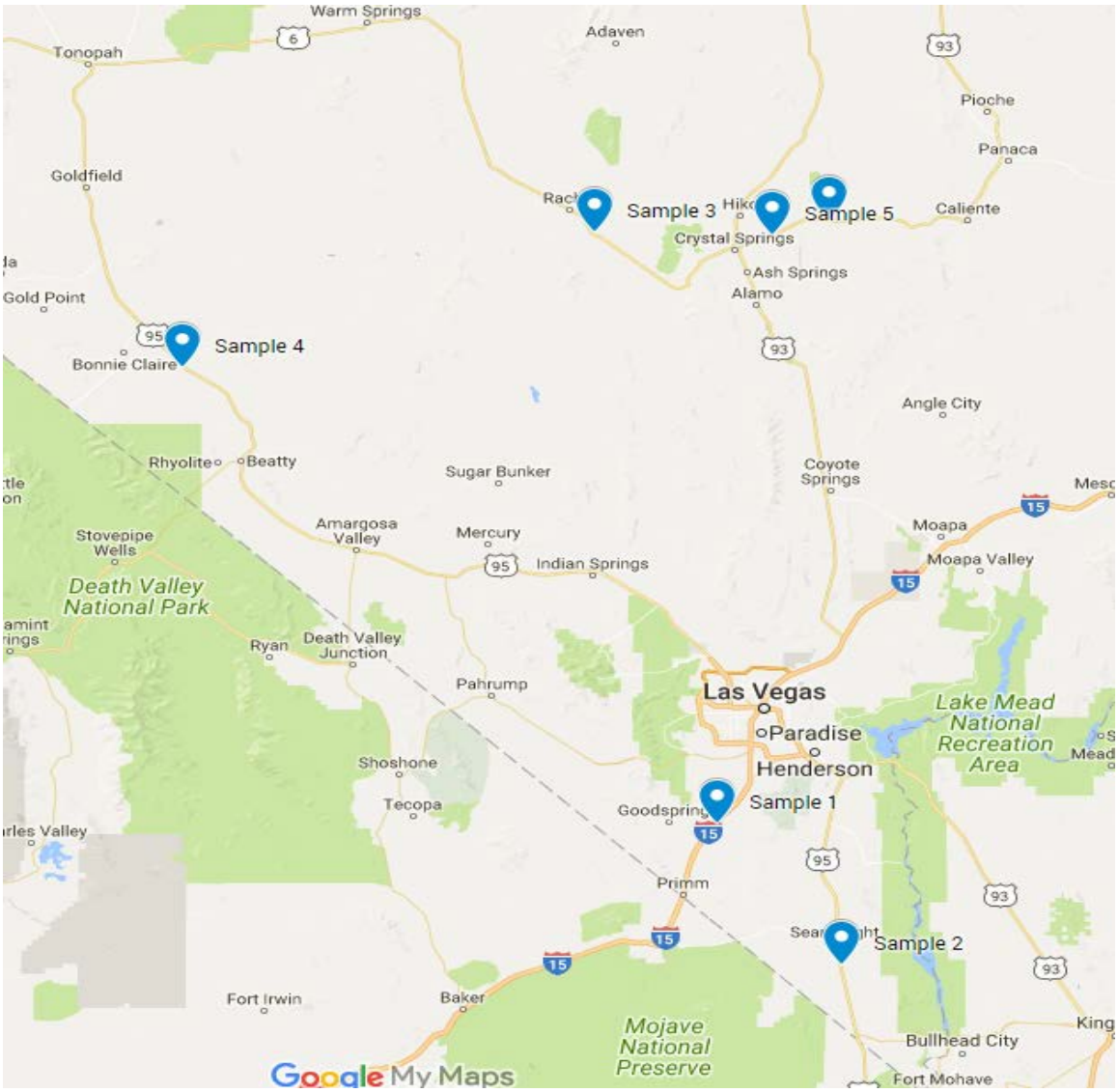

Figure 3.3. Subgrade sample locations.

Table 3.3. Collected Subgrade Materials.

Subgrade Source	NDOT Route/City	Quantity (Bags)
Sample 1	I-15/Goodsprings	10
Sample 2	US-95/Searchlight	10
Sample 3	NV-375/Rachel	10
Sample 4	US-95/Bonnie Claire	10
Sample 5	US-93/Crystal Spring MP62	10
Sample 6	US-93/Crystal Spring MP67	10

Chapter 4. LABORATORY TESTING

This chapter presents the laboratory testing of the base, borrow, and subgrade materials that were sampled from NDOT District 1. The materials were subjected to five groups of laboratory testing: Soil Classification, Moisture-density Relationship, Repeated Load Triaxial Resilient Modulus, Unconfined Compressive Strength, and Resistance Value "R-value". The following sections briefly describe the test methods and presents the data generated from each testing group.

4.1. Soil Classification Testing

The selected materials were classified using particle size analysis and Atterberg limits following both AASHTO and USCS systems which are widely used in practice. The particle size analysis for the aggregate and soil materials was conducted in accordance with NDOT test method Nev.T206 and ASTM D421 and D422 respectively. NDOT test methods Nev. T 210J, T 211J, and T 212J were used to determine the Liquid Limit (LL), Plastic Limit (PL), and Plasticity Index (PI) of the selected materials, respectively. The Materials Division Testing Manual for the NDOT test methods can be found online at (last accessed on February 2018): https://www.nevadadot.com/doing-business/about-ndot/ndot-divisions/operations/materials-section/materials-test-manual.

4.1.1. Particle Size Analysis of Base, Borrow, and Subgrade Materials

Aggregate from base and borrow materials were split into the sample size around 3000g and dried until to a constant weight at a temperature not exceeding 110°C. The dry aggregate was washed over sieve #10 and sieve #200. Retained materials on sieve #10, sieve #200, and washing vessel were transferred into a pan, dried at 110°C, and sieved through a set of sieves in a mechanical sieve shaker. Results of sieve analysis are summarized in Table 4.1 and Figure 4.1 for base materials and in Table 4.2 and Figure 4.2 for borrow materials. All base materials satisfied the NDOT specifications for Type 1 Class B aggregate type.

Materials from subgrade samples were split into the required sample size and dried at 60°C. The dry material was pulverized by using a rubber head hammer. Washing was performed on sieve #10 and poured through sieve #200 until clear water appears. Retained materials on sieve #10 and sieve #200 were carefully transferred in to a pan and dried at a temperature of 60°C. The dry material was pulverized again and sieve analysis was done in a mechanical sieve shaker. The sieve analysis results for the subgrade are summarized in Table 4.3 and Figure 4.3.

Table 4.1. Summary of Sieve Analysis for Base Materials.

Size / mm	% Passing						
	NDOT Spec	Contract No.					
		3546	3583	3597	3605	3613	3607
25.0 mm (1")	80-100	100	100	100	100	100	99.3
19.0 mm (3/4")		96.8	98.1	97.7	90.2	88.9	92.7
12.5 mm (1/2")		76.4	86.7	83.9	66.3	67.8	68.7
9.5 mm (3/8")		62.3	76.3	69.4	54.1	57.6	56.1
4.75 mm (No. 4)	30-65	40.8	45.6	43.4	35.3	38.6	45.4
2.36 mm (No. 8)		27.5	31.2	27.2	25.1	27.9	32.1
2.00 mm (No. 10)		25.2	29.1	24.7	23.3	26.1	28.9
1.18 mm (No. 16)	15-40	19.5	24.4	18.8	19.0	21.6	22.8
0.6 mm (No. 30)		14.9	20.4	14.1	15.0	18.3	17.8
0.425 mm (No. 40)		13.3	19.3	12.6	13.5	17.2	16.0
0.3 mm (No. 50)		12.0	17.0	11.4	12.1	15.8	14.5
0.15 mm (No. 100)		10.3	12.4	9.7	9.9	10.4	12.4
0.075 mm (No. 200)	2-12	8.8	8.7	8.3	7.7	5.3	10.0

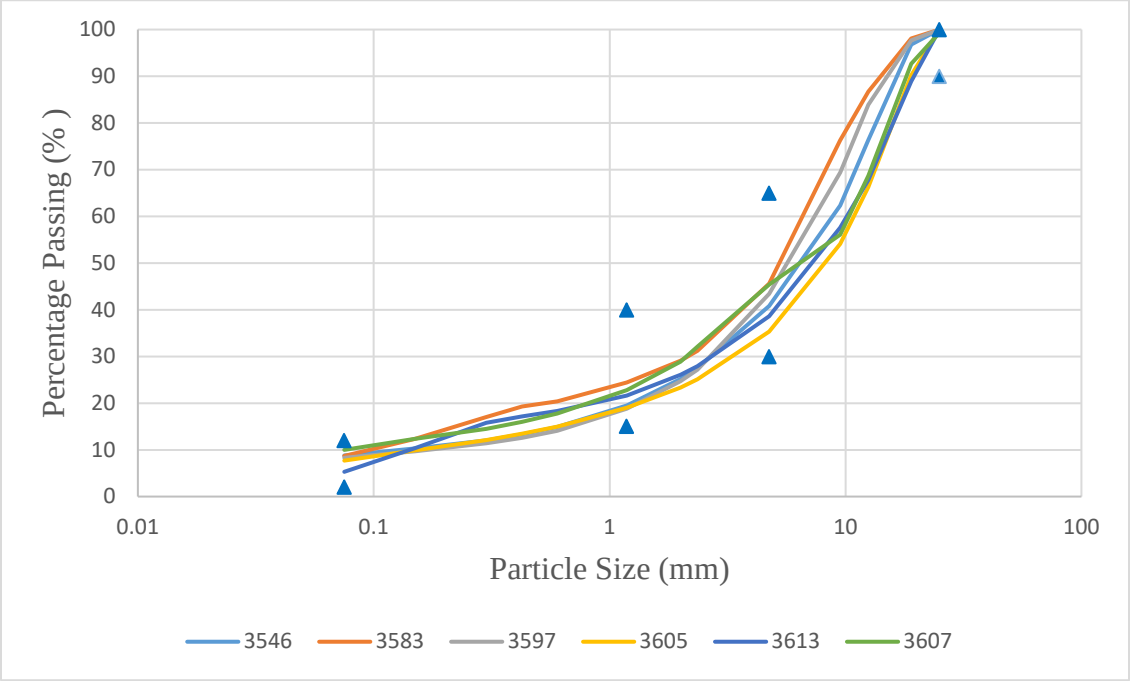

Figure 4.1. Gradation curves for base materials.

Table 4.2. Summary of Sieve Analysis for Borrow Materials.

Size / mm	% Passing					
	NDOT Spec	Contract No.				
		3546	3583	3597	3613	3607
75 mm (3")	100	100	100	100	100	100
50 mm (2")		100	100	100	100	100
37.5 mm (1.5")		100	100	100	97.4	100
25.0 mm (1")		100	99.1	97.7	89.9	98.0
19.0 mm (3/4")		100	95.5	96.0	85.3	94.5
12.5 mm (1/2")		100	92.9	90.2	76.8	89.9
9.5 mm (3/8")		99.9	91.1	85.6	69.8	86.2
4.75 mm (No. 4)		79.9	88.1	71.7	53.3	75.9
2.36 mm (No. 8)		48.6	86.7	56.7	40.8	65.3
2.00 mm (No. 10)		43.0	86.4	53.3	38.1	62.6
1.18 mm (No. 16)		28.6	85.6	42.1	32.4	54.0
0.6 mm (No. 30)		18.4	84.6	32.4	27.9	43.0
0.425 mm (No. 40)		15.4	84.2	28.7	26.3	37.6
0.3 mm (No. 50)		13.3	83.5	25.7	24.0	32.0
0.15 mm (No. 100)		11.4	80.6	20.9	14.3	23.7
0.075 mm (No. 200)		10.5	66.9	16.4	7.3	16.4

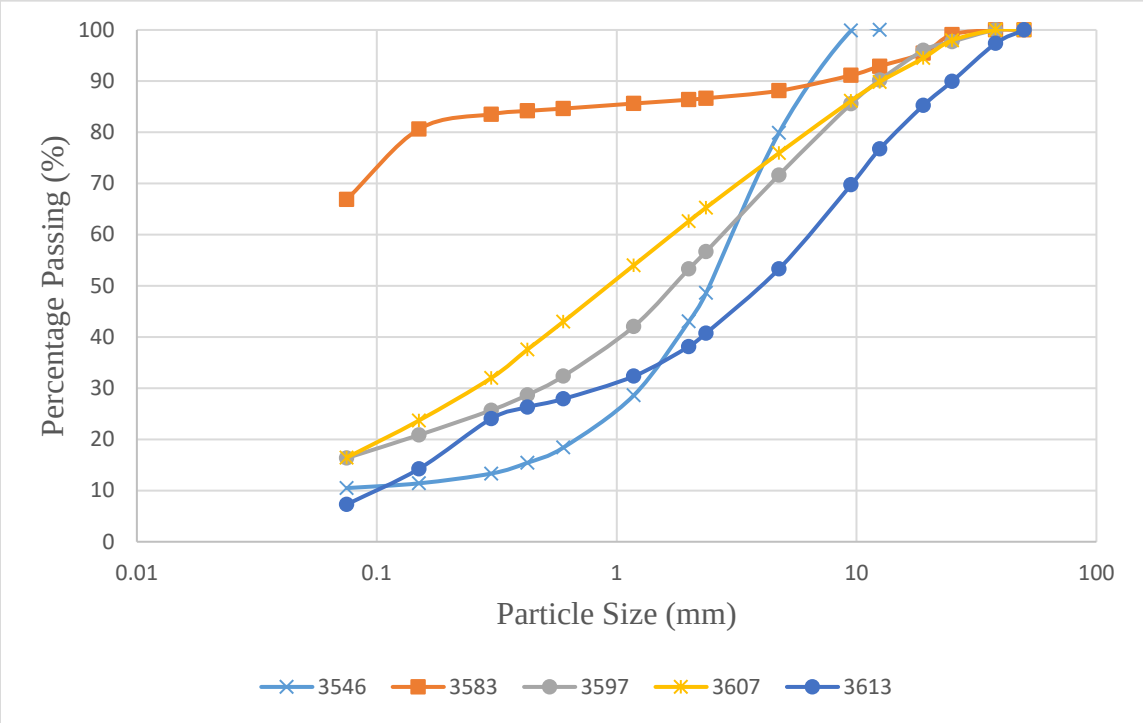

Figure 4.2. Gradation curves for borrow materials.

Table 4.3. Summary of Sieve Analysis for Subgrade Materials.

Size / mm	% Passing					
	Sample Source					
	I-15/ Goodspring	US-95/ Searchlight	NV-375/ Rachel	US-95/ Bonnie Claire	US-93/ Crystal Spring MP62	US-93/ Crystal Spring MP67
50.0 mm (2")	97.5	100	100	100	100	100
25.0 mm (1")	83.5	96.7	87.5	98.8	100	100
9.5 mm (3/8")	57.2	92.7	52.2	95.4	99.3	97.2
4.75 mm (No. 4)	43.4	87.8	33.5	92	95.6	89.3
2.00 mm (No. 10)	34.4	68.7	23.2	84.3	81.4	77.2
0.425 mm (No. 40)	28	43.9	15.2	37.6	44.5	52.6
0.3 mm (No. 50)	26.6	39.3	13.4	25.2	37.1	46.7
0.15 mm (No. 100)	22.6	31.5	9.6	11.7	25.5	35.7
0.075 mm (No. 200)	14.6	23.9	5.4	5.5	18.1	26

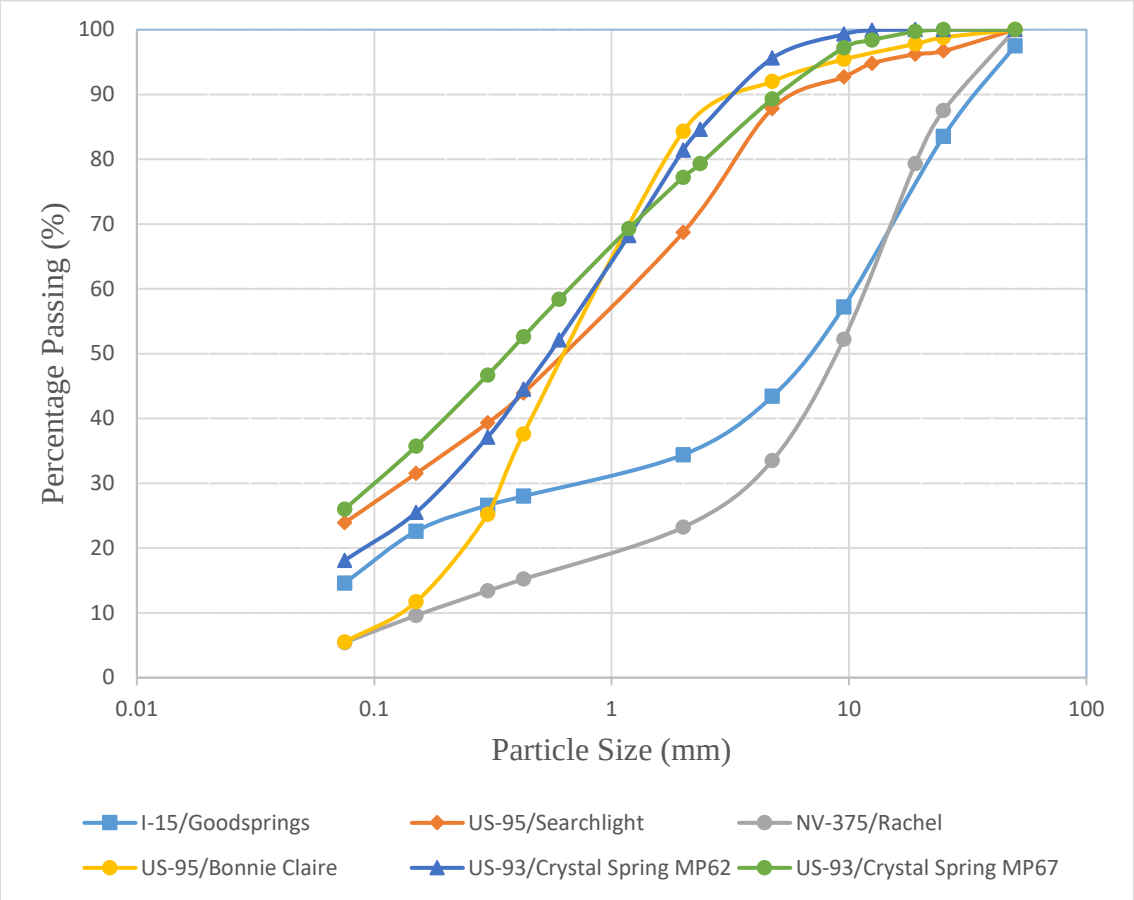

Figure 4.3. Gradation curves for subgrade materials.

4.1.2. Atterberg Limits

Liquid limit and plastic limit are often referred to as “Atterberg Limits.” Based on its moisture content, soil can be in the state of liquid, plastic, semi-solid, or solid. Liquid limit is the moisture content at which the soil transforms from plastic to liquid. Plastic limit is the moisture content at which the soil transforms from semi-solid to plastic. Liquid limit and plastic limit tests were conducted according to NDOT test method Nev. T 210J and T 211J, respectively. The plasticity index was then calculated as the numerical difference between the liquid limit and the plastic limit of the soil following NDOT test method Nev. T 212J.

A representative sample with minimum weight of 150g was obtained from passing sieve #40. Moisture was added and mixed until a uniform color is achieved. For the liquid limit test, the Casagrande apparatus was used to determine the number of blows to close the 13mm groove. The moisture content was changed in order to obtain three sets of number of blows in the range of; 25-35, 20-30, and 15-25. Around 8 grams of soil from the 25-35 was used for the plastic limit test. The sample was divided into 1.5-2 g portion and rolled on a glass plate until it forms a 3mm thread. This process was continued until the thread crumbles at which the moisture content was obtained. Figure 4.4 shows the apparatus and tools used for the liquid limit and plastic limit tests.

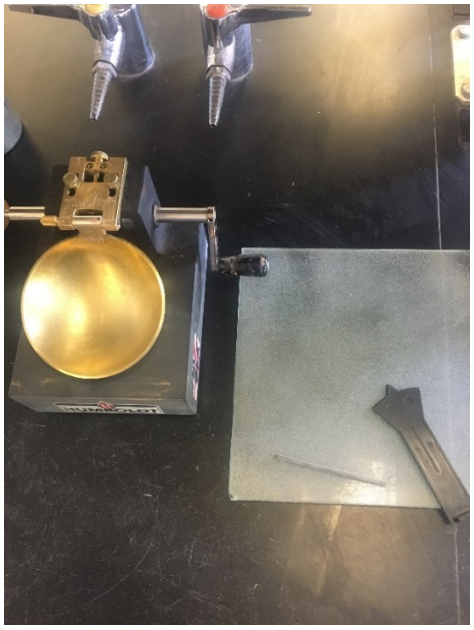

Figure 4.4. Atterberg limits test apparatus and tools.

The moisture content of the sample which gives 25 blows to close the groove by 13 mm is considered as the liquid limit. All base materials were classified as non-plastic indicating that the plastic limit was not defined. Figure 4.5 shows at typical liquid limit plot for subgrade. The summary of the Atterberg limits for the borrow and subgrade materials are shown in Table 4.4 and Table 4.5, respectively.

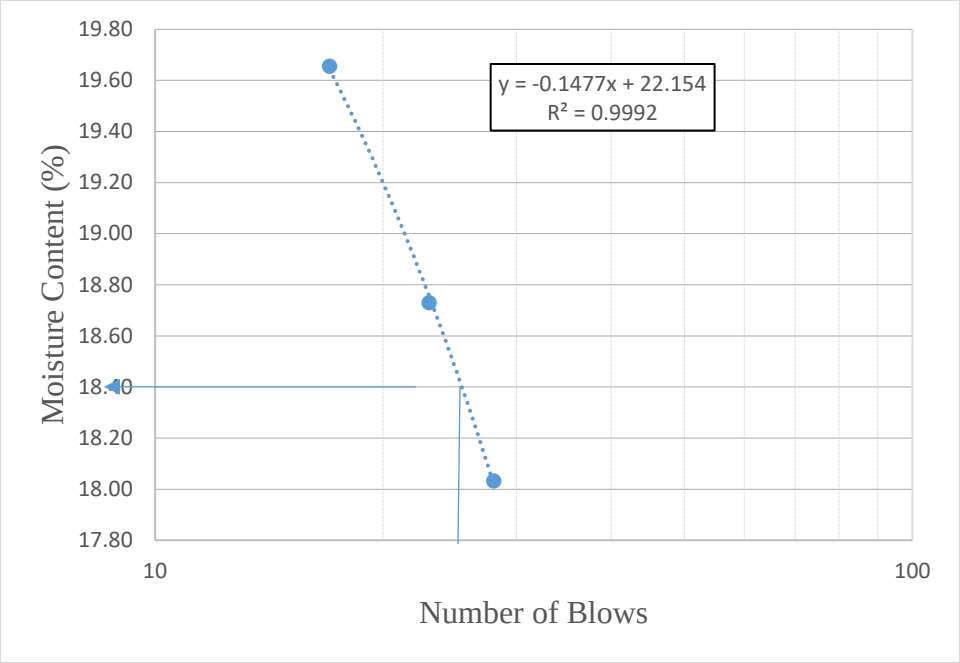

Figure 4.5. Liquid limit test results for subgrade (I-15/Goodsprings).

Table 4.4. Summary of Atterberg Limits for Borrow Materials.

Contract No.	Liquid Limit	Plastic Limit	Plasticity Index
3546	16.5	14.5	2.0
3583	23.5	18.8	4.7
3597	22.2	18.9	3.3
3607	23.2	23.1	0.1
3613	N/A	NP	0

Table 4.5. Summary of Atterberg Limits for Subgrade Materials.

Soil Source	Liquid Limit (%)	Plastic Limit (%)	Plasticity Index
I-15/Goodsprings	18.4	16.9	1.5
US-95/Searchlight	N/A	NP	0
NV-375/Rachel	30.9	26.6	4.3
US-95/Bonnie Claire	21.1	20.1	1
US-93/Crystal Spring MP62	19.6	17.7	1.9
US-93/Crystal Spring MP67	22.2	17.8	4.5

4.1.3. Soil Classification

The classifications of the subgrade materials were done according to AASHTO and USCS methods. Liquid limit, plasticity index, and particle size distribution were used for the classification process. The AASHTO classification method (AASHTO M 145) is presented in

Table 4.6 and Table 4.7 summarizes the AASHTO classification of the subgrade materials. The USCS classification method (ASTM -2487) is presented in Table 4.8 and Table 4.7 summarizes the UCS classification of the subgrade materials.

Table 4.6. AASHTO Soil Classification Method.

General Classification	Granular Materials (35 Percent or Less Passing 75 µm)						
	A-1			A-2			
Group Classification	A-1-a	A-1-b	A-3	A-2-4	A-2-5	A-2-6	A-2-7
Sieve analysis, percent passing:							
2.00 mm (No. 10)	50 max	—	—	—	—	—	—
0.425 mm (No. 40)	30 max	50 max	51 min	—	—	—	—
75 µm (No. 200)	15 max	25 max	10 max	35 max	35 max	35 max	35 max
Characteristics of fraction passing 0.425 mm (No. 40):							
Liquid limit	—		—	40 max	41 min	40 max	41 min
Plasticity index	6 max		NP	10 max	10 max	11 min	11 min
Usual types of significant constituent materials	Stone fragments, gravel and sand		Fine sand	Silty or clayey gravel and sand			
General rating as subgrade	Excellent to Good						

Table 4.7. Classification of Subgrade Materials with AASHTO and UCS Methods.

Classification Method	I-15/ Goodspring	US-95/ Searchlight	NV-375/ Rachel	US-95/ Bonnie Claire	US-93/ Crystal Spring MP62	US-93/ Crystal Spring MP67
AASTHO	A-1-a	A-1-b	A-1-a	A-1-b	A-1-b	A-2-4
USCS	GM	SM	GP-GM	SW-SM	SM	SC

Table 4.8. Unified Soil Classification Method.

Criteria for Assigning Group Symbols and Group Names Using Laboratory Tests[A]				Soil Classification	
				Group Symbol	Group Name[B]
COARSE-GRAINED SOILS	Gravels (More than 50 % of coarse fraction retained on No. 4 sieve)	Clean Gravels (Less than 5% fines[C])	Cu≥4 and 1≤Cc ≤3[D]	GW	Well-graded gravel[E]
			Cu<4 and/or [Cc<1orCc>3][D]	GP	Poorly graded gravel[E]
		Gravels with Fines (More than 12 % fines[C])	Fines classify as ML or MH	GM	Silty gravel[E,F,G]
			Fines classify as CL or CH	GC	Clayey gravel[E,F,G]
More than 50% retained on No. 200 sieve	Sands (50% or more of coarse fraction passes No. 4 sieve)	Clean Sands (Less than 5% fines[H])	Cu≥6 and 1≤Cc ≤3[D]	SW	Well-graded sand[I]
			Cu<6 and/or [Cc<1orCc>3][D]	SP	Poorly graded sand[I]
		Sands with Fines (More than 12 % fines[H])	Fines classify as ML or MH	SM	Silty sand[F,G,I]
			Fines classify as CL or CH	SC	Clayey sand[F,G,I]
FINE-GRAINED SOILS	Silts and Clays Liquid limit less than 50	inorganic	PI>7 and plots on or above "A" line[J]	CL	Lean clay[K,L,M]
			PI<4 or plots below "A" line[J]	ML	Silt[K,L,M]
		organic	Liquid limit−oven dried / Liquid limit−not dried < 0.75	OL	Organic clay[K,L,M,N] Organic silt[K,L,M,O]
50% or more passes the No. 200 sieve	Silts and Clays Liquid limit 50 or more	inorganic	PI plots on or above "A" line	CH	Fat clay[K,L,M]
			PI plots below "A" line	MH	Elastic silt[K,L,M]
		organic	Liquid limit−oven dried / Liquid limit−not dried < 0.75	OH	Organic clay[K,L,M,P] Organic silt[K,L,M,Q]
HIGHLY ORGANIC SOILS	Primarily organic matter, dark in color, and organic odor			PT	Peat

4.2. Moisture-Density Relationship (T 108B)

Compaction is the densification process of the material by applying mechanical energy. As the moisture content increases, water particles fill the air voids and increase the density of the material. This densification process occurs up to a certain moisture content, after which any additional water will displace the solid particles leading to reduction in the density. The corresponding moisture content at the maximum density is labeled as the optimum moisture content (OMC).

The moisture-density relationships for the various selected materials were established and the optimum moisture content corresponding to the maximum dry unit weight were identified in accordance with NDOT test method Nev. T108B. For method A, a 4 inch diameter sample was compacted in five equal lifts with 25 blows in each lift. For method B, a 6 inch diameter mold was compacted in five equal lifts with 54 blows in each lift. Both compaction methods used a 10 lb rammer with an 18 inch drop. Top lift was compacted with an extension collar and sample was trimmed to the mold surface level. Two moisture content samples were taken; one near top and one near bottom of compacted sample. Typical moisture-density curves are shown in Figure 4.6, Figure 4.7, and Figure 4.8. Summaries of the moisture density test results for the base, borrow, and subgrade materials are summarized in Table 4.9, Table 4.10, and Table 4.11, respectively.

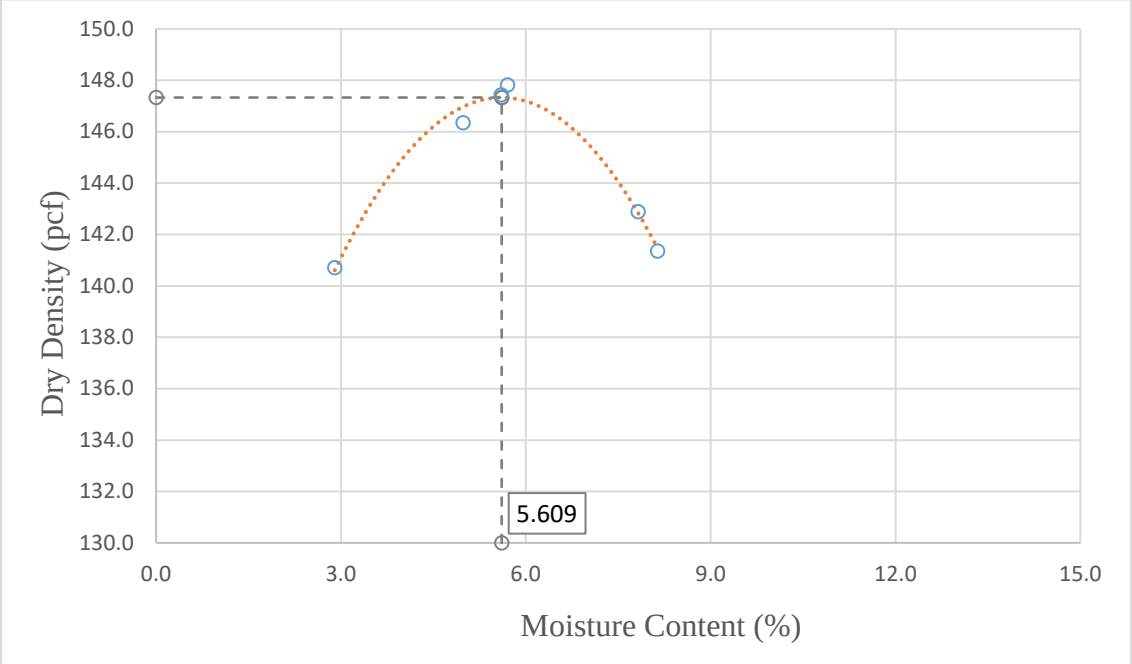

Figure 4.6. Moisture-density curve for base material (contract 3583).

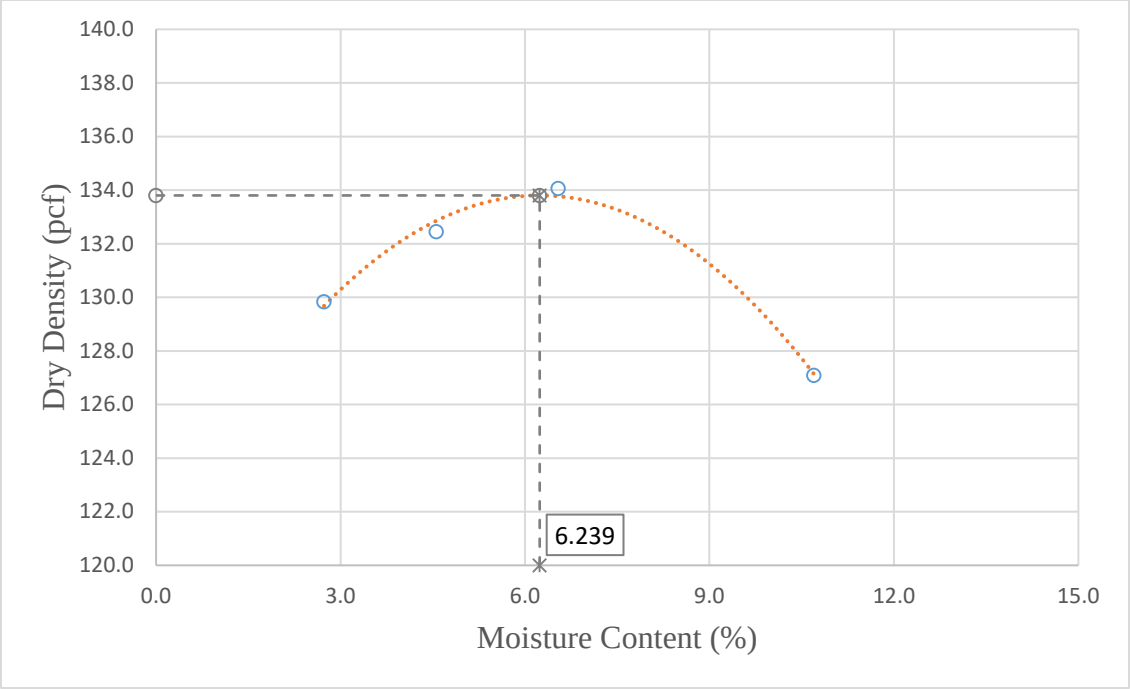

Figure 4.7. Moisture-density curve for borrow materials (contract 3597).

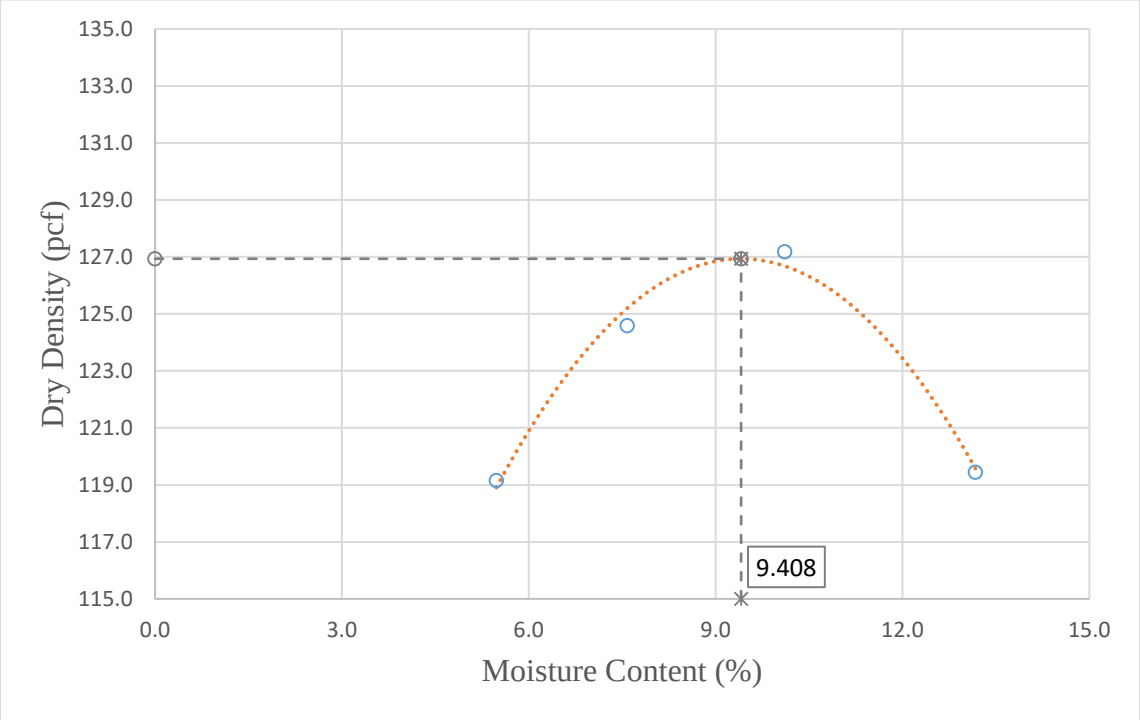

Figure 4.8. Moisture-density curve for subgrade materials (US-93/Bonnie Claire).

Table 4.9. Summary of Moisture-Density Test Results for Base Materials.

Contract No.	Max Dry Density (pcf)	OMC (%)
3546	144.7	5.0
3583	147.3	5.6
3597	143.0	3.9
3605	147.5	5.0
3607	135.8	6.7
3613	141.6	3.5

Table 4.10 Summary of Moisture-Density Test Results for Borrow Materials.

Contract No.	Max Dry Density (pcf)	OMC (%)
3546	136.9	7.2
3583	119.4	10.7
3597	133.8	6.2
3607	125.6	11.3
3613	143.2	5.4

Table 4.11. Sumarry of Moisture-Density Test Results for Subgrade Materials.

Subgrade Source	Max Dry Density (pcf)	OMC (%)
I-15/Goodsprings	134.9	6.3
US-95/Searchlight	133.3	6.6
NV-375/Rachel	139.2	6.1
US-95/Bonnie Claire	126.9	9.4
US-93/Crystal Spring MP62	122.4	9.8
US-93/Crystal Spring MP67	123.8	9.3

4.3. Resilient Modulus Testing

Resilient modulus is an important parameter in the pavement design which represents the stress-dependent stiffness of the base, borrow, and subgrade materials under a certain pattern of repeated loading and confinement stress level using a triaxial set-up. AASHTO T 307 is the most commonly used test for Mr of unbound materials (i.e. 22 out of 30 agencies/DOTs). Therefore, AASHTO T 307 standard procedure was followed for determining the Mr of the sampled materials. The loading pattern for the Mr test consists of a repeated axial cyclic stress of fixed amplitude with a loading duration of 0.1 second followed by a rest period of 0.9 second. The AASHTO standard stipulates detailed testing procedures for unbound materials, which include loading sequences, confining pressures, maximum axial stresses, cyclic stresses, constant stresses, and the number of loading applications. Overall, base materials are subjected to higher stresses during the testing than the subgrade soils despite the similarities in the testing sequences. The loading sequence for the base and borrow materials is presented in Table 4.12 and the loading sequence for the subgrade materials is summarized in Table 4.13.

Table 4.12. Testing Sequence for Base and Subbase Materials.

Sequence No.	Confining Pressure (psi)	Max. Axial Stress (psi)	Cyclic Stress (psi)	Contact Stress (psi)	No. of Load Application
0	6	4	3.6	0.4	500-1000
1	6	2	1.8	0.2	100
2	6	4	3.6	0.4	100
3	6	6	5.4	0.6	100
4	6	8	7.2	0.8	100
5	6	10	9.0	1.0	100
6	4	2	1.8	0.2	100
7	4	4	3.6	0.4	100
8	4	6	5.4	0.6	100
9	4	8	7.2	0.8	100
10	4	10	9.0	1.0	100
11	2	2	1.8	0.2	100
12	2	4	3.6	0.4	100
13	2	6	5.4	0.6	100
14	2	8	7.2	0.8	100
15	2	10	9.0	1.0	100

Table 4.13. Testing Sequence for Subgrade Materials.

Sequence No.	Confining Pressure (psi)	Max. Axial Stress (psi)	Cyclic Stress (psi)	Contact Stress (psi)	No. of Load Application
0	15	15	13.5	1.5	500-1000
1	3	3	2.7	0.3	100
2	3	6	5.4	0.6	100
3	3	9	8.1	0.9	100
4	5	5	4.5	0.5	100
5	5	10	9.0	1.0	100
6	5	15	13.5	1.5	100
7	10	10	9.0	1.0	100
8	10	20	18.0	2.0	100
9	10	30	27.0	3.0	100
10	15	10	9.0	1.0	100
11	15	15	13.5	1.5	100
12	15	30	27.0	3.0	100
13	20	15	13.5	1.5	100
14	20	20	18.0	2.0	100
15	20	40	36.0	4.0	100

4.3.1. Sample Preparation

According to AASTHO T 307, the minimum diameter of the sample must be five times the maximum particle size. In this testing a 4 inch dimeter and 8 inch height mold was used and particles exceeding the limit were scalped. All samples were prepared at optimum moisture content and 90% of the maximum dry unit weight. The required amount of material was calculated based on the volume of the mold and dry density. The OMC was added to the material and kept in the sealed plastic bag for 16 – 48 hours. A vibratory compactor was used for the compaction as shown in Figure 4.9. The specimens were compacted in six lifts of equal mass. After compaction, the sample was extruded and a membrane was installed immediately. Figure 4.10 shows the sample after extrusion and Figure 4.11 shows the membrane installed on the sample. Porous stones with filter papers were placed at the top and bottom of the sample with membrane. Finally, the sample with membrane and porous stones was sealed very carefully by using an 'O' ring.

Figure 4.9. Vibratory compactor and sample mold.

Figure 4.10. Extruded compacted sample.

Figure 4.11. Compacted sample with membrane, porous stones and O-rings.

4.3.2. Testing

The prepared sample was carefully installed inside the triaxial chamber. The drainage valves connected to the top and bottom of the samples and a vacuum pressure was applied through the drainage vales to make sure there was no leakage. Figure 4.12 shows the sample inside the chamber after vacuum was applied. LVDT's were mounted in the outside of the chamber and connected to the load cell to measure the axial deformation of the sample as shown in Figure 4.13. The loading protocol for the base, borrow and subgrade materials was controlled by the software. Frequent manual checks were made to confirm that the machine was applying the correct cyclic stress, confinement, and contact stress.

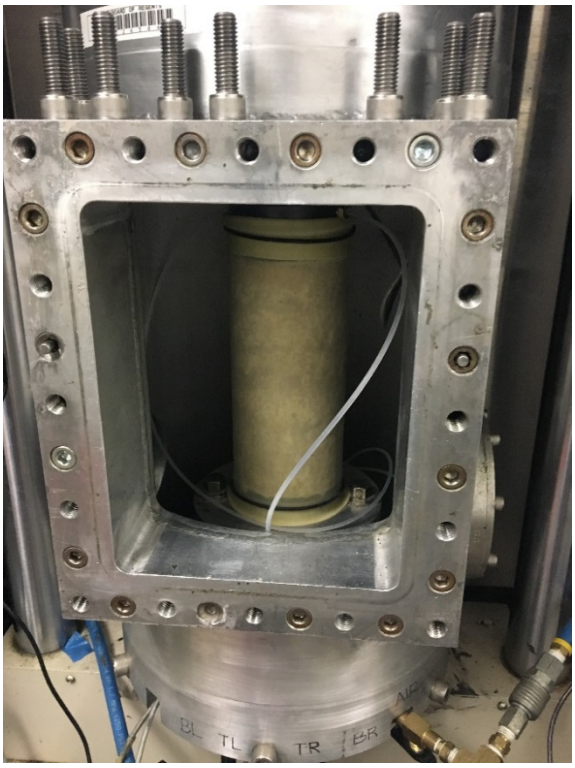

Figure 4.12. Sample inside the triaxial chamber.

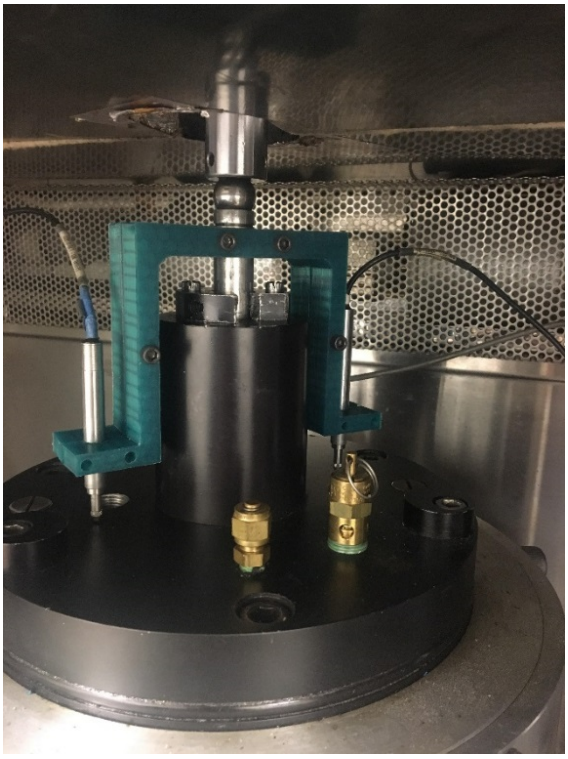

Figure 4.13. LVDT's connected on the outside of the triaxial chamber.

4.3.3. Development of Mr Models

The results of the triaxial testing of the base, borrow, and subgrade materials were used to develop the non-linear models that relate the Mr to the stress conditions. For the base and borrow materials, the Theta model (25) was used to represent the stress-hardening behavior. For the subgrade material the Uzan and the Universal models (26) were used. The constitutive model equations are given below.

$$\text{Theta Model:} \quad M_R = K\theta^n \tag{27}$$

Where;

K and n: regression coefficients
θ: bulk stress, psi

$$\text{Uzan Model} \quad M_R = K\theta^n\sigma_d^m \tag{28}$$

Where;

K, m: regression coefficients
σ_d: deviator stress, psi

$$\text{Universal Model} \quad M_r = k_1 p_a \left(\frac{\theta}{p_a}\right)^{k_2} \left(\frac{\tau_{oct}}{p_a} + 1\right)^{k_3} \tag{29}$$

Where;

k_1, k_2, k_3: regression coefficients
P_a: atmospheric pressure, psi
τ_{oct}: octahedral shear stress, psi

Resilient modulus value was obtained from the average value of the last five cycles for each sequence. The method of least squares in Microsoft Excel was used to develop the regression coefficients in the constitutive models. Table 4.14 presents typical data from the testing of a base sample and the necessary input parameters for the regression analysis. The Theta model showed good correlation for the base and borrow materials as shown in Figure 4.14 and Figure 4.15. Both the Universal and Uzan models showed good correlations for the subgrade materials as shown in Figure 4.16 and Figure 4.17, respectively. The constitutive model regression parameters for the base, borrow and subgrade materials are summarized in Table 4.15, Table 4.16, and Table 4.17, respectively. One of the borrow material's (Contract 3583) constitutive model was similar to subgrade material. The variation of resilient modulus with different state of stress for the base, borrow, and subgrade materials are presented in Figure 4.18, Figure 4.19, and Figure 4.20, respectively.

Table 4.14. Summary of Resilient Modulus Test Results for Base Material (Contract 3546).

Sequence	Cyclic Axial Stress (psi)	Contact Stress (psi)	Confine Stress (psi)	Axial Resilient Modulus (psi)	Deviator Stress, σ_d (psi)	Major Principal Stress, σ_1 (psi)	Minor Principal Stress, σ_3 (psi)	Bulk Stress, θ (psi)	Octahedral Shear Stress (psi)
1	13.5	1.5	14.8	46,385	15.0	29.8	14.8	59.5	7.1
2	2.7	0.3	2.8	22,854	3.0	5.8	2.8	11.4	1.4
3	5.3	0.6	2.8	23,661	5.9	8.8	2.8	14.4	2.8
4	8.1	0.9	2.8	25,371	9.0	11.8	2.8	17.5	4.2
5	4.5	0.5	4.8	25,231	5.0	9.9	4.8	19.5	2.4
6	9.0	1.0	4.8	28,698	10.0	14.8	4.8	24.4	4.7
7	13.5	1.5	4.8	30,357	15.0	19.9	4.8	29.5	7.1
8	9.0	1.0	9.8	35,372	10.0	19.8	9.8	39.4	4.7
9	18.0	2.0	9.8	41,542	20.0	29.8	9.8	49.5	9.4
10	26.8	3.0	9.8	43,812	29.8	39.7	9.8	59.3	14.1
11	9.0	1.0	14.8	39,750	10.0	24.8	14.8	54.5	4.7
12	13.5	1.5	14.8	43,625	15.0	29.8	14.8	59.4	7.1
13	26.8	3.0	14.8	49,674	29.8	44.6	14.8	74.3	14.0
14	13.7	1.5	19.8	49,374	15.2	35.0	19.8	74.6	7.1
15	18.1	2.0	19.8	53,101	20.1	39.9	19.8	79.6	9.5
16	34.6	4.0	19.8	59,304	38.6	58.4	19.8	98.0	18.2

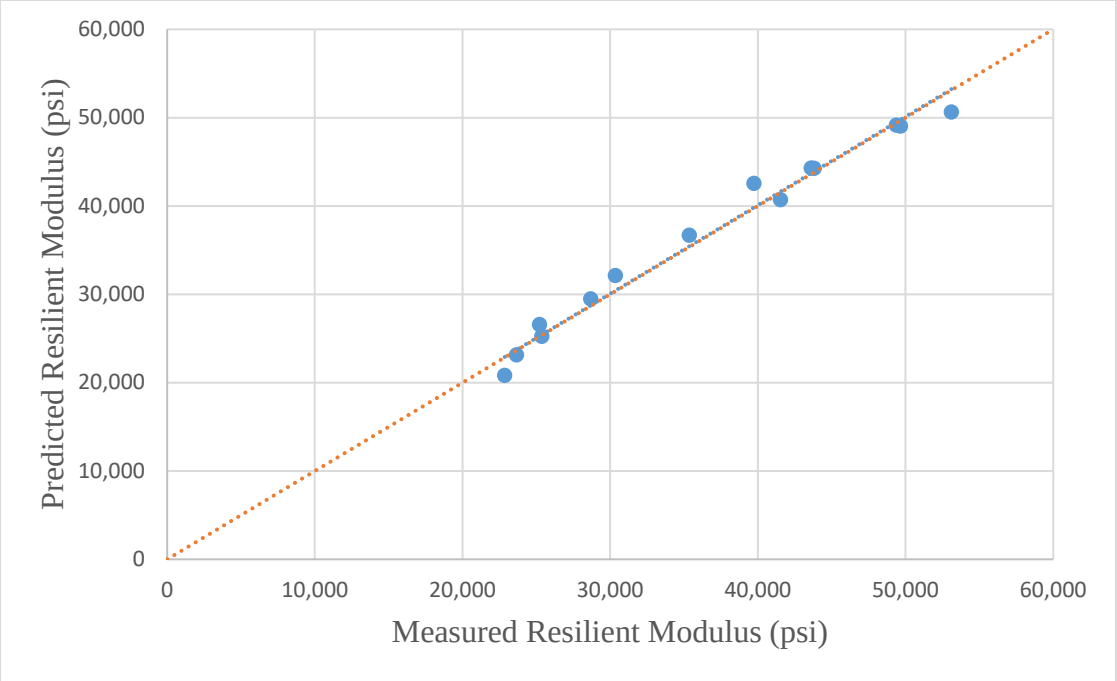

Figure 4.14. Theta model for base material (contract 3546).

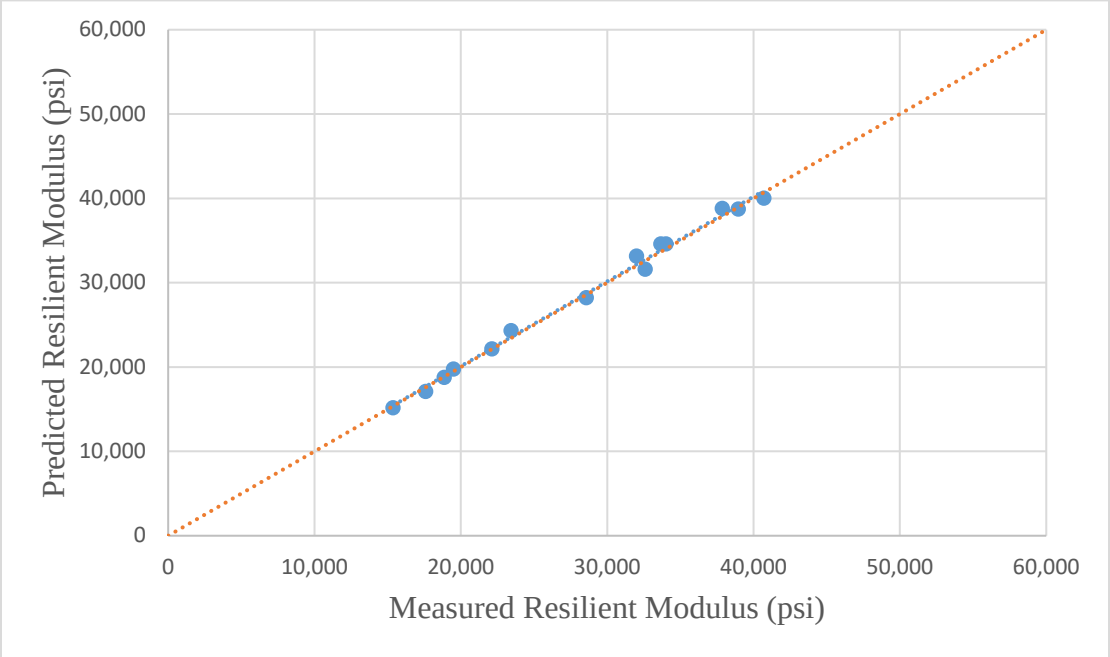

Figure 4.15. Theta model for borrow material (contract 3546).

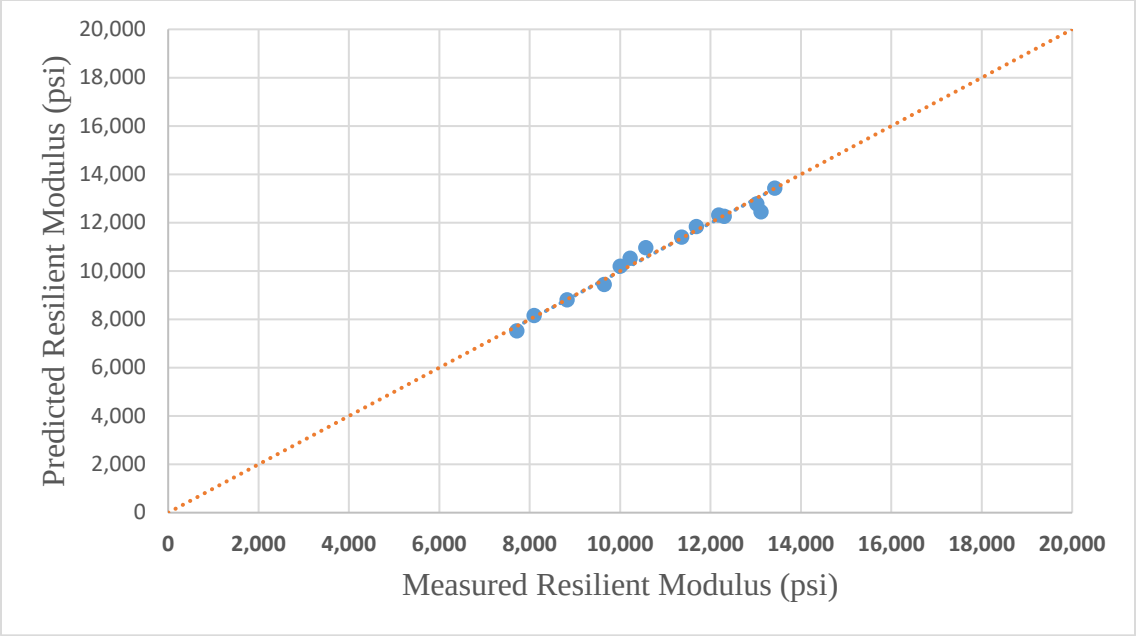

Figure 4.16. Uzan model for subgrade (US-93/Crystal Spring MP62).

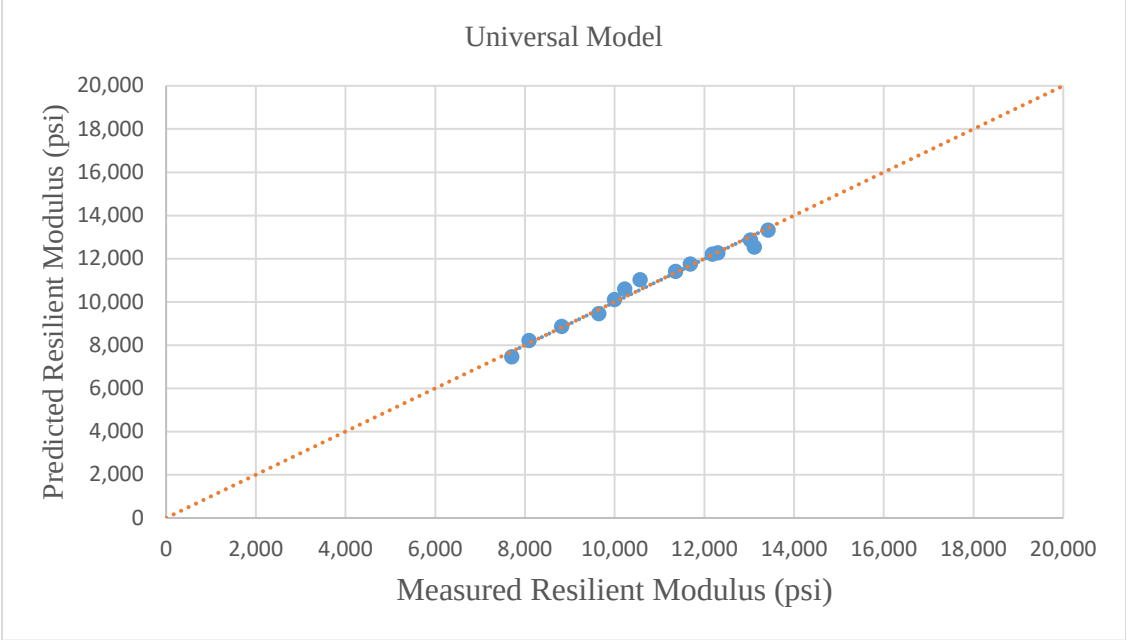

Figure 4.17. Universal model for subgrade (US-93/Crystal Spring MP62).

Table 4.15. Regression Coefficients of Mr Model for Base Materials.

Model	Regression Coefficient	Contract Number					
		3546	**3583**	**3605**	**3607**	**3613**	**3597**
Theta	K	6808	5806	3818	3497	5257	5806
	n	0.4585	0.4423	0.5492	0.5770	0.4722	0.4782

Table 4.16. Table 16. Regression Coefficients of Mr Model for Borrow Materials.

Model	Regression Coefficient	Contract Number		
		3546	**3613**	**3597**
Theta	K	4514	4610	5534
	n	0.4990	0.4980	0.4379

Table 4.17 Regression Coefficients of Mr Model for Subgrade Materials.

Soil Source	Universal Model			Uzan Model		
	k_1	k_2	k_3	k	n	m
I-15/Goodsprings	1126	0.4538	-0.2688	4938	0.4547	-0.0356
US-95/Searchlight	971	0.4322	-0.5369	4797	0.4147	-0.0695
NV-375/Rachel	1041	0.5011	-0.2569	4030	0.5023	-0.0364
US-95/Bonnie Claire	748	0.3842	-0.2786	3949	0.3863	-0.0382
US-93/Crystal Spring MP62	742	0.5087	-0.4097	2837	0.5087	-0.055
US-93/Crystal Spring MP67	989	0.4009	-0.7937	5136	0.397	-0.1085
3583 Borrow	811	0.4418	-0.8092	4377	0.5278	-0.3195

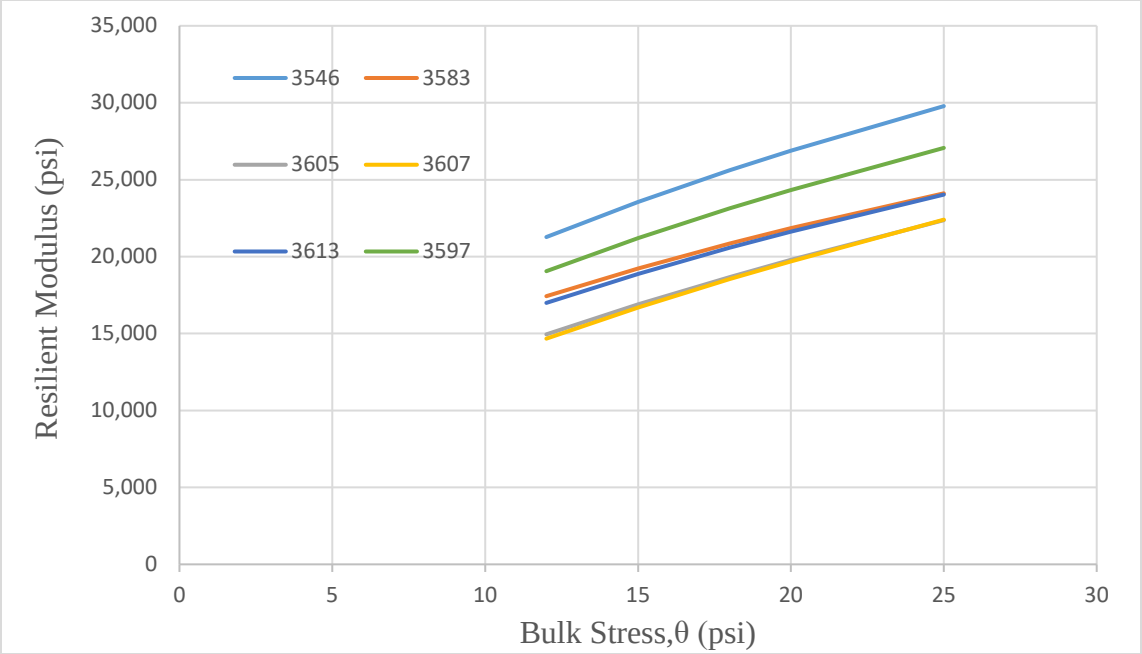

Figure 4.18. Variation of resilient modulus of base materials with bulk stress.

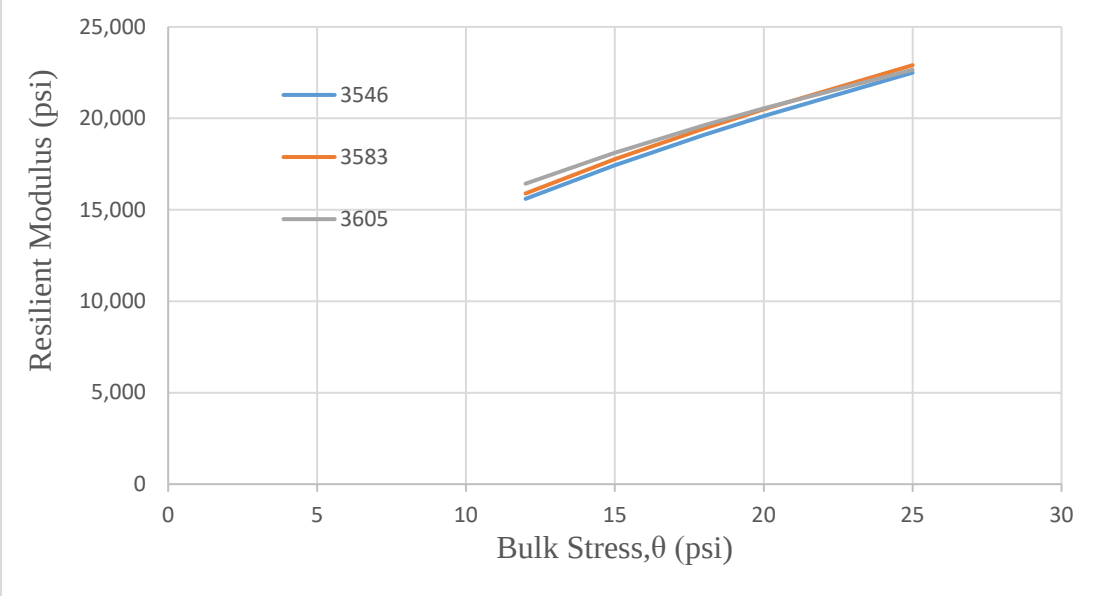

Figure 4.19. Variation of resilient modulus of borrow materials with bulk stress.

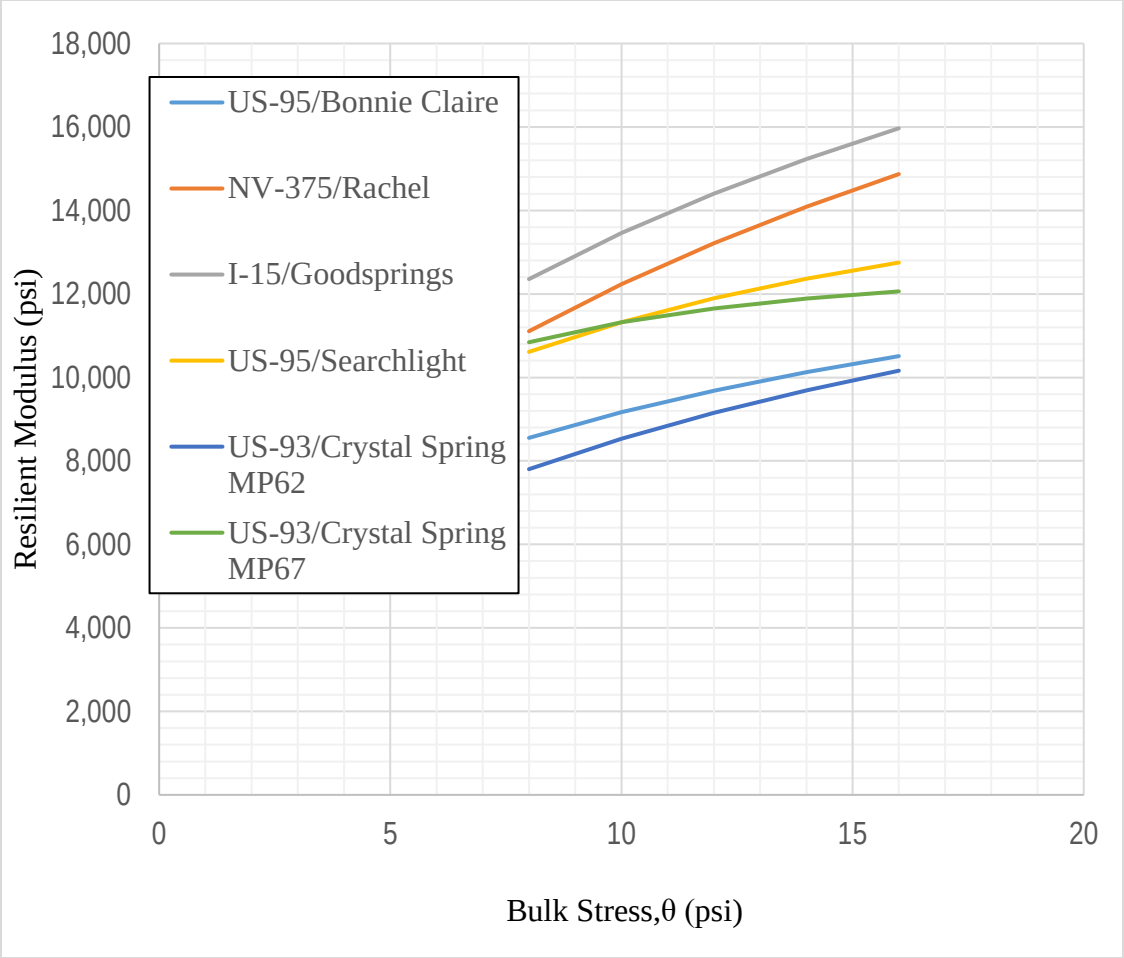

Figure 4.20. Variation of resilient modulus of subgrade materials with bulk stress.

4.4. Unconfined Compressive Strength

the unconfined compressive strength (UCS) tests were conducted in accordance with AASHTO T 208. The continuous stress-strain responses were recorded to produce a complete stress-strain diagram. As was discovered in the literature review, the inclusion of the stress-strain parameters may significantly improve the correlation.

Samples were prepared at the optimum moisture content and maximum dry density with the vibratory compactor. A 6 inch diameter and 12 inch height mold was used to meet the requirement of; maximum particles size has to be smaller than one-sixth of the specimen diameter. Tests were conducted at a strain rate between 0.2 and 2 percent per minute. Two replicates were tested for each source of material. Figure 4.21 shows and extruded sample and Figure 4.22 shows the sample after testing is completed. Typical UCS stress-strain curves are shown in Figure 4.23, Figure 4.24, and Figure 4.25 for base, borrow, and subgrade materials, respectively. Table 4.18 summarizes the unconfined compressive strength properties for the base, borrow, and subgrade materials.

Figure 4.21. Extruded UCS sample.

Figure 4.22. Sample after the UCS test.

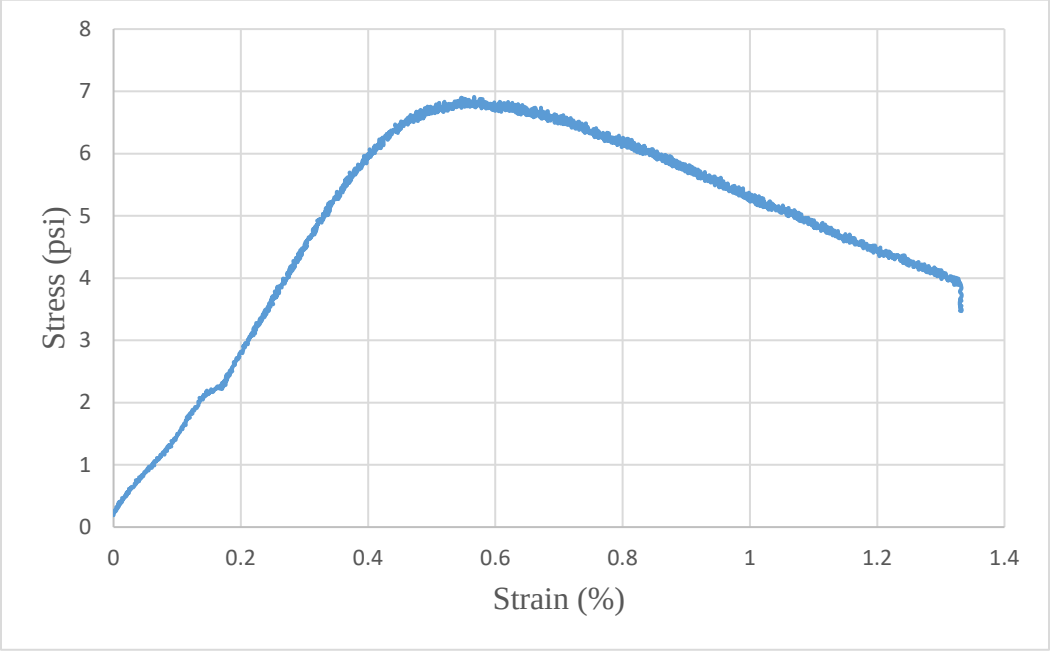

Figure 4.23. UCS stress-strain curve for base materials (contract 3583).

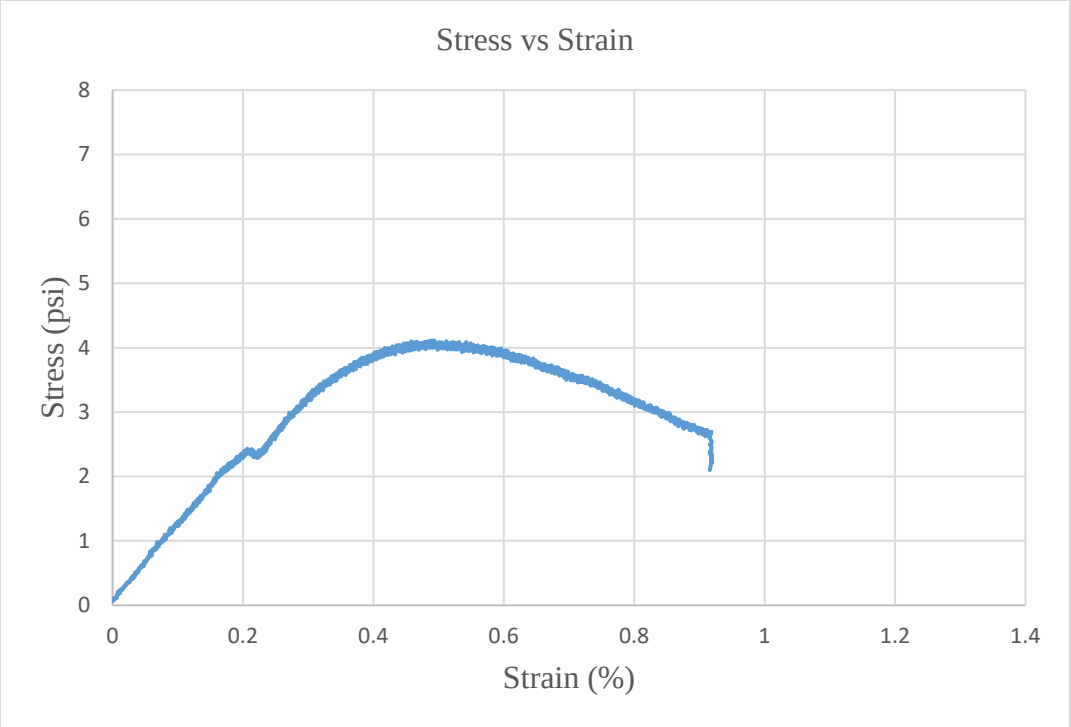

Figure 4.24. UCS stress-strain curve for borrow material (contract 3613).

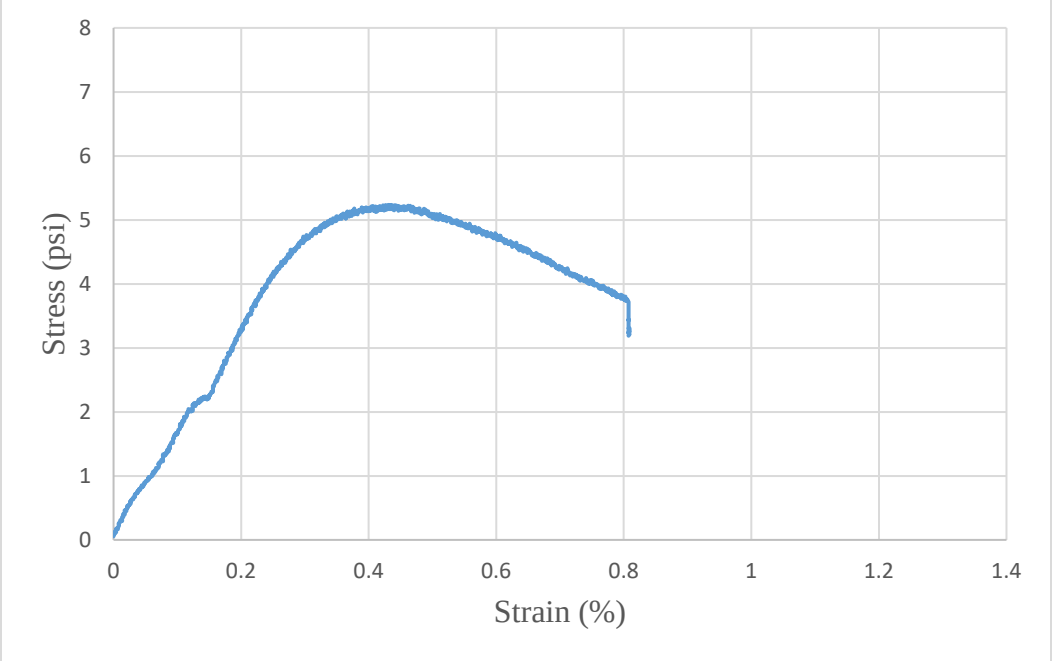

Figure 4.25. UCS stress-strain curve for subgrade material (I-15/Goodsprings).

Table 4.18. Summary of Unconfined Compressive Strength Test Results.

Material		UC (psi)	Strain (%)
Base	3546	2.8	0.65
	3583	7.3	0.51
	3597	3.4	0.60
	3605	6.6	0.64
	3607	9.7	0.72
	3613	3.7	0.51
Borrow	3546	1.3	0.60
	3583	5.6	0.80
	3597	6.6	0.78
	3613	4.1	0.54
Subgrade	I-15/Goodsprings	5.1	0.50
	US-95/Searchlight	8.5	0.57
	NV-375/Rachel	2.7	0.76
	US-95/Bonnie Claire	7.6	0.78
	US-93/Crystal Spring MP62	8.8	0.70
	US-93/Crystal Spring MP67	8.9	0.72

4.5. R-value Test (T 115D)

The R-value testing is an empirical measure of unbound materials strength and expansion potential which has been used in designing flexible pavements in Nevada. The R-value of the collected base, borrow and subgrade materials were determined in accordance with the NDOT test method Nev. T115D. Sample was split in to the required size and based on the gradation, four 1200g samples were batched for the R-value test. The initial moisture content was measured and different amount of water was added to get different moisture content. Steel mold with the diameter of 4 inch and height of 5 inch was used to prepare the sample. The mechanical kneading compactor was used to compact the sample as shown Figure 4.26. For the compaction 100 tamps were applied to the specimen (using 200 psi foot pressure).

The mold was placed on the exudation device as shown in Figure 4.27 after the compaction. A uniformly increasing load at a rate of 2000 lb per minute was applied until exudation was achieved. The exudation pressure was calculated by taking the exudation load and dividing the area of the specimen. Then the sample was kept undisturbed for 16- 20 hours with the addition of approximately 200 mL of water to calculate the expansion pressure as shown in Figure 4.28. After the specimen tested for expansion, it was forced into stabilometer as shown in Figure 4.29. Horizontal pressure and displacement were obtained at vertical pressure of 160 psi.

Figure 4.26. Kneading compactor.

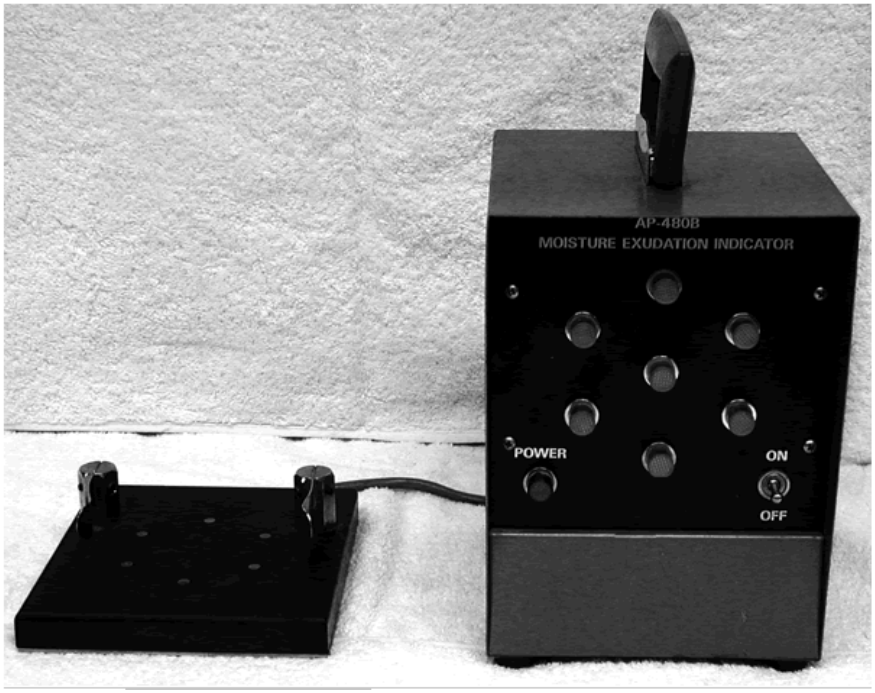

Figure 4.27. Exudation-indicator device.

Figure 4.28. Expansion pressure device.

Figure 4.29. R-value testing equipment.

The R-value was calculated from the Equation 30. Plot the R-value against the exudation pressure and R-value was determined from the graph for the 300 psi exudation pressure. The R-value tests were conducted by Black Eagle Consulting Company. Figure 4.30 presents the R-value test results for base material. The summary of R-value test results is shown in Table 4.19. R-value correction was done for the specimens if the specimen heights were not in the range of 2.45 – 2.55 inch. According NDOT standard specifications, the Type 1 Class B aggregate base and borrow materials have to have a minimum R-Value of 70 and 45 respectively.

$$R = 100 - \frac{100}{\left[\frac{2.5*(Pv-1)}{D*Ph}+1\right]} \quad (30)$$

Where;

R: R-value
Pv: vertical pressure (160 psi)
D: turns displacement reading
Ph: horizontal pressure (Stabilometer gauge reading at 160 psi vertical pressure)

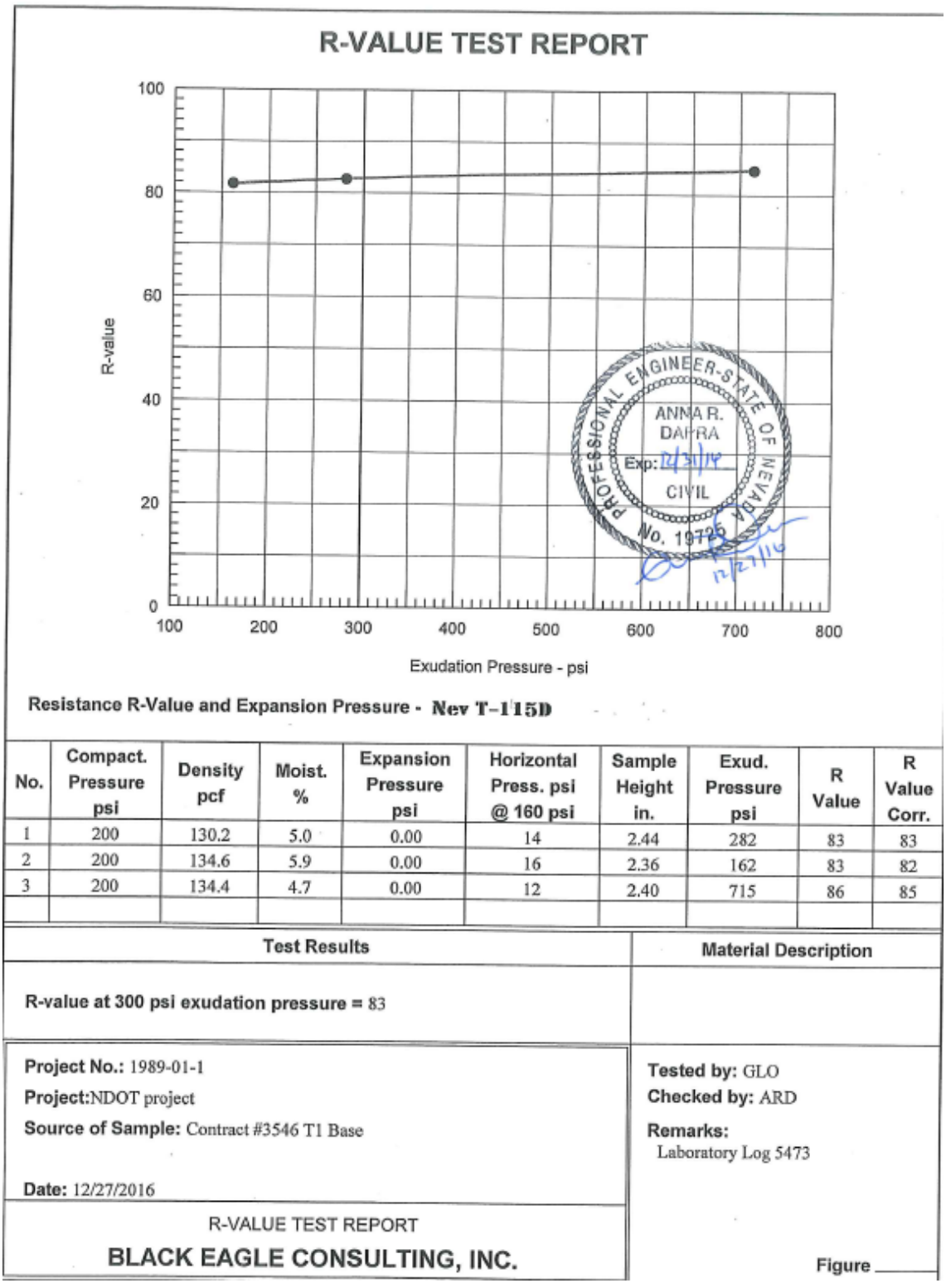

No.	Compact. Pressure psi	Density pcf	Moist. %	Expansion Pressure psi	Horizontal Press. psi @ 160 psi	Sample Height in.	Exud. Pressure psi	R Value	R Value Corr.
1	200	130.2	5.0	0.00	14	2.44	282	83	83
2	200	134.6	5.9	0.00	16	2.36	162	83	82
3	200	134.4	4.7	0.00	12	2.40	715	86	85

Figure 4.30. R-value test results for base material (contract 3546).

Table 4.19. Summary of R-value Test Results.

Contract	Sample No.	Density (pcf)	Moisture (%)	Exudation Pressure (psi)	R-Value @300 psi Exud. Pressure		
					Measured	Corr.	Average
3546 (Base)	1	130.2	5.0	282	83	83	
	2	134.6	5.9	162	83	82	83
	3	134.4	4.7	715	86	85	
3583 (Base)	1	138.9	6.8	100	79	78	
	2	138.1	5.8	333	81	80	80
	3	140.2	5.5	518	83	82	
3597 (Base)	1	121.0	3.9	608	82	82	
	2	125.6	4.5	478	77	75	71
	3	127.3	4.8	204	73	71	
3605 (Base)	1	132.4	5.4	354	83	81	
	2	135.3	5.2	540	86	86	78
	3	134.0	6.0	275	77	77	
3607 (Base)	1	125.7	6.6	530	85	85	
	2	124.3	7.6	298	85	85	85
	3	122.9	7.2	175	84	84	
3613 (Base)	1	135.0	5.0	699	87	87	
	2	138.7	5.9	204	84	82	83
	3	136.3	5.5	388	85	84	
3546 (Borrow)	1	123.8	5.0	727	84	84	
	2	123.4	6.5	441	82	82	78
	3	124.2	6.9	287	79	78	
3583 (Borrow)	1	116.8	13.5	125	32	32	
	2	119	11.8	734	70	70	44
	3	118.6	12.6	355	47	47	
3597 (Borrow)	1	136.1	8.1	149	74	71	
	2	134.4	7.2	731	85	85	78
	3	137.0	7.8	411	83	82	
3607 (Borrow)	1	119.7	13	100	57	57	
	2	119.3	12.2	271	76	76	78
	3	120.1	11.1	587	81	81	
3613 (Borrow)	1	138.3	5.9	361	85	85	
	2	139.6	6.7	227	83	83	84
	3	141.5	5.5	566	85	85	
I-15/ Goodsprings	1	131.9	7.9	188	78	78	
	2	129.5	7.2	468	82	82	82
	3	130.8	7.5	268	81	81	
US-95/ Searchlight	1	130.9	8.4	148	71	69	
	2	130.1	7.9	682	80	80	75
	3	130.7	8.2	254	74	74	
NV-375/ Rachel	1	129.5	8.8	302	80	81	
	2	130.7	9.5	171	76	76	80
	3	130.3	8.1	663	85	85	
US-95/ Bonnie Claire	1	121.8	11.4	172	72	71	
	2	121.1	10.2	719	74	74	74
	3	120.9	10.6	391	75	75	
US-93/ Crystal Spring MP62	1	119.2	10.5	404	80	81	
	2	119.8	10.9	225	66	68	74
	3	119.5	9.9	694	78	78	
US-93/Crystal Spring MP67	1	120.5	11.3	231	51	51	
	2	120.8	10.8	323	77	77	71
	3	119.6	10.1	628	78	78	

Chapter 5. DESIGN RESILIENT MODULUS FOR NEW PROJECTS

The subgrade and unbound layers have a definite effect on pavement performance and must be properly characterized for structural design (new and rehabilitation). Resilient modulus is the primary material property that is used to characterize the subgrade soil and other unbound structural layers for flexible pavement design in the AASHTO 1993 Design Guide (27) and in the new MEPDG developed under NCHRP project 1-37A (28) and currently being implemented as the AASHTOWare® Pavement ME design software (28).

This Chapter focuses on the identification of the resilient modulus properties for subgrade and unbound layers for the design of new flexible pavements as recommended by the AASHTO MEPDG. In order to develop correlations between the Mr and other properties of the subgrade and unbound materials such as R-value, UCS, Atterberg limits, etc…, the design value of the Mr for each layer must be established.

5.1. Procedure for Identification of Resilient Modulus Design Value

The steps to determine the design value for the unbound layers (aggregate base, borrow materials and subgrade soil) using repeated load triaxial resilient modulus tests are listed and defined below. These steps are in accordance with the MEPDG Manual of Practice (1) as well as in the final report for NCHRP project 1-37A (28) for both flexible and rigid pavements.

1. Based on previous experience, a trial flexible pavement structure is assumed that can satisfy the requirements of traffic loads and available materials.
2. Use the trial pavement structure to calculate the at-rest stress state from the overburden pressures for the aggregate base layer, embankment, and/or subgrade. The at-rest stress state for the aggregate base layer and embankment are determined at their quarter depth, while the at-rest stress state for the subgrade is determined 18 inches into the subgrade. These material characterization depths were established by comparing laboratory resilient modulus values to backcalculated elastic layer modulus values. These depths were selected for estimating the c-factor included in the 1993 AASHTO Design Guide, as well as in the MEPDG Manual of Practice.
3. Start with the subgrade or lowest unbound layer and move upward in the pavement structure to establish the design resilient modulus for all unbound material layers using a linear elastic layer program for calculating layer responses or stresses at the locations defined in step 1. Assume the resilient modulus for the unbound layers above which the design resilient modulus is being estimated.
4. For the design truck axle load and season, calculate the load-related vertical and horizontal stresses using a linear elastic layered program to be consistent with the Pavement ME Design pavement response program. The load-related stresses are calculated at the material/soil characterization depths listed above (see step #number 2).
5. Calculate the at-rest horizontal and vertical stresses from overburden at the same critical points or locations in the unbound layers used to calculate the load-related

stresses. The at-rest vertical pressure (p_1) and the at-rest horizontal stresses (p_2 and p_3) are calculated as follows.

$$p_0 = \left(D_{HMA}\gamma_{HMA} + D_{Base}\gamma_{Base} + D_{Soil}\gamma_{Soil}\right) \quad (31)$$

$$p_1 = p_0 \quad (32)$$

$$p_2 = p_3 = p_0 K_0 \quad (33)$$

Where;

p_0 and p_1: at-rest vertical or overburden pressure from the layers above a specific point

p_2, p_3: at-rest horizontal stress

K_0: at-rest earth pressure coefficient

D_{HMA}: thickness of the asphalt concrete layers

D_{Base}: thickness of the unbound aggregate base and/or embankment layers – If determining the at-rest stresses in the unbound base layer the point or depth into the base is ¼ of its thickness (see step 1)

D_{Soil}: point for computing at rest stress state in subgrade, 18 inches

γ_{HMA}: average in place density of the asphalt concrete layers

γ_{Base}: average in place wet density of the unbound aggregate base and/or embankment layers

γ_{Soil}: average in place wet density of the subgrade soil

6. Superimpose the at-rest and load-related stresses in the vertical and horizontal directions. In other words, add the at-rest and load-related vertical stresses, and add the at-rest and load related horizontal stresses.
7. Superimpose the total stress state versus resilient modulus calculated with linear elastic layer theory and the repeated load resilient modulus values versus stress state measured in the laboratory. The stress state at which the elastic modulus and laboratory resilient modulus are equal is the design value to be used in the Pavement ME Design software for quasi-input level 1.
8. Check the design resilient modulus determined for the lower unbound layers to be sure it is the same, as previously determined. This step is an iterative process to determine a stable design resilient modulus.

5.2. Identification of Resilient Modulus Design Value for Typical NDOT Pavements

This section identified the Mr design values for subgrade and unbound layers for typical NDOT flexible pavement sections. The typical pavement sections were designed using the Pavexpress software which is based on the AASHTO 1993 (27) design procedure. Three different traffic levels were considered for the pavement design. The NDOT *Pavement Structural Design Manual* was used as a reference for the input parameters as shown in Table 5.1. Structural coefficients for the asphalt concrete layer, base layer, and borrow layer were selected in accordance with the NDOT manual to be; 0.35, 0.10, and 0.07, respectively. Two different levels of subgrade resilient modulus were considered for the

design; strong at 14,000 psi and weak at 8,000 psi. Resilient modulus of the base layer was kept constant at 26,000 psi. Table 5.2 presents the pavement structures for different traffic levels.

For pavements on weak subgrade, borrow material was used as a subbase. For this case, the resilient modulus for the base, borrow, and subgrade were assumed to be; 26,000, 11,250, and 6,800 psi, respectively. The pavement structures with the borrow material are shown in Table 5.3.

Table 5.1. Major Inputs for Pavexpress Software.

Traffic Level	Design Traffic in Million ESALs (MESALs)	Reliability Level (%)	Initial Serviceability index	Terminal serviceability index	Standard Deviation (S_o)
Low	5	85	4.2	2	0.45
Medium	15	90	4.2	2.5	0.45
High	30	95	4.2	2.5	0.45

Table 5.2. Pavement Structures for Different Traffic Levels.

Traffic Level	Mr (Subgrade) (psi)	Thickness (inch)	
		AC	Base
Low	14,000	5	16
	8,000	7	16
Medium	14,000	7	18
	8,000	9.5	18
High	14,000	8	23
	8,000	10.5	23

Table 5.3. Pavement Structure with Borrow Materials.

Traffic Level	Thickness (inch)		
	AC	Base	Borrow
Low	5.5	16	10
Medium	8.5	18	10
High	9.5	23	10

The load-induced principal stresses were calculated using the 3D-Move analysis software (30) for a single wheel load of 9,000 lb and tire pressure of 80 psi as recommended in previous studies (31). The asphalt concrete layer was divided into sublayers to capture the

viscoelastic behavior. Sublayer thicknesses were obtained from the MEPDG procedure as shown in Figure 5.1.

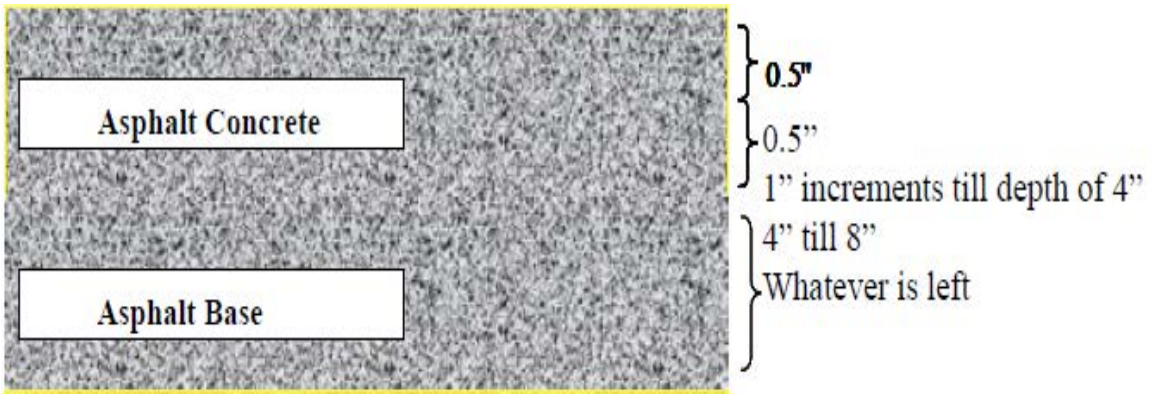

Figure 5.1. Sublayer thicknesses for the AC layer.

3D-Move models the AC layer as a viscoelastic material where the modulus changes with the temperature and frequency. The median temperature of District 1 of 110°F was used to calculate the dynamic modulus of the AC layer. For this analysis, a vehicle speed of 45 mph was considered. The loading frequency imparted by the moving vehicle changes with depth in the AC layer. The dynamic modulus master curve used in this analysis was developed for District 1 by using a representative mean dynamic modulus data for a PG76-22NV mixture as summarized in Table 5.4 and illustrated in Figure 5.2 (2).

Table 5.4. Mean Dynamic Modulus Values for District 1 PG76-22NV Mixture (2).

Frequency (Hz)	Temperature (°F)				
	14	40	70	100	130
0.1	2,437,149	1,142,867	231,733	49,451	22,928
0.5	2,796,769	1,566,757	371,867	79,212	29,081
1	2,929,984	1,786,152	459,860	99,621	38,053
5	3,189,069	2,208,295	700,905	174,052	65,800
10	3,280,392	2,398,327	841,850	225,042	77,131
25	3,384,391	2,819,783	1,041,907	335,073	107,196

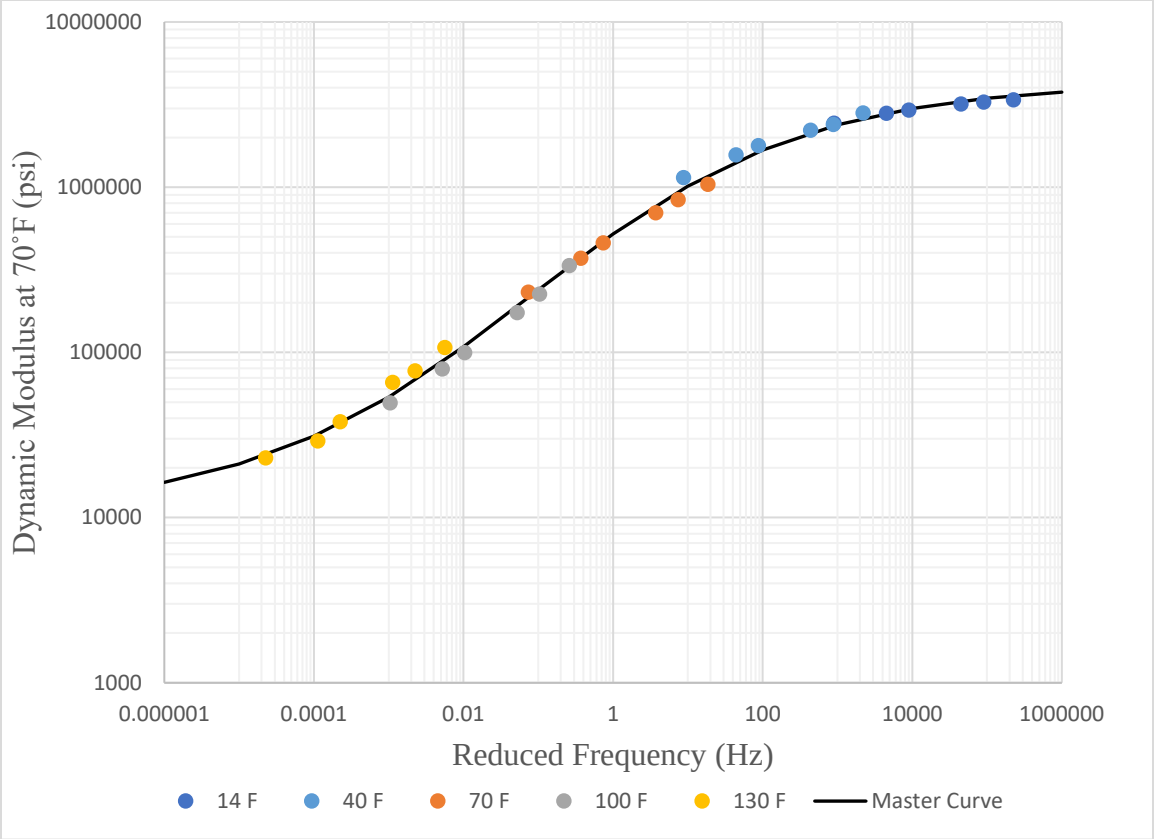

Figure 5.2. Dynamic modulus master curve for mixtures used in District 1.

The thicknesses of the asphalt concrete sublayers were transformed into equivalent thicknesses by using the method of equivalent thickness (MET) as shown in Figure 5.3.

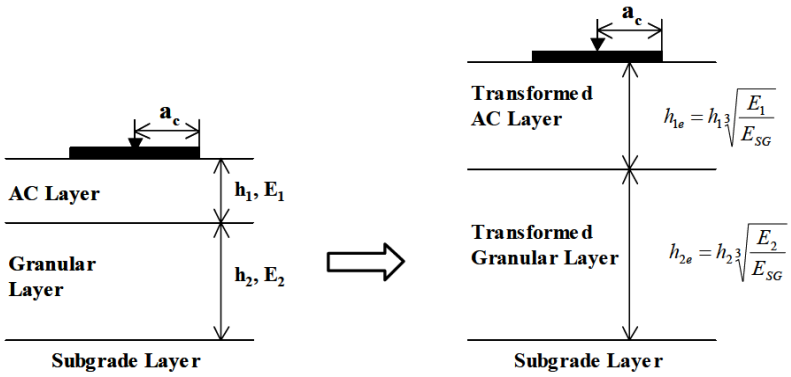

Figure 5.3. Equivalent thickness transformation using MET.

The pulse time was calculated using Equation 34. The calculation of effective length was done according to the MEPDG procedure as shown in Figure 5.4. The frequency for each sublayer was obtained from the pulse time. Dynamic modulus master curve was used to calculate the dynamic modulus for the corresponding frequencies for each sublayer. The calculated parameters and dynamic modulus values for each sublayer for a 5-inch AC layer are shown in Table 5.5.

$$t = \frac{L_{eff}}{17.6 v_s} \quad (34)$$

Where;

t: time of load (sec)
L_{eff} : effective length (inch)
V_s :velocity (mph)

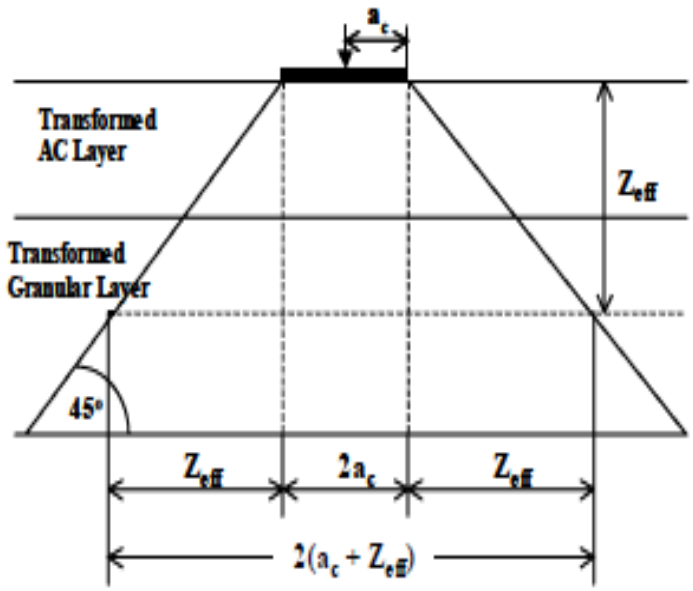

Figure 5.4, Effective length computation for single axle load configuration.

Table 5.5. Summary of Sublayers for a 5-inch AC Layer.

Sublayer	Thickness (inch)	Z_{eff} (in)	L_{eff} (in)	Pulse time (sec)	E* (psi)
Sublayer 1	0.5	1.35	14.51	0.01832	277,310
Sublayer 2	0.5	2.68	17.17	0.02167	261,579
Sublayer 3	1.0	5.25	22.31	0.02817	238,711
Sublayer 4	1.0	7.77	27.34	0.03452	222,347
Sublayer 5	1.0	10.23	32.27	0.04075	209,822
Sublayer 6	1.0	12.66	37.12	0.04687	199,798

The AC layer was subdivided and used in the 3D-Move (30) analysis. The Poisson's ratio for the AC, base, and subgrade was assumed to be 0.3, 0.35, and 0.45, respectively. The responses were obtained at the center and edge of the tire at the locations specified in step 1. Principal stresses were obtained from the software and converted into octahedral and shear stress (Equations 35 and 36).

$$\sigma_{oct} = \frac{1}{3}(\sigma_1 + \sigma_2 + \sigma_3) \quad (35)$$

$$|\boldsymbol{\tau}_{\mathbf{oct}}| = \frac{1}{3}\sqrt{(\sigma_1 - \sigma_2)^2 + (\sigma_2 - \sigma_3)^2 + (\sigma_1 - \sigma_3)^2} \quad (36)$$

Where;

σ_1: major principal stress
σ_2: minor principal stress
σ_3: intermediate principal stress

Triaxial state of stress can be obtained from the octahedral normal stress and shear stress. The deviator stress (σ_d) and confining stress (σ_c) are expressed in equations 37 and 38, respectively (32,33).

$$\sigma_d = \frac{3}{\sqrt{2}}|\tau_{oct}| \quad (37)$$

$$\sigma_c = \sigma_{oct} - \frac{\sigma_d}{3} \quad (38)$$

Stresses from the overburden pressure were also converted into triaxial state of stress and superimposed on the load induced stresses. The theta model (25) and universal model (26) were used to calculate the resilient modulus for base and subgrade layers, respectively. Table 5.6 and Table 5.7 present the iterative process for a pavement structure with 5-inch AC layer and 16-inch base layer. The iterative process was continued until the error becomes less than one percent. In this case, the identified design resilient modulus for the base and subgrade layers are 27,250 and 12,500 psi, respectively under centerline of the tire.

Table 5.6. Sate of Stress from Load-Induced Stress and Overburden Stress.

Trial	Layer	Location	3-D Move Stress (psi)							Static (psi)	
			σ_1	σ_2	σ_3	τ_{oct}	σ_d	σ_{oct}	σ_c	σ_d	σ_c
Trial 1	CAB	Center	19.42	-0.27	-0.29	9.28	19.69	6.29	-0.28	0.38	0.38
	CAB	Edge	15.90	-0.33	-0.73	7.75	16.43	4.95	-0.53	0.38	0.38
	SG	Center	1.94	0.05	0.04	0.89	1.90	0.68	0.04	1.59	1.59
	SG	Edge	1.89	0.05	0.04	0.87	1.85	0.66	0.04	1.59	1.59
Trial 2	CAB	Center	19.42	-0.27	-0.29	9.28	19.69	6.29	-0.28	0.38	0.38
	CAB	Edge	15.90	-0.33	-0.73	7.75	16.43	4.95	-0.53	0.38	0.38
	SG	Center	1.94	0.05	0.04	0.89	1.90	0.68	0.04	1.59	1.59
	SG	Edge	1.89	0.05	0.04	0.87	1.85	0.66	0.04	1.59	1.59

Table 5.7. Predicted Resilient Modulus from the State of Stress.

Trial	Layer	Location	Total (psi)		Bulk Stress θ (psi)	Octahedral Shear Stress (psi)	Assumed MR (psi)	Predicted Mr (psi)	Error (%)
			σ_d	σ_c					
Trial 1	CAB	Center	20.08	0.11	20.40	9.47	26,000	27,130	4.3
	CAB	Edge	16.81	-0.14	16.38	7.93	26,000	24,536	5.6
	SG	Center	3.49	1.63	8.38	1.64	13,000	12,469	4.1
	SG	Edge	3.44	1.63	8.34	1.62	13,000	12,441	4.3
Trial 2	CAB	Center	20.08	0.11	20.40	9.47	27,250	27,130	0.4
	CAB	Edge	16.81	-0.14	16.38	7.93	27,250	24,536	10.0
	SG	Center	3.49	1.63	8.38	1.64	12,500	12,469	0.2
	SG	Edge	3.44	1.63	8.34	1.62	12,500	12,441	0.5

The subgrade materials were divided into two categories based on the resilient modulus test results. The subgrade from I-15/Goodsprings and NV-375/Rachel were identified as strong while the rest of the subgrade materials were identified as weak. Summary of resilient modulus for the base, borrow, and subgrade materials are shown in Table 5.8, Table 5.9, and Table 5.10.

Table 5.8. Summary of Resilient Modulus for Pavement Structure on Strong Subgrade.

Material		Traffic Level / SG Strength			
		Low/High 5 inch AC & 16 inch CAB		Medium/High 7 inch AC & 18 inch CAB	
		Mr (psi)		Mr (psi)	
Base	Subgrade	Base	Subgrade	Base	Subgrade
3546	I-15/Goodsprings	27,250	12,500	22,000	12,750
3546	NV-375/Rachel	27,000	11,250	22,000	11,500
3583	I-15/Goodsprings	21,600	12,500	17,800	12,750
3583	NV-375/Rachel	21,600	11,250	17,800	11,500
3597	I-15/Goodsprings	24,300	12,500	19,500	12,750
3597	NV-375/Rachel	24,300	11,250	19,500	11,500
3605	I-15/Goodsprings	19,500	12,500	15,200	12,750
3605	NV-375/Rachel	19,300	11,300	15,200	11,550
3607	I-15/Goodsprings	19,300	12,500	14,900	12,750
3607	NV-375/Rachel	19,000	11,250	14,800	11,500
3613	I-15/Goodsprings	21,400	12,500	17,400	12,750
3613	NV-375/Rachel	21,400	11,250	17,400	11,500

Table 5.9. Summary of Resilient Modulus for Pavement Structure on Weak Subgrade.

Material		Traffic Level / SG Strength					
		Low/Low 7 inch AC & 16 inch CAB		Medium/Low 9.5 inch AC & 18 inch CAB		High/Low 10.5 inch AC&23 inch CAB	
		Resilient Modulus (psi)		Resilient Modulus (psi)		Resilient Modulus (psi)	
Base	**Subgrade**	**CAB**	**SG**	**CAB**	**SG**	**CAB**	**SG**
3546	US-95/Bonnie Claire	21,200	8,600	18,000	8,700	17,400	9,000
3546	US-95/Searchlight	21,800	10,600	18,500	10,900	17,800	11,250
3546	US-93/Crystal Spring MP62	21,000	7,700	17,800	8,000	17,200	8,300
3546	US-93/Crystal Spring MP67	21,800	10,600	18,500	10,900	17,800	11,250
3546	Borrow 3583	21,200	8,500	18,000	8,700	17,400	9,000
3583	US-95/Bonnie Claire	17,200	8,600	14,800	8,700	14,300	9,000
3583	US-95/Searchlight	17,700	10,600	15,300	10,900	14,600	11,250
3583	US-93/Crystal Spring MP62	17,000	7,700	14,600	8,000	14,200	8,300
3583	US-93/Crystal Spring MP67	17,700	10,600	15,300	10,900	14,600	11,250
3583	Borrow 3583	17,200	8,500	14,800	8,700	14,300	9,000
3597	US-95/Bonnie Claire	19,000	8,600	16,000	8,700	15,300	9,000
3597	US-95/Searchlight	19,400	10,600	16,500	10,900	15,800	11,250
3597	US-93/Crystal Spring MP62	18,700	7,700	15,800	8,000	15,200	8,300
3597	US-93/Crystal Spring MP67	19,400	10,600	16,500	10,900	15,800	11,250
3597	Borrow 3583	19,000	8,500	16,000	8,700	15,300	9,000
3605	US-95/Bonnie Claire	14,600	8,600	12,200	8,700	11,600	9,000
3605	US-95/Searchlight	15,200	10,650	12,700	10,900	11,900	11,250
3605	US-93/Crystal Spring MP62	14,400	7,750	12,000	8,000	11,400	8,300
3605	US-93/Crystal Spring MP67	15,200	10,650	12,700	10,900	11,900	11,250
3605	Borrow 3583	14,600	8,500	12,200	8,700	11,600	9,000
3607	US-95/Bonnie Claire	14,300	8,600	11,800	8,700	11,200	9,000
3607	US-95/Searchlight	14,800	10,600	12,300	10,900	11,500	11,250
3607	US-93/Crystal Spring MP62	14,100	7,700	11,600	7,950	11,000	8,300
3607	US-93/Crystal Spring MP67	14,800	10,600	12,300	10,900	11,500	11,250
3607	Borrow 3583	14,300	8,500	11,800	8,700	11,200	9,000
3613	US-95/Bonnie Claire	16,700	8,600	14,200	8,700	13,700	9,000
3613	US-95/Searchlight	17,200	10,600	14,700	10,900	14,000	11,250
3613	US-93/Crystal Spring MP62	16,500	7,700	14,000	8,000	13,500	8,300
3613	US-93/Crystal Spring MP67	17,200	10,600	14,700	10,900	14,000	11,250
3613	Borrow 3583	16,700	8,500	14,200	8,700	13,700	9,000

Table 5.10. Summary of Resilient Moduli values for Pavement Structures with Borrow Layer.

Material			5.5inch AC, 16 inch CAB and 10 inch Borrow			8.5inch AC, 18 inch CAB and 10 inch Borrow		
			Resilient Modulus (psi)			Resilient Modulus (psi)		
Base	Borrow	Subgrade	CAB	Borrow	SG	CAB	Borrow	SG
3583	3546	US-93/Crystal Spring MP62	20,300	11,800	8,200	15,900	11,700	8,500
3583	3546	Borrow 3583	20,300	11,900	8,900	15,900	11,900	9,200
3583	3597	US-93/Crystal Spring MP62	20,300	12,700	8,200	16,000	12,600	8,500
3583	3597	Borrow 3583	20,400	12,900	8,900	16,000	12,800	9,200
3583	3613	US-93/Crystal Spring MP62	20,300	11,900	8,200	16,000	11,900	8,500
3583	3613	Borrow 3583	20,300	12,100	8,900	16,000	12,100	9,200

Chapter 6. DESIGN RESILIENT MODULUS FOR REHABILITATION PROJECTS

The MEPDG approach described in Chapter 5 generated good results when applied on new pavement design projects. In the case of rehabilitation projects (i.e. overlay), which is the most common type of projects for NDOT, a relationship between the backcalculated and design resilient modulus is needed for the implementation of the AASHTOWare® Pavement ME Design software (29). This chapter focuses on the methodology to develop representative resilient modulus values for unbound materials for the pavement design of rehabilitation projects. The effort will examine correlations between Mr of unbound materials and the corresponding R-value, UCS, and other physical properties. A stepwise mechanistic analysis approach for determining a representative Mr value for the unbound materials in base, subbase, and subgrade layers was applied. The ILLI-PAVE 2005 finite element (FE) pavement analysis program (34) was employed as an advanced structural model for computing stresses as well as deflection basins in typical NDOT's flexible pavement structures under standard traffic loading.

The main unique features of ILLI-PAVE in comparison with other pavement analysis software are:

- Inclusion of constitutive models (a total of six different models are readily available) allowing for the characterization of the non-linear "stress-dependent" resilient behavior of granular materials and fine-grained soils under repetitive loading which is unavailable in Linear Elastic Programs (LEP).
- Implementation of Mohr-Coulomb failure criteria (c and ϕ) for unbound materials.
- Substantially lower computational effort because of the use of axi-symmetric FE formulation.
- Ability to handle a flexible pavement structure with up to ten different layers.

It should be noted that the ILLI-PAVE is the only model that allows the use of the constitutive Mr equations developed from the AASHTO T 307 tests.

6.1. Procedure for Identification of Design Resilient Modulus for Rehabilitation Designs

The stepwise mechanistic approach using ILLI-PAVE implemented for the determination of Mr values for rehabilitation designs is summarized as follows.

- Step 1- Select Representative Pavement Structures**:** The analysis is initiated by establishing representative NDOT's flexible pavement structures.
- Step 2- Pavement Layer Properties:
  - Asphalt Concrete (AC): in order to incorporate the viscoelastic behavior of the AC mixture in the ILLI-PAVE model, the AC layer was divided into sublayers and the dynamic modulus master curve for the asphalt mixture commonly used in NDOT District 1 was utilized to properly assign an elastic modulus for each of the sublayers using the appropriate loading frequency and temperature.

  - Crushed Aggregate Base (CAB), Borrow, and Subgrade (SG): The constitutive stress-dependent models developed from the T 307 Mr tests as well as the laboratory determined Mohr-Coulomb failure criteria (c and ϕ) were used in the ILLI-PAVE model.

- Step 3- Pavement Responses: When considering the non-linearity of the unbound materials, the Mr property varies at different locations within the respective layer. In other words, the state of stresses at each point in the layer results in a different Mr value caused by the stress-dependency of the unbound material. Hence, calculating the Mr from a determined state of stresses at a specific location within the layer under the center of load and assigning the Mr value to the entire layer might be questionable. In this study, surface deflection basins (i.e. vertical deflection at various radial distances from the applied load) were generated through the ILLI-PAVE model for the representative pavement structures under the allowable maximum tire load in Nevada on a circular plate. The generated surface deflection basins obtained are then employed in a backcalculation analysis to identify the Mr of each pavement layer including the base, borrow, and subgrade.
- Step 4- Establish the Mr Correlation Equations: Using the backcalculated moduli values for various types of unbound materials and pavement structures, correlations between Mr and R-value, UCS, or physical properties were developed and examined for their effectiveness.

6.2. Identification of Resilient Modulus for Rehabilitation Design

Flexible pavement sections used for the new designs were also used for this analysis. The AC layer was divided into sublayers as explained earlier. In the case of modulus for the AC mix, the damaged dynamic modulus master curve was used in order to simulate the in-situ AC layer of the flexible pavement in need for rehabilitation. The following steps were completed to develop the damaged dynamic modulus master curve:

1. Use the dynamic shear modulus and phase angle properties for a typical District 1 asphalt binder of PG76-22NV (as shown in Table 6.1) to estimate the viscosity of the binder at different temperatures.
2. Determine the regression parameters for equation 39.
3. The damage factor for the AC layer, d_{AC}, in Equation 40 can be determined based on the condition of the Ac layer as follows: a) Excellent condition, d_{AC} between 0.00 and 0.20, b) Good condition, d_{AC} between 0.20 and 0.40, c) Fair condition d_{AC} between 0.40 and 0.80, d) Poor condition d_{AC} between 0.80 and 1.20, and e) Very Poor condition d_{AC} greater than 1.20. in this research, a Fair condition was assumed for the existing AC layer and a damage value of 0.6 was selected for use in Equation 40.
4. Using Equation 40, determine the damaged dynamic modulus of the AC layer for different frequencies and temperatures as shown in Table 6.2.

Table 6.1. Representative Mean Dynamic Shear Modulus and Phase angle for PG 76-22 NV.

Temperature (F)	Binder G* (Pa)	Phase angle (deg)
147	7355	58.9
158	4638	58.4
169	2873	60.0

$$\log(E^*) = \delta + \frac{\alpha}{1 + e^{\beta+\gamma\log(t_r)}} \quad (39)$$

Where;

E^*: asphalt concrete moduli, psi
Δ: regression parameter
t_r: reduced time
α, β and γ: regression parameters

$$E^*dam = 10^{\delta} + \frac{E^* - 10^{\delta}}{1 + e^{-0.3+5*\log(d_{AC})}} \quad (40)$$

Figure 6.1 presents the master curves for the undamaged and damaged dynamic modulus of the AC layer for a typical District 1 asphalt binder of PG76-22NV. It should be noted that the scales in Figure 6.1 are logarithmic, therefore, any small changes in the master curves represents large differences in the actual values of the dynamic modulus. The AC layer was divided into sublayers and each sublayer was assigned an appropriate damaged dynamic modulus value using the damaged modulus master curve.

Table 6.2. Damaged Dynamic Modulus Input Values at Different Temperatures and Frequencies.

Frequency (Hz)	Temperature (F)				
	14	40	70	100	130
0.1	1,997,842	828,806	172,699	44,108	20,482
0.5	2,301,555	1,181,348	299,833	70,823	27,379
1	2,414,573	1,342,907	376,385	88,597	31,821
5	2,635,369	1,716,813	611,987	153,256	47,935
10	2,713,571	1,870,344	738,021	194,959	58,616
25	2,802,917	2,061,039	924,129	267,061	77,985

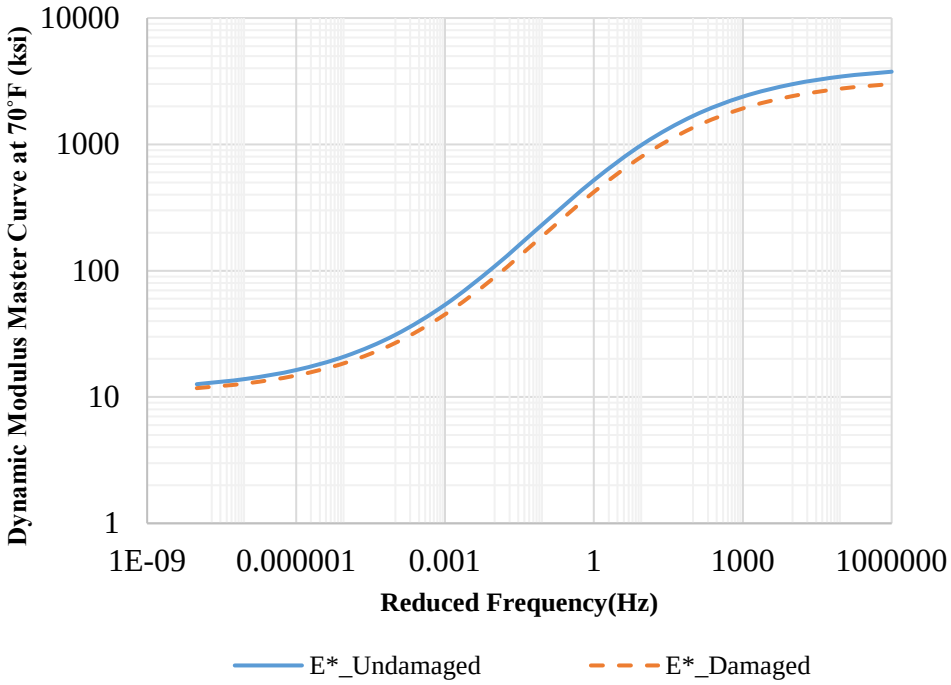

Figure 6.1. Damaged and undamaged dynamic modulus master curve.

For the base and borrow materials, the theta model (25) was used as an input to the ILLIPAVE software whereas for the subgrade, the Uzan model (26) was used. The values of the Poisson's ratios and the classification of subgrade quality were kept similar to the case of new designs. The Falling Weight Deflectometer (FWD) test was simulated in the ILLIPAVE model by applying a circular load of 9,000 lbs with a radius of 5.9 inch. The cohesion and friction angle properties for one base and one subgrade material were determined in the laboratory while the properties for the reaming materials were estimated based on their corresponding USCS classifications. The laboratory measured values as shown in Table 6.3 were close to the ones estimated based on the USCS classifications.

Table 6.3. Cohesion and Friction Angle from the Laboratory Testing.

Material	Cohesion (psi)	Friction angle (deg)
Base (Contract 3583)	4.1	48.9
Subgrade (I-15/Goodsprings)	8.2	33.8

The computer software, Modulus-6.1, was used to backcalculate the modulus values of the various layers using the deflection basins obtained from the ILLIPAVE analysis. An apparent rigid layer was introduced in the Modulus-6.1 software to capture the nonlinearity of the unbound materials. The backcalculation process was considered complete when the deflections basins calculated by the Modulus-6.1 model closely matched the deflections generated by the ILLIPAVE model. At this stage, the identified modulus values were assigned for the corresponding layers.

A sample calculation for a flexible pavement structure with 5.0 inch AC and 16.0 inch base material from contract 3546 on top of the subgrade material from the US-95/Bonnie Claire location is presented in this section. The forward calculation of the deflections by the ILLIPAVE model are summarized in Table 6.4. These deflections were used as input in the Modulus-6.1 model and the resulted backcaluated deflections are summarized in Table 6.5. Figure 6.2 presents the comparison between forward calculated and backcalculated deflections. The backcalculated moduli of the various layers are summarized in Table 6.6. The absolute error was 0.97 and E4/stiffness ratio was 5.5. Summary of the results from this analysis are presented in Table 6.7, Table 6.8 and Table 6.9 for different pavement structures.

Table 6.4. Deflections at various Radial Distances generated by the ILLIPAVE Model.

Radial Distance (inch)	Vertical Defection (mils)
0	23.08
8	16.39
12	12.68
18	8.73
24	6.28
36	3.63
48	1.99
60	1.04
72	0.55

Table 6.5. Deflection at Various Distances Backcalculated by the Modulus 6.1 Model.

Radial Distance (inch)	Defection (mils)
0	23.14
8	16.29
12	12.65
24	6.43
36	3.55
48	1.99
60	1.13

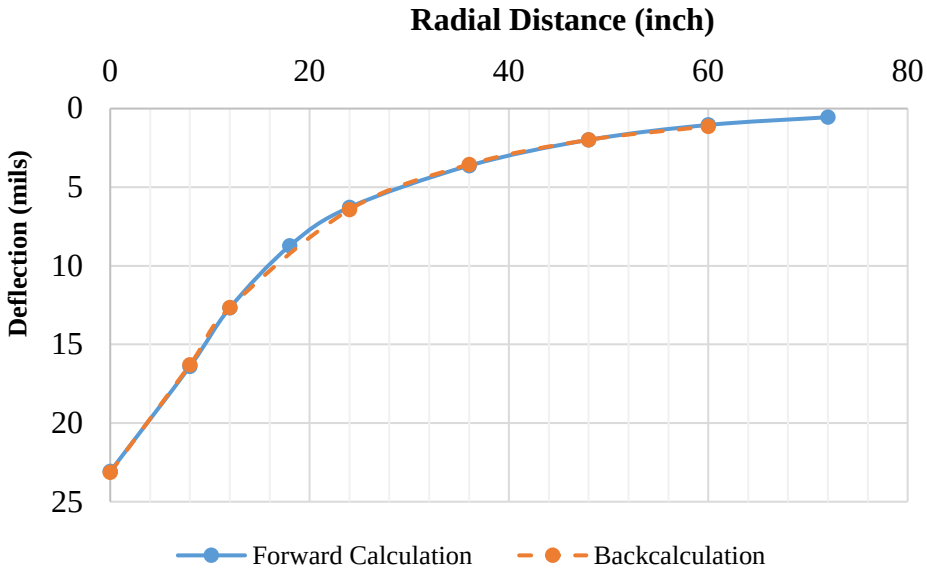

Figure 6.2. Forward calculated and backcalculated deflections.

Table 6.6. Backcalculated Modulus for Each Layer.

Layer	Backcalculated Moduli (psi)
AC	195,400
CAB	22,900
SG	8,400

Table 6.7. Summary of Backcalculated Moduli values for Pavement Structures with Borrow Layer.

Material			Pavement Structure			
			7 inch AC & 18 inch CAB			
			Backcalculated Moduli (psi)			
CAB	Borrow	Subgrade	SG	Borrow	CAB	AC
3546	3546	US-95/Bonnie Claire	5,400	11,900	16,500	191,000
3546	3546	US-95/Searchlight	6,300	13,300	16,800	189,400
3546	3596	US-93/Crystal Spring MP62	5,400	13,900	16,300	192,900
3546	3596	US-93/Crystal Spring MP67	6,300	15,500	16,500	192,800
3546	3613	Borrow 3583	5,600	10,700	17,100	186,300
3583	3613	US-95/Bonnie Claire	7,000	10,600	17,700	183,500

Table 6.8. Summary of Backcalculated Moduli for Pavement Structures on Strong Subgrade.

Material		Traffic Level / SG Strength					
		Low/High 5 inch AC & 16 inch CAB			Medium/High 7 inch AC & 18 inch CAB		
		Backcalculated Moduli (psi)			Backcalculated Moduli (psi)		
CAB	SG	CAB	SG	AC	CAB	SG	AC
3546	I-15/Goodsprings	22,900	8,400	195,400	22,300	8,200	176,700
3546	NV-375/Rachel	22,400	7,700	197,200	21,600	7,700	178,400
3586	I-15/Goodsprings	19,800	8,400	187,900	19,300	8,100	173,200
3583	NV-375/Rachel	19,700	7,600	185,900	19,100	7,400	172,800
3597	I-15/Goodsprings	21,300	8,200	191,700	20,600	8,000	174,700
3597	NV-375/Rachel	20,800	7,400	193,000	19,900	7,500	176,600
3605	I-15/Goodsprings	17,900	7,600	187,500	17,000	7,300	173,900
3605	NV-375/Rachel	17,600	6,900	187,800	16,700	6,900	173,100
3607	I-15/Goodsprings	17,800	7,200	186,700	16,500	7,200	174,700
3607	NV-375/Rachel	17,200	6,800	189,900	16,100	6,800	175,000
3613	I-15/Goodsprings	19,700	8,000	186,400	19,000	7,700	172,800
3613	NV-375/Rachel	19,100	7,500	187,800	18,500	7,300	172,500

Table 6.9. Summary of Backcalculated Moduli for Pavement Structures on Weak Subgrade.

Material		Traffic Level / SG Strength					
		Low/Low 7 inch AC & 16 inch CAB			Medium/Low 9.5 inch AC & 18 inch CAB		
		Backcalculated Moduli (psi)			Backcalculated Moduli (psi)		
CAB	SG	CAB	SG	AC	CAB	SG	AC
3546	US-95/Bonnie Claire	20,500	6,600	170,300	19,800	6,800	158,000
3546	US-95/Searchlight	22,800	7,300	165,200	21,000	7,700	158,000
3546	US-93/Crystal Spring MP62	20,600	5,700	167,700	19,000	6,400	158,600
3546	US-93/Crystal Spring MP67	22,800	7,300	166,100	21,100	7,800	157,600
3546	Borrow 3583	22,300	6,900	164,600	20,500	7,500	158,100
3583	US-95/Bonnie Claire	17,900	6,600	167,900	17,400	6,500	157,100
3583	US-95/Searchlight	19,300	7,600	164,800	18,300	7,500	157,000
3583	US-93/Crystal Spring MP62	17,600	6,000	167,500	17,200	6,000	156,400
3583	US-93/Crystal Spring MP67	19,400	7,600	164,300	18,400	7,500	156,600
3583	Borrow 3583	18,900	7,100	164,300	18,100	7,200	156,500
3597	US-95/Bonnie Claire	18,500	6,700	170,800	18,200	6,600	157,500
3597	US-95/Searchlight	20,100	7,600	167,700	19,100	7,600	158,000
3597	US-93/Crystal Spring MP62	18,400	6,000	168,100	17,500	6,200	158,200
3597	US-93/Crystal Spring MP67	20,200	7,600	167,400	19,500	7,500	156,300
3597	Borrow 3583	19,800	7,200	165,700	19,100	7,200	155,900
3605	US-95/Bonnie Claire	16,100	6,000	165,000	15,100	6,100	156,700
3605	US-95/Searchlight	16,900	7,200	164,600	16,000	7,000	155,600
3605	US-93/Crystal Spring MP62	15,300	5,700	167,600	14,500	5,800	156,900
3605	US-93/Crystal Spring MP67	17,000	7,100	164,800	16,000	7,000	156,200
3605	Borrow 3583	16,700	6,700	162,900	15,600	6,700	155,900
3607	US-95/Bonnie Claire	15,600	5,900	166,200	14,800	5,900	155,300
3607	US-95/Searchlight	16,500	7,000	165,300	15,600	6,900	155,600
3607	US-93/Crystal Spring MP62	14,800	5,500	168,400	14,000	5,700	157,400
3607	US-93/Crystal Spring MP67	16,900	6,800	164,000	15,600	6,800	155,700
3607	Borrow 3583	16,200	6,600	164,000	15,300	6,500	155,200
3613	US-95/Bonnie Claire	17,400	6,500	166,700	17,000	6,400	155,900
3613	US-95/Searchlight	18,900	7,400	164,100	17,800	7,400	156,500
3613	US-93/Crystal Spring MP62	17,100	5,800	166,500	16,300	6,100	157,300
3613	US-93/Crystal Spring MP67	19,000	7,200	168,800	17,900	7,300	156,100
3613	Borrow 3583	18,400	7,000	164,000	17,500	7,000	155,900

Chapter 7. RESILIENT MODULUS PREDICTION MODEL DEVELOPMENT

The goal of this analysis is to develop a prediction model for Mr value to be used in the design of flexible pavements as function of empirical and physical properties for the unbound materials. The properties considered in the development of the prediction model, included; R-value, unconfined compressive strength, materials passing sieves #200, #40, 3/8", maximum dry density, optimum moisture content, and plasticity index. In addition, the pavement equivalent thickness in terms of the base, borrow, or the subgrade layer were identified as critical parameters in the determination of the design Mr for unbound layers. The layer thicknesses above the base, borrow, and subgrade used for the state of stress calculations were transformed into equivalent thickness of base, borrow, or subgrade using the method of equivalent thickness (MET) as presented in Equations 41, 42, and 43.

$$\mathbf{H_{eq,\,CAB} = h_{AC}}\left(\frac{\mathbf{E_{AC}} * (\mathbf{1} - \boldsymbol{\nu}_{\mathbf{SG}}{}^{\mathbf{2}})}{\mathbf{E_{SG}} * (\mathbf{1} - \boldsymbol{\nu}_{\mathbf{AC}}{}^{\mathbf{2}})}\right)^{(1/3)} + \frac{\mathbf{h_{CAB}}}{\mathbf{4}} * \left(\frac{\mathbf{E_{CAB}} * (\mathbf{1} - \boldsymbol{\nu}_{\mathbf{SG}}{}^{\mathbf{2}})}{\mathbf{E_{SG}} * (\mathbf{1} - \boldsymbol{\nu}_{\mathbf{CAB}}{}^{\mathbf{2}})}\right)^{(1/3)} \quad \textbf{(41)}$$

$$\mathbf{H_{eq,\,BOR}} = \boldsymbol{h_{AC}}\left(\frac{\boldsymbol{E_{AC}} * (\mathbf{1} - \boldsymbol{\nu_{SG}}{}^{\mathbf{2}})}{\boldsymbol{E_{SG}} * (\mathbf{1} - \boldsymbol{\nu}_{\mathbf{AC}}{}^{\mathbf{2}})}\right)^{(1/3)} + \boldsymbol{h_{CAB}} * \left(\frac{\boldsymbol{E_{CAB}} * (\mathbf{1} - \boldsymbol{\nu_{SG}}{}^{\mathbf{2}})}{\boldsymbol{E_{SG}} * (\mathbf{1} - \boldsymbol{\nu_{SG}}{}^{\mathbf{2}})}\right)^{(1/3)} + \frac{\mathbf{h_{BOR}}}{\mathbf{4}} * \left(\frac{\mathbf{E_{BOR}} * (\mathbf{1} - \boldsymbol{\nu}_{\mathbf{SG}}{}^{\mathbf{2}})}{\mathbf{E_{SG}} * (\mathbf{1} - \boldsymbol{\nu}_{\mathbf{BOR}}{}^{\mathbf{2}})}\right)^{(1/3)} \quad \textbf{(42)}$$

$$\mathbf{H_{eq,\,SG}} = \boldsymbol{h_{AC}}\left(\frac{\boldsymbol{E_{AC}} * \left(\mathbf{1} - \boldsymbol{\nu_{SG}}{}^{\mathbf{2}}\right)}{\boldsymbol{E_{SG}} * (\mathbf{1} - \boldsymbol{\nu}_{\mathbf{AC}}{}^{\mathbf{2}})}\right)^{\left(\frac{1}{3}\right)} + \boldsymbol{h_{CAB}} * \left(\frac{\boldsymbol{E_{CAB}} * \left(\mathbf{1} - \boldsymbol{\nu_{SG}}{}^{\mathbf{2}}\right)}{\boldsymbol{E_{SG}} * (\mathbf{1} - \boldsymbol{\nu_{SG}}{}^{\mathbf{2}})}\right)^{\left(\frac{1}{3}\right)} + \mathbf{18} \quad \textbf{(43)}$$

Where;

$H_{eq,\,CAB}$: equivalent thickness of the base layer, inch
$H_{eq,\,BOR}$: equivalent thickness of the borrow layer, inch
$H_{eq,\,SG}$: equivalent thickness of the subgrade layer, inch
E_{AC}: modulus of AC layer, psi
E_{CAB}: resilient modulus of base layer, psi
E_{CAB}: resilient modulus of borrow layer, psi
E_{SG}: resilient modulus of subgrade layer, psi
ν_{AC}: Poisson's ratio of AC layer
ν_{CAB}: Poisson's ratio of base layer
ν_{BOR}: Poisson's ratio of borrow layer
ν_{SG}: Poisson's ratio of subgrade layer

7.1. Statistical Analysis

Multi linear regression analysis was conducted using the R software (35). The following assumptions were checked for each model:

- If errors are following a normal distribution
- Multi-collinearity

Anderson-Darling normality test (36) and variance inflation factors (37) were used to check the normality and multi-collinearity respectively. A backward elimination method was used to identify the best fit model. First, all of the identified variables were included in the analysis and tested for statistical significance. Next, the non-significant variables (i.e., p-value greater than 0.05) were removed and the analysis was repeated until all the significant variables were identified.

Based on the results of the statistical analysis, it is observed that the design resilient modulus of the subgrade does not change with the pavement structure. However, the design resilient modulus of base and borrow layers change significantly with the pavement structure. Accordingly, the data for the base and borrow layers were combined to develop a single prediction model while the prediction model for the subgrade layer was established separately. The ranges of data that were used for the model development are shown in Table 7.1.

Table 7.1. Range of Variables for the Design Mr Models Development.

Parameter	Range of Data					
	Subgrade		Base		Borrow	
	Min	Max	Min	Max	Min	Max
R-value	44	82	71	85	78	83
P#200(%)	5.4	66.9	5.3	10	7.3	16.4
P#40(%)	15.2	84.2	12.6	19.3	15.4	28.7
P# 3/8(%)	52.2	99.3	54.1	76.3	69.8	99.9
Maximum dry density (pcf)	119.4	139.2	135.8	147.5	133.8	143.2
Optimum moisture content (%)	6.1	10.7	3.5	6.7	5.4	7.2
UCS (psi)	2.7	8.9	2.8	9.7	1.3	6.6
PI	1	4.7	0	0	0	3.3
H_{eq} (inch)	48.5	80.8	17.1	35.3	38.3	54.4
Mr (new design)	7,700	13,200	11,000	27,250	11,700	20,400
Mr (rehabilitation)	5,400	8,400	14,000	22,900	10,600	15,500

Two sets of models were examined; a) a prediction model with the UCS and without the R-value and b) a prediction model without the UCS and with the R-value. The summary of the developed models for new design and rehabilitation projects with UCS and R-value are presented in Table 7.2 and Table 7.3, respectively. The typical residual plot and normality plot from the R software are shown in Figure 7.1 and Figure 7.2. The residual

plot should look random, in other words, there should not be any pattern. The normality plot has to be linear in order to satisfy the linear regression assumption. The data seem to satisfy the normality condition and the regression assumptions.

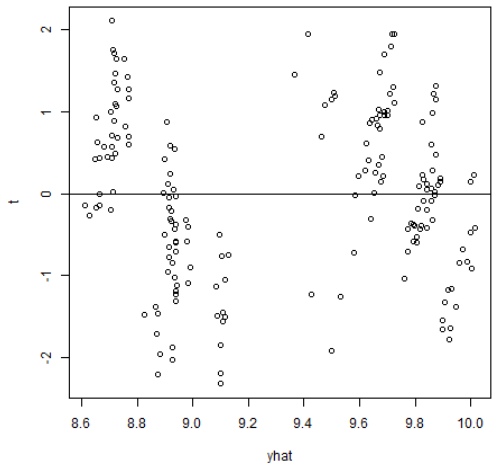

Figure 7.1. Residual error plot for the prediction model.

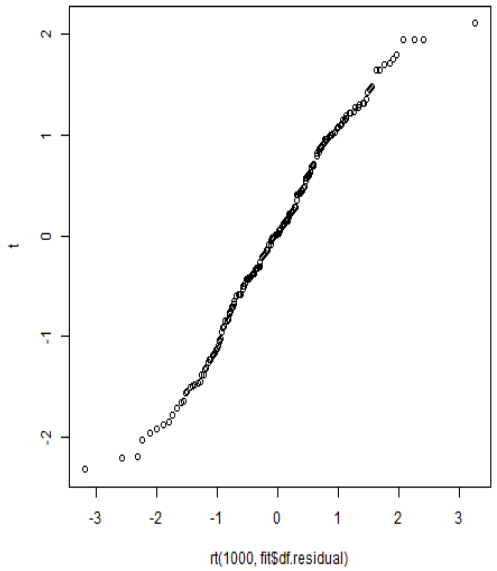

Figure 7.2. Normality plot for the prediction model.

Table 7.2. Summary of Design Resilient Modulus Models with UCS.

Ln(Mr)	Intercept	P#200 (%)	P#40 (%)	P#3/8 (%)	γ_d (pcf)	OMC (%)	UCS (psi)	PI	H_{eq} (inch)	Norm*	Mul. Col**	R-Square
$Ln(Mr_{SG-New})$	7.4514	0.0036		-0.0129	0.0158		0.0973	0.0311		Fail	Fail	0.8818
$Ln(Mr_{SG-Reh})$	9.2335	0.0028		-0.0045		-0.0401	0.0318	0.0158		Pass	Fail	0.6180
$Ln(Mr_{CAB-New})$	9.8294		0.0060	0.0066		0.1122	-0.0878		-0.0270	Pass	Pass	0.9641
$Ln(Mr_{CAB-Reh})$	9.8130			0.0031		0.0738	-0.0597		-0.0088	Fail	Pass	0.8469
$Ln(Mr_{BOR-New})$	10.0307	0.0165	0.0245			0.0740	-0.0818		-0.0286	Fail	Pass	0.8479
$Ln(Mr_{BOR-Reh})$	10.3677	0.0160	-0.0087				-0.0234		-0.0165	Pass	Pass	0.6339

Table 7.3. Summary of Design Resilient Modulus Models with R-value.

Ln(Mr)	Intercept	R-value	P#40 (%)	P#3/8 (%)	γ_d (pcf)	OMC (%)	PI	H_{eq} (inch)	Norm*	Mul. Col**	R-Square
$Ln(Mr_{SG-New})$	3.1784	0.0180	0.0136		0.0315		0.0433		Fail	Fail	0.8272
$Ln(Mr_{SG-Reh})$	5.3982	0.0134	0.0125	-0.0032	0.0168		0.0177		Pass	Fail	0.7065
$Ln(Mr_{CAB-New})$	7.3224	0.0366	-0.0656	0.0256		-0.0893		-0.0270	Fail	Pass	0.9644
$Ln(Mr_{CAB-Reh})$	8.0140	0.0261	-0.0485	0.0161		-0.0659		-0.0089	Fail	Pass	0.8542
$Ln(Mr_{BOR-New})$	8.9671	0.0102		0.0123		-0.0743		-0.0189	Fail	Pass	0.6000
$Ln(Mr_{BOR-Reh})$	9.2304	0.0136	-0.0229	0.0079		-0.0661		-0.0127	Fail	Pass	0.6594

**Multi-collinearity, *Normality, γ_d: Maximum dry unit weight, PI: Plasticity index

Based on the analysis of the multiple models, the resilient modulus of the subgrade can be estimated from the R-value or the UCS. However, for the base and borrow materials, the R-value only should be used to predict the resilient modulus. The UCS of the base and borrow materials is not a good indicator of their Mr property. Within the pavement structure, base and borrow materials are subjected to confinement and deviator stresses. Therefore, the UCS test is not a representative strength test for the in-situ conditions of the base and borrow layers. However, in the case of subgrade, since the confinement and deviator stresses are relatively low, the UCS test values can be used as a strength property as was shown in several past studies.

Based on the analysis of the data generated from this experiment, a correlation was found possible between the equivalent thickness and depth from pavement surface to the location where the state of stress was calculated (D) as shown in Figure 7.3. The depth of location for state of the stress calculation was defined in the MEPDG procedure (see step number 2 under Section 5.1 – for the aggregate base layer and embankment stresses are determined at their quarter depth, while for the subgrade, stresses are determined 18 inches into the subgrade). According to the MEPDG procedure, a trial pavement structure must be assumed in the design process. Therefore, using the assumed pavement structure, the depth to the state of stress calculation can be determined for each layer and used to calculate the equivalent thickness in terms of the layer being analyzed using Equations 44 to 47 (different equations for New and Rehabilitation designs and for CAB and Borrow materials). Once the equivalent thickness is computed, the resilient modulus of the layer being analyzed can be estimated from the models presented in Table 7.2 and Table 7.3 and can be used as a Level 2 input for the AASHTOWare® Pavement ME Design software (29).

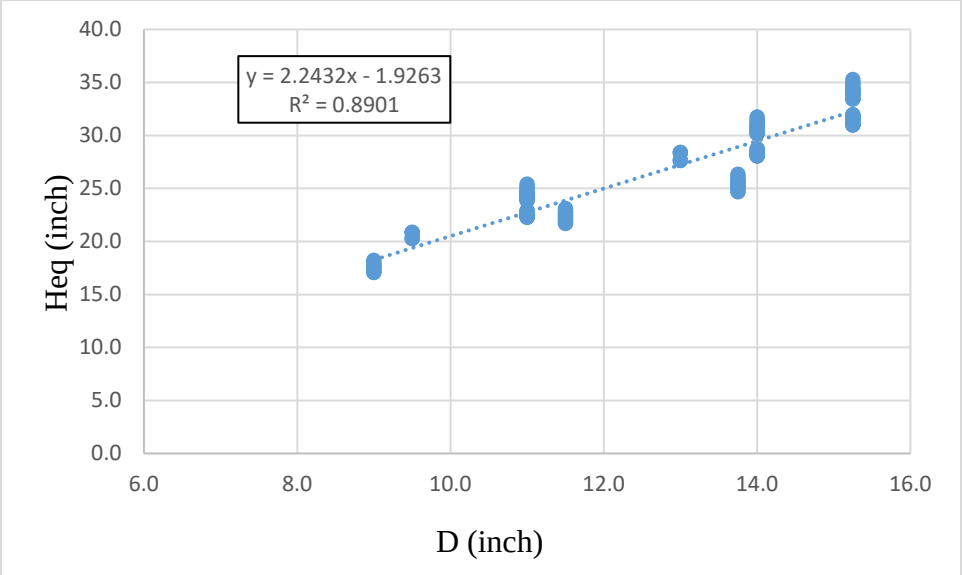

Figure 7.3. Correlation between H_{eq} and D for new design.

$$H_{eqNew-CAB} = 2.2432 * D - 1.9263 \quad (44)$$

$$H_{eqNew-Bor} = 1.3211 * D + 9.6409 \quad (45)$$

$$H_{eqReh-CAB} = 2.399 * D - 1.7468 \quad (46)$$

$$H_{eqReh-BOR} = 1.543 * D + 8.044 \quad (47)$$

Where;
$H_{eqNew-CAB}$: equivalent thickness of the base layer for new design, inch
$H_{eqNew-BOR}$: equivalent thickness of the borrow layer for new design, inch
$H_{eqReh-CAB}$: equivalent thickness of the base layer for rehabilitation design, inch
$H_{eqReh-BOR}$: equivalent thickness of the borrow layer for rehabilitation, inch
D: depth of location for state of stress calculation (base, borrow, and subgrade), inch

7.2. Comparison of Resilient Modulus Prediction Models

The comparison between the design resilient modulus and predicted resilient modulus of subgrade by using the UCS for the new design and rehabilitation projects is presented in Figure 7.4 and Figure 7.5, respectively. Figure 7.6 and Figure 7.7 presents the comparison of design resilient modulus and predicted resilient modulus for the new design and rehabilitation projects using the R-value, respectively. It can be easily observed that the prediction of the design resilient modulus for the borrow material can be improved with additional data points.

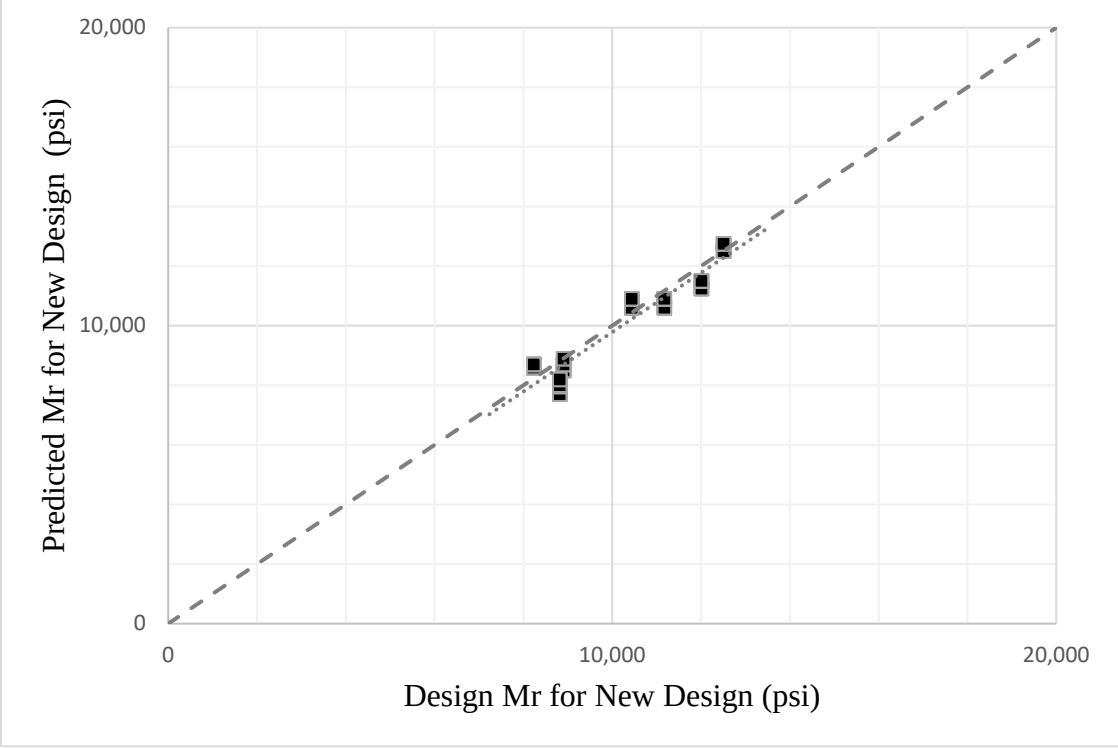

Figure 7.4. Variation of design resilient modulus versus predicted resilient modulus of subgrade (using UCS) for new design.

Figure 7.5. Variation of design resilient modulus versus predicted resilient modulus of subgrade (using UCS) for rehabilitation design.

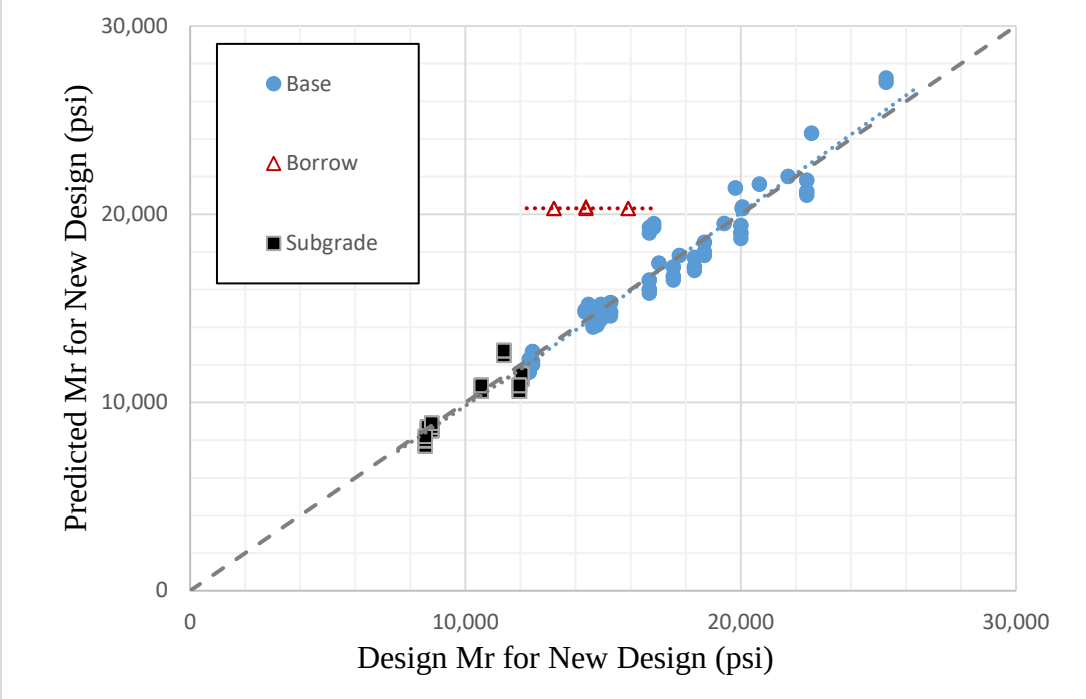

Figure 7.6. Variation of design resilient modulus with predicted resilient modulus (using R-value) for new design.

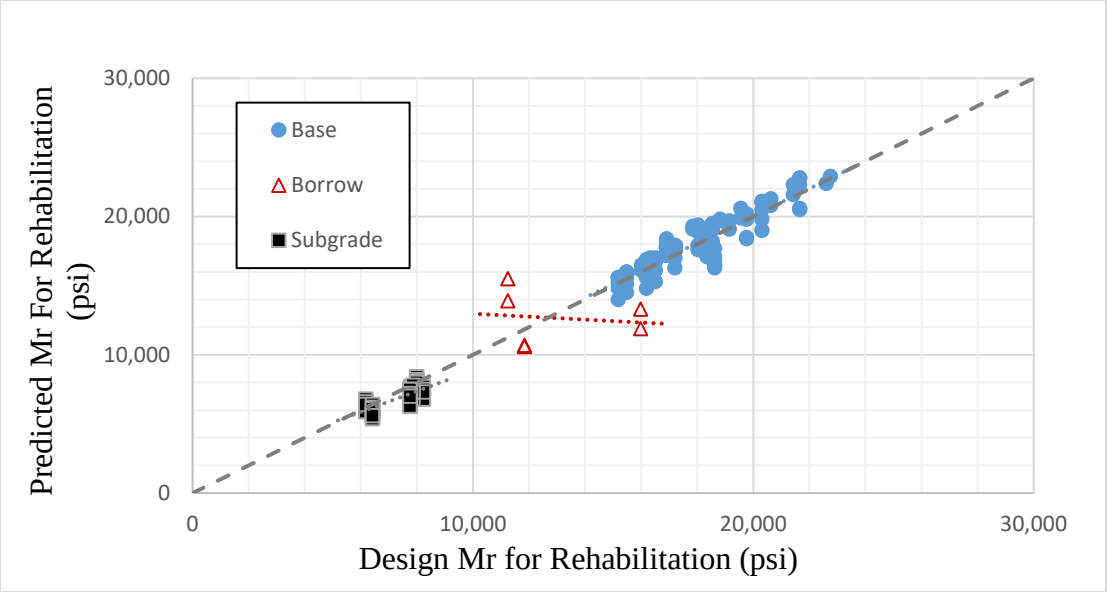

Figure 7.7. Variation of rehabilitation design resilient modulus with predicted resilient modulus (using R-value) for rehabilitation design.

The comparison of resilient modulus prediction models for the new and rehabilitation designs based on R-value is presented in Figure 7.8. It can be seen that the predicted resilient modulus for the subgrade materials for new design is consistently higher than rehabilitation design while a better agreement is achieved for the base layer.

A comparison between resilient modulus prediction from the current NDOT equation and the model for the design resilient modulus developed using R-value is presented in Figure 7.9. It can be seen that the current NDOT resilient modulus equation in terms of R-value consistently overestimates the resilient modulus for all layers and for both new and rehabilitation designs. This further supports the need to establish prediction models for the design resilient modulus of unbound and subgrade layers that are based on the strength and physical properties of locally available granular materials and in-place natural soils.

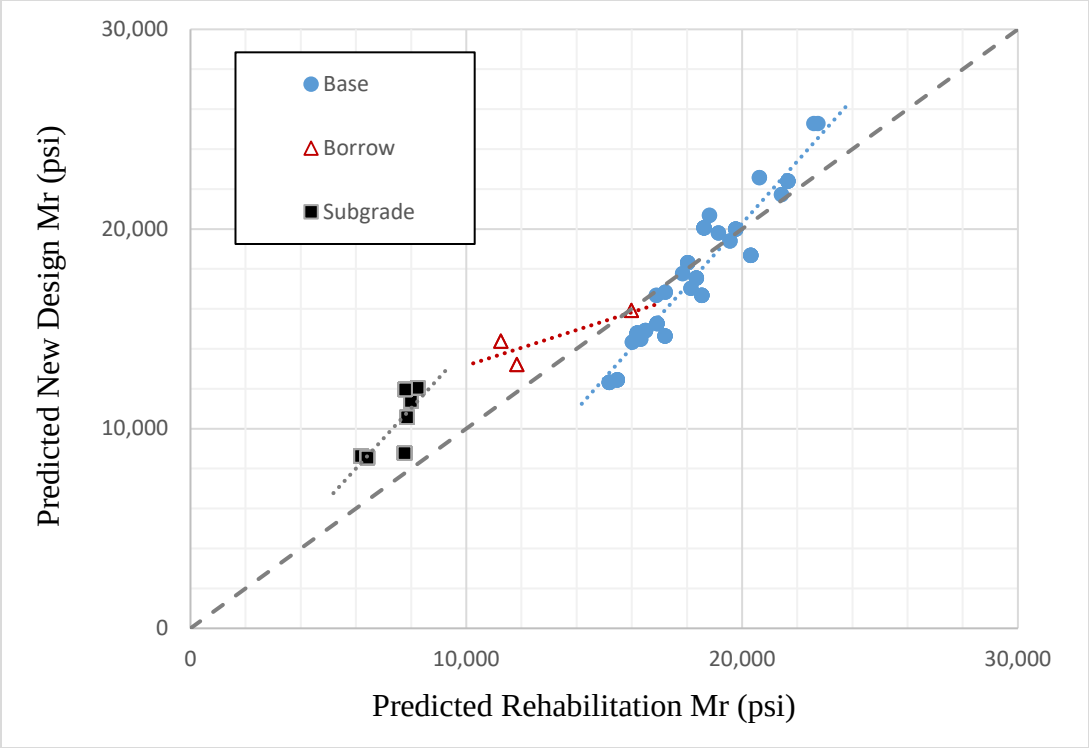

Figure 7.8. Comparison of predicted rehabilitation and new design Mr (R-value).

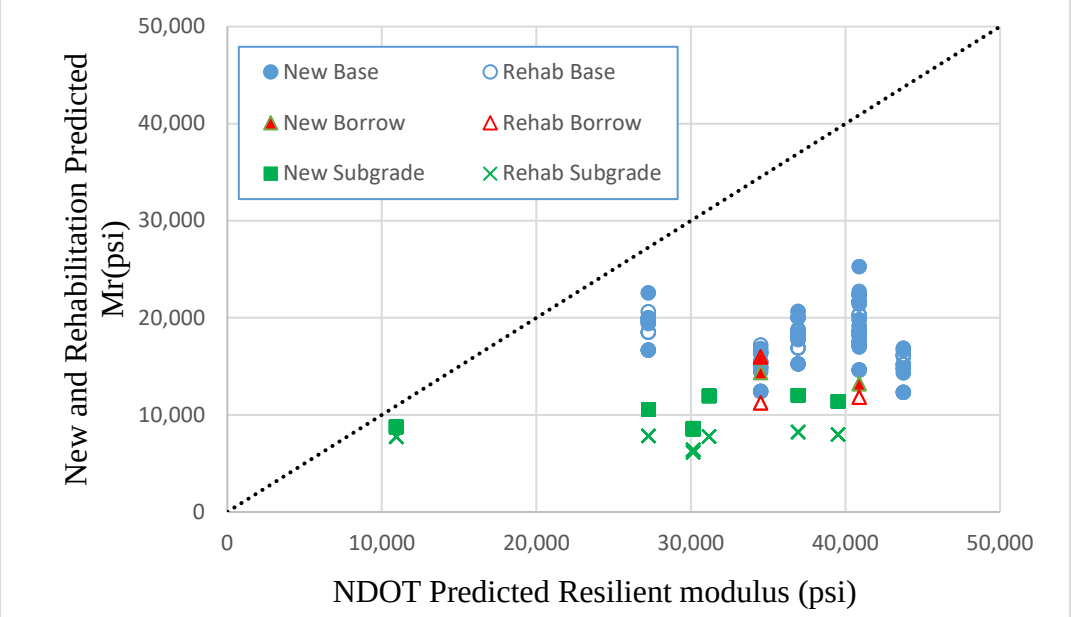

Figure 7.9. Variation of NDOT predicted Mr and predicted Mr for new and rehabilitation design (R-value).

7.3. AASHTOWare® Pavement ME Comparison

The effect of the design resilient modulus models developed in this research on the design of typical flexible pavements was evaluated by using the AASHTOWare® Pavement ME design software. The design was done for 10 million design ESALs. The design inputs were obtained from the NDOT manual (2). The input resilient modulus and design pavement structure without borrow material is shown in Table 7.4 and Table 7.5, respectively. The current NDOT manual specifies a resilient modulus for the base layer of 26,000 psi regardless of the R-value. It can be observed that the design thickness of the asphalt concrete layer is increased by 0.5 – 1.0 inch when using the design resilient modulus model based on the R-value. Similar observation was found in the pavement structure with borrow materials as shown in Table 7.6 and Table 7.7.

Table 7.4. Resilient Modulus of Unbound materials (without Borrow Material).

Strength Properties	Base	Subgrade
R-value	80	44
Resilient Modulus(psi) (NDOT)	36,929	10,918
Resilient Modulus(psi)(Developed model)	18,458	8,779

Table 7.5. Design Flexible Pavement Structure.

Mr Equation	Pavement Thickness (inch)	
	AC	Base
Current NDOT	6	16
Developed Model	7	16
Developed Model with 26000 psi Base	6.5	16

Table 7.6. Resilient Modulus of Unbound materials (with Borrow Material).

Strength Properties	Base	Borrow	Subgrade
R-value	80	78	44
Resilient Modulus(psi) (NDOT)	36,929	34,511	10,918
Resilient Modulus(psi)(Developed model)	20,214	16,289	8,779

Table 7.7. Design Pavement Structure (With Borrow Material).

Mr Equation	Pavement Thickness (inch)		
	AC	Base	Borrow
Current NDOT	6	10	8
Developed Model	7	10	8
Developed Model with 26000 psi Base	6.5	10	8

Chapter 8. CONCLUSIONS AND RECOMMENDATIONS

The major objective of this study is to develop a resilient modulus prediction model for unbound materials to be used for new design and rehabilitation projects in NDOT District 1. This objective was achieved by sampling and testing of different base, borrow, and subgrade materials from District 1. The classifications of materials were conducted according to AASHTO and UCSE systems. The maximum dry density and optimum moisture content relationships were obtained by conducting moisture-density tests for all materials. The resilient modulus and unconfined compressive strength tests were conducted on the evaluated materials at the optimum moisture content. Two different approaches were used to determine the design resilient modulus; a) for new design and b) for rehabilitation design.

Based on the generated data conducted from the experiment and the statistical analyses, the following observations and conclusions can be made:

- The stress dependent behavior of the resilient modulus for the base and borrow material fits very well the Theta model.
- The stress dependent behavior of resilient modulus for the subgrade materials fits very well both the universal model and Uzan model.
- The resilient modulus of base and borrow materials is significantly influenced by the pavement structure.
- The design resilient modulus of the subgrade layer for new pavement designs can be predicted based on UCS or R-value from the following models.

$$\ln(Mr_{SG-New}) = 7.4514 + 0.0036*P\#200 - 0.0129*P\#3/8 + 0.0158*\gamma_d + 0.0973*UCS + 0.0311*PI \quad (48)$$

$$\ln(Mr_{SG-New}) = 3.1784 + 0.018*\text{R-value} + 0.0136*P\#40 + 0.0315*\gamma_d + 0.0433*PI \quad (49)$$

- The design resilient modulus of the subgrade layer for rehabilitation pavement designs can be predicted based on UCS or R-value from the following models.

$$\ln(Mr_{SG-Reh}) = 9.2335 + 0.0028*P\#200 - 0.0045*P\#3/8 - 0.0401*OMC + 0.0318*UCS + 0.0158*PI \quad (50)$$

$$\ln(Mr_{SG-Reh}) = 5.3982 + 0.0134*\text{R-value} + 0.0125*P\#40 - 0.0032*P\#3/8 + 0.0168*\gamma_d + 0.0177*PI \quad (51)$$

- The design resilient modulus of the base layer for new pavement and rehabilitation pavement designs can be predicted based on R-value from the following models.

$$\ln(Mr_{CAB-New}) = 7.3224 + 0.0366 * \text{R-value} - 0.0656 * P\#40 + 0.0256 * P\#3/8 - 0.0893 * OMC - 0.0270 * H_{eq} \quad (52)$$

$$\ln(Mr_{CAB-Reh}) = 8.0140 + 0.0261 * \text{R-value} - 0.0485 * P\#40 + 0.0161 * P\#3/8 - 0.0659 * OMC - 0.0089 * H_{eq} \quad (53)$$

- The design resilient modulus of the borrow layer for new pavement and rehabilitation pavement designs can be predicted based on R-value from the following models.

$$\ln(Mr_{BOR-New}) = 8.9671 + 0.0102 * \text{R-value} + 0.0123 * P\#3/8 - 0.0743 * OMC - 0.0189 * H_{eq} \quad (54)$$

$$\ln(Mr_{BOR-Reh}) = 9.2304 + 0.0136 * \text{R-value} - 0.0229 * P\#40 + 0.0079 * P\#3/8 - 0.0661 * OMC - 0.0127 * H_{eq} \quad (55)$$

- The equivalent thickness (H_{eq}) is calculated for the layer being analyzed using Equations 56 to 59 based on the depth of location for state of stress calculation (base, borrow, and subgrade).

$$H_{eqNew-CAB} = 2.2432 * D - 1.9263 \quad (56)$$

$$H_{eqNew-Bor} = 1.3211 * D + 9.6409 \quad (57)$$

$$H_{eqReh-CAB} = 2.399 * D - 1.7468 \quad (58)$$

$$H_{eqReh-BOR} = 1.543 * D + 8.044 \quad (59)$$

  For example:

  - New Design:
    - 5 inch of AC layer on top of 10 inch of CAB layer on top of SG.
    - Depth of interest for the CAB layer is at its quarter depth, D = 5 + 10/4 = 7.5 inch.
    - Using Equation 56 and D of 7.5 inch, the equivalent thickness is: $H_{eqNew-CAB} = 2.2432 * 7.5 - 1.9263 = 14.90\ inch$
  - Rehabilitation Design:
    - 5 inch of AC layer on top of 10 inch of CAB layer on top of SG.
    - Depth of interest for the CAB layer is at its quarter depth, D = 5 + 10/4 = 7.5 inch.
    - Using Equation 58 and D of 7.5 inch, the equivalent thickness is: $H_{eqReh-CAB} = 2.399 * 7.5 - 1.7468 = 16.25\ inch$

It should be noted that the recommended models are best applicable for the range of data used in the development efforts. Similar effort is highly recommended for unbound and subgrade materials encountered in NDOT Districts 2 and 3. As additional materials from Districts 2 and 3 are evaluated, more robust prediction models can be developed and extensive database can be developed for the implementation of the AASHTO MEPDG.

Chapter 9. REFERENCES

1. AASHTO. (2008). *Mechanistic-Empirical Pavement Design Guide: A Manual of Practice: Interim Edition*. American Association of State Highway and Transportation Officials.
2. Hajj, E.Y., Sebaaly, P.E., and Nabhan, P. (2015). *Manual for Designing Flexible Pavements in Nevada using the AASHTOWare Pavement ME,* Western Regional Superpave Center, University of Nevada, Reno, Draft Final Report to Nevada DOT.
3. Schwartz, C. W., Li, R., Kim, S., Ceylan, H., and Gopalakrishnan, K. (2013). "Global Sensitivity Analysis of Mechanistic Empirical Pavement Design Guide for Flexible Pavements." *Transportation Research Record*, 2368, 12–23.
4. Von Quintus, H. L., Boudreau, R., and Cooley, A. (2015). *Precision and Bias of Resilient Modulus Test*. Washington D.C.
5. ARA, and ERES Consultants (2004). *Guide for Mechanistic-Emperical Design of New and Rehabilitated Pavement Structures - Final Report Chapter 2: Design Inputs-Material Characterizations*. National Cooperative Highway Research Program, Washington D.C.
6. Puppala, A. J. (2008). *Estimating Stiffness of Subgrades and Unbound Materials for Pavement Design*. Transportation Research Board, Washington D.C.
7. Yau, A., and Von Quintus, H. (2002). *Study of LTPP Laboratory Resilient Modulus Test Data and Response Characteristics*. Federal Highway Administration, Washington, D.C.
8. Ceylan, H., Kim, S., Gopalakrishnan, K., and Smadi, O. G. (2009). *MEPDG Work Plan Task No. 8 : Validation of Pavement Performance Curves for the Mechanistic-Empirical Pavement Design Guide MEPDG Work Plan Task No . 8 : Validation of Pavement Performance Curves for the Mechanistic-Empirical Pavement Design Guide Final R*. Iowa Department of Transportation, Ames, IA.
9. Mokwa, R., and Akin, M. (2009). *Measurement and Evaluation of Subgrade Soil Parameters: Phase I–Synthesis of Literature*. Montana Department of Transportation, Helena, MT.
10. Asphalt Institute (1981). *Thickness design--asphalt pavements for highways and streets* (No. 1).
11. ARA (2015). *Characterization of Material Properties for M-E Pavement Design in Wyoming - Draft Final Report*. University of Wyoming.
12. Yeh, S.-T., and Su, C.-K. (1989). *Resilient Properties of Colorado Soils*. Colorado Department of Highways, Denver, CO.
13. Mallela, J., Titus-Glover, L., Sadasivam, S., Bhattacharya, B., Darter, M., and Von Quintus, H. (2013). *Implementation of the AASHTO Mechanistic-Empirical Pavement Design Guide for Colorado*. Colorado Department of Transportation.
14. Von Quintus, H. L., Darter, M. M., Mallela, J., Bhattacharya, B., and Sadasivam, S.

(2013). *Verification and Local Calibration/Validation of the MEPDG Performance Models for Use in Georgia: Validation of the MEPDG Transfer Functions Using the LTPP Test Sections in Georgia Task 2 Interim Report*. Georgia Department of Transportation, Atlanta, GA.

15. Bayomy, F., El-Badawy, S., and Awed, A. (2011). *Implementation of the MEPDG for Flexible Pavements in Idaho*. Idaho Transportation Department, Boise, ID.
16. Baladi, G. Y., Dawson, T., and Sessions, C. (2009). *Pavement Subgrade MR Design Values for Michigan's Seasonal Changes, Final Report*. Michigan Department of Transportation, Construction and Technology Division, P.O. Box 30049, Lansing, MI 48909, Lansing, .
17. George, K. P. (2004). *Prediction of Resilient Modulus from Soils Index Proprieties*. Mississippi Department of Transportation.
18. George, K. P. (2003). *Falling Weight Deflectometer for Estimating Subgrade Moduli*. Mississippi Department of Transportation.
19. James, R. S., Cooley, A., and Ahlrich, R. C. (2010). *Summary of Lessons Learned from the MDOT MEPDG Materials Library Study*. Mississippi Department of Transportation.
20. Richardson, D., Petry, T., Ge, L., Han, Y.-P., and Lusher, S. M. (2009). *Resilient Moduli of Typical Missouri Soils and Unbound Granular Base Materials*. Missouri Department of Transportation.
21. Darter, M. I., Titus-Glover, L., and Von Quintus, H. L. (2009). *Mechanistic-Empirical Pavement Design Guide in Utah: Validation, Calibration, and Development of the UDOT MEPDG User's Guide*. Utah Department of Transportation, Salt Lake City.
22. Jackson, K. D. (2015). "Laboratory Resilient Modulus Measurements of Aggregate Base Materials in Utah." Brigham Young University.
23. Titi, H., Elias, M., and Helwany, S. (2006). *Determination of Typical Resilient Modulus Values for Selected Soils in Wisconsin*. Wisconsin Department of Transportation, Wisconsin.
24. Eggen, P., and Brittnacher, D. (2004). *Determination of Influences on Support Strength of Crushed Aggregate Base Course Due to Gradational , Regional and Source Variations*. Wisconsin Department of Transportation, Wisconsin.
25. Hicks, R. G., & Monismith, C. L. (1971). Factors influencing the resilient response of granular materials. *Highway research record*, (345).
26. Uzan, J., Witczak, M. W., Scullion, T., & Lytton, R. L. (1992). Development and validation of realistic pavement response models. In *International Conference on Asphalt Pavements, 7th, 1992, Nottingham, United Kingdom* (Vol. 1).
27. AASHTO Design Guide (1993). *Guide for Design of Pavement Structures.* American Association of State Highway and Transportation Officials, p. 700.

28. NCHRP 1-37A (2004). "Guide for Mechanistic-Empirical Design of New and Rehabilitated Pavement Structures." Final Report for NCHRP 1-37A Project. Available online at: http://www.trb.org/mepdg/guide.htm

29. AASHTOWare Pavement ME Design software. American Association of State Highway and Transportation Officials (AASHTO), http://me-design.com/MEDesign/.

30. 3D-Move Analysis software® V2.1. (2013). Reno, NV. Available online at: http://www.arc.unr.edu/Software.html#3DMove, last accessed September 19, 2017.

31. Khazanovich, L., Celauro, C., Chadbourn, B., Zollars, J., & Dai, S. (2006). Evaluation of subgrade resilient modulus predictive model for use in mechanistic-empirical pavement design guide. *Transportation Research Record: Journal of the Transportation Research Board*, *1947*, pp. 155-166.

32. Nabizadeh, H., Hajj, E. Y., Siddharthan, R., Elfass, S., Sebaaly, P. E. (2016). "Estimation of In-Situ Shear Strength Parameters for Subgrade Layer Using Non-destructive Testing." *The Roles of Accelerated Pavement Testing in Pavement Sustainability*, pp. 525-538, Springer, Cham

33. Nabizadeh, H., Hajj, E. Y., Siddharthan, R., Elfass, S., Nimeri, N. (2017). "Application of Falling Weight Deflectometer for the Estimation of in-situ Shear Strength Parameters of Subgrade layer." *Bearing Capacity of Roads, Railways and Airfields*, pp. 743-749, Taylor & Francis Group.

34. Thompson, M. R., & Elliot, R. P. (1985). ILLI-PAVE based response algorithms for design of conventional flexible pavements. *Transportation Research Record: Journal of the Transportation Research Board*, *1043*, 50-57.

35. R Core Team (2017). R: A language and environment for statistical computing. R Foundation for Statistical Computing, Vienna, Austria.

36. D'Agostino, R. B. (1986). Tests for the normal distribution. *Goodness-of-fit techniques*, *68*, p. 576.

37. Fox, J., & Monette, G. (1992). Generalized collinearity diagnostics. *Journal of the American Statistical Association*, *87*(417), pp. 178-183.

APPENDIX A

Laboratory test results are shown in this appendix, including moisture density and resilient modulus test.

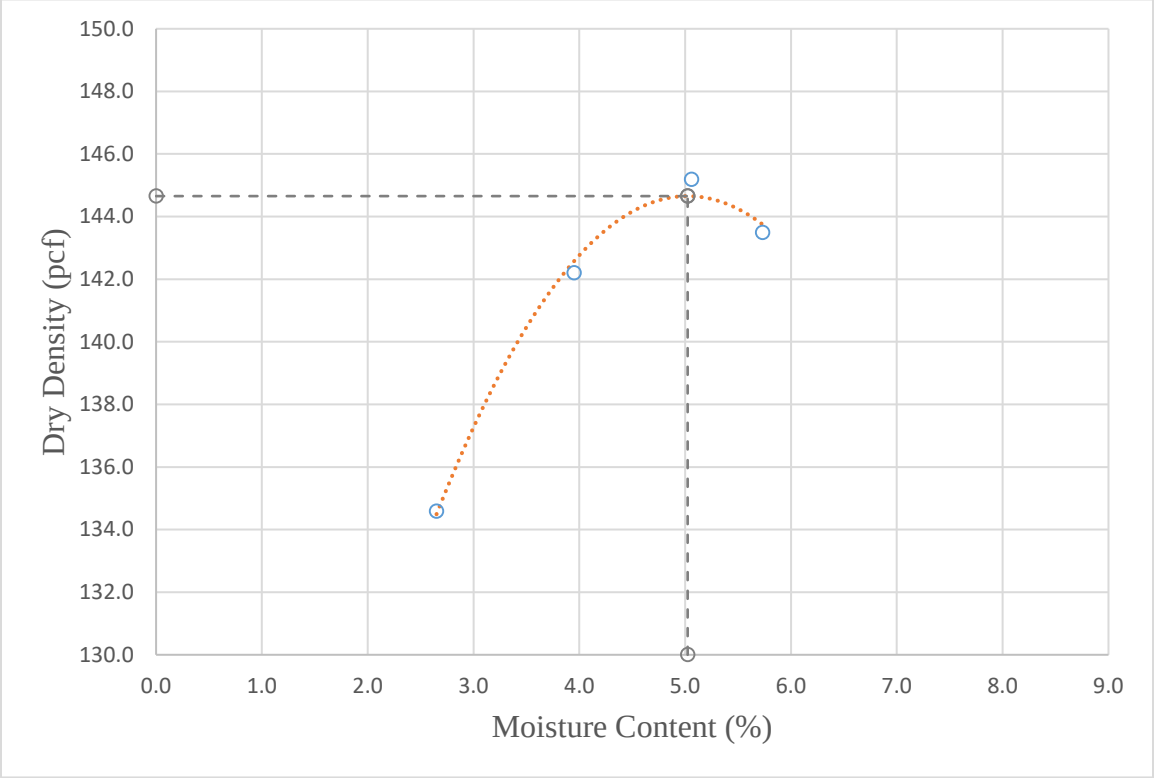

Figure A.1. Moisture-density curve for base material (contract 3546).

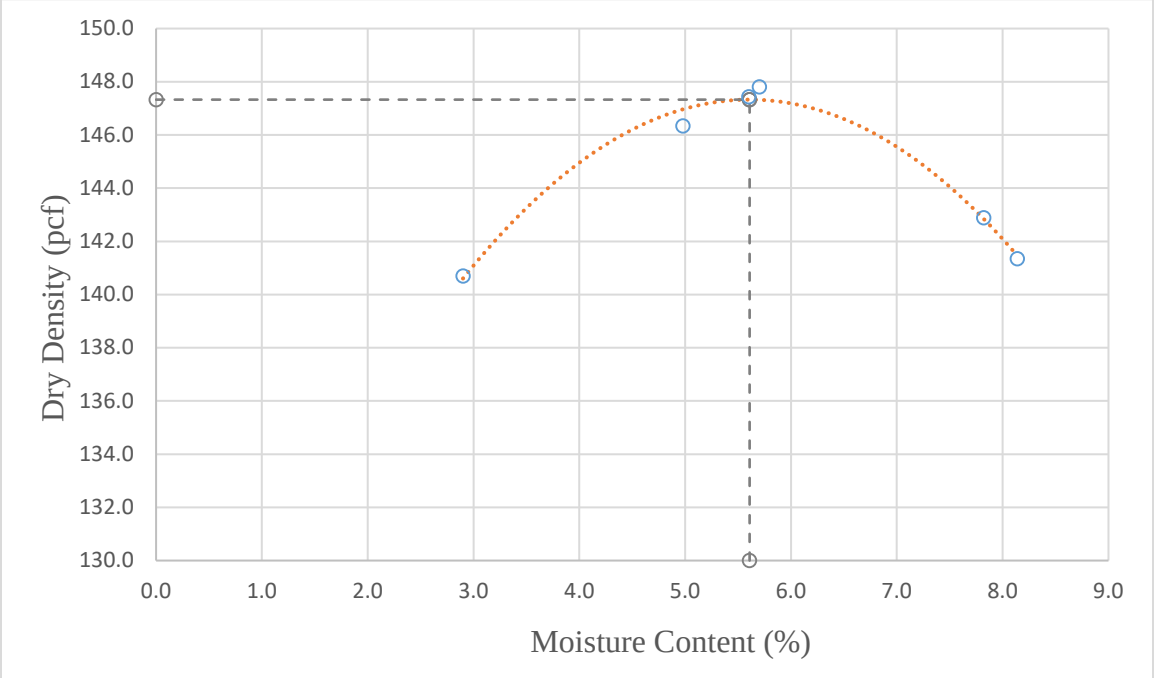

Figure A.2. Moisture-density curve for base material (contract 3583).

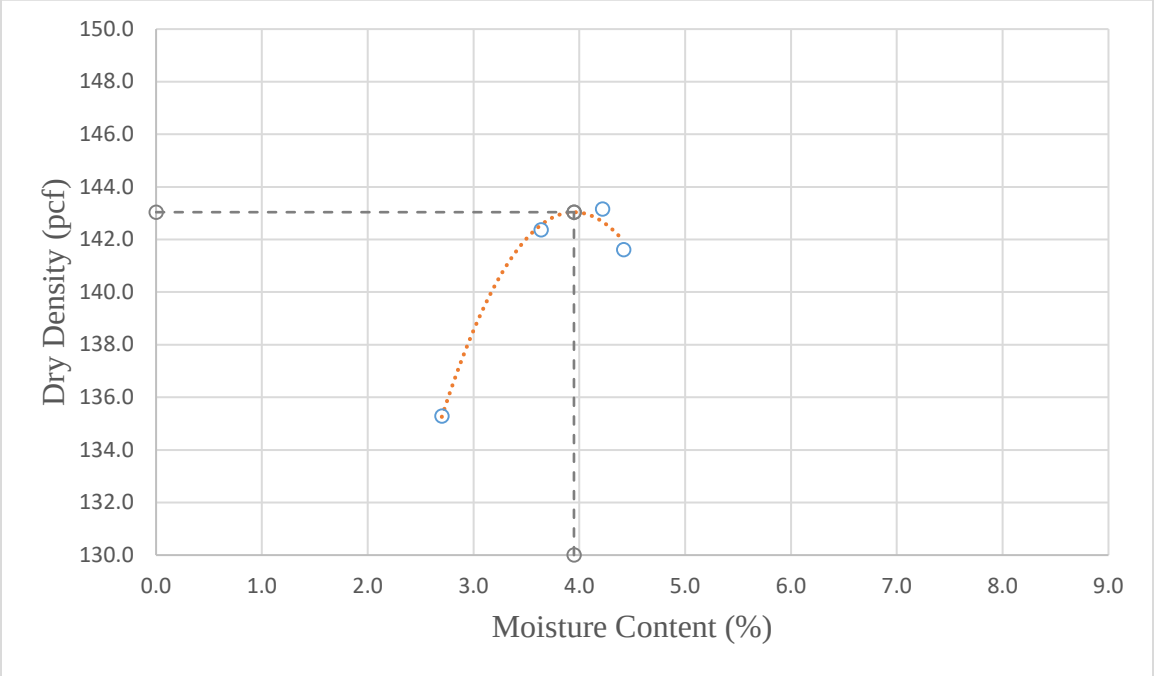

Figure A.3. Moisture-density curve for base material (contract 3597).

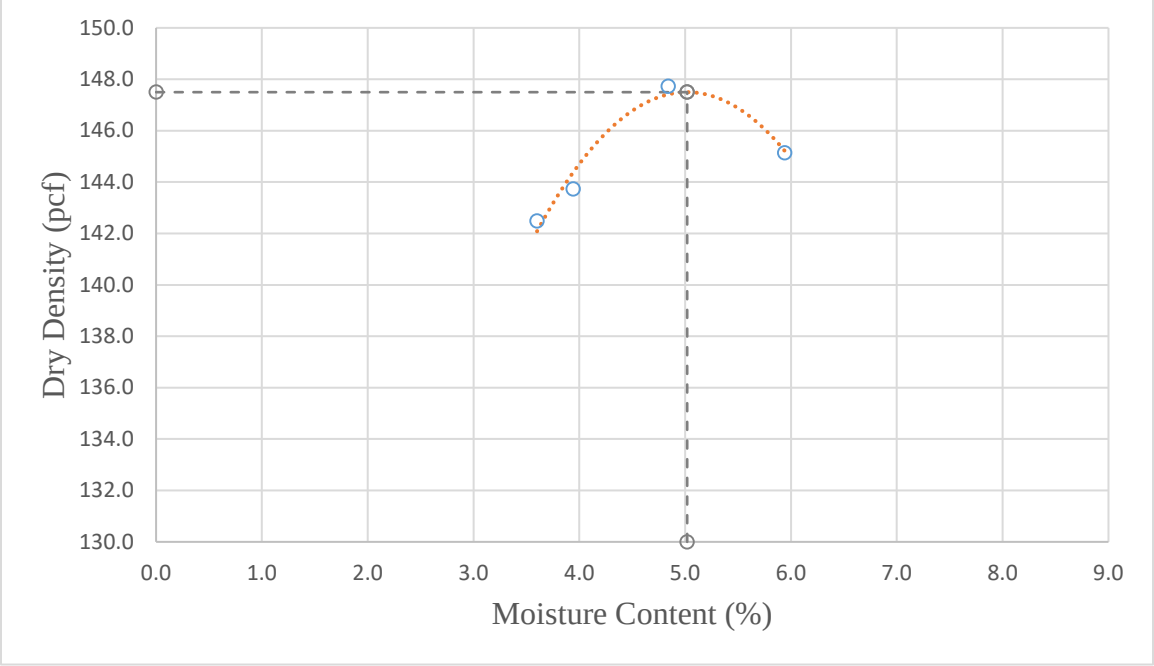

Figure A.4. Moisture-density curve for base material (contract 3605).

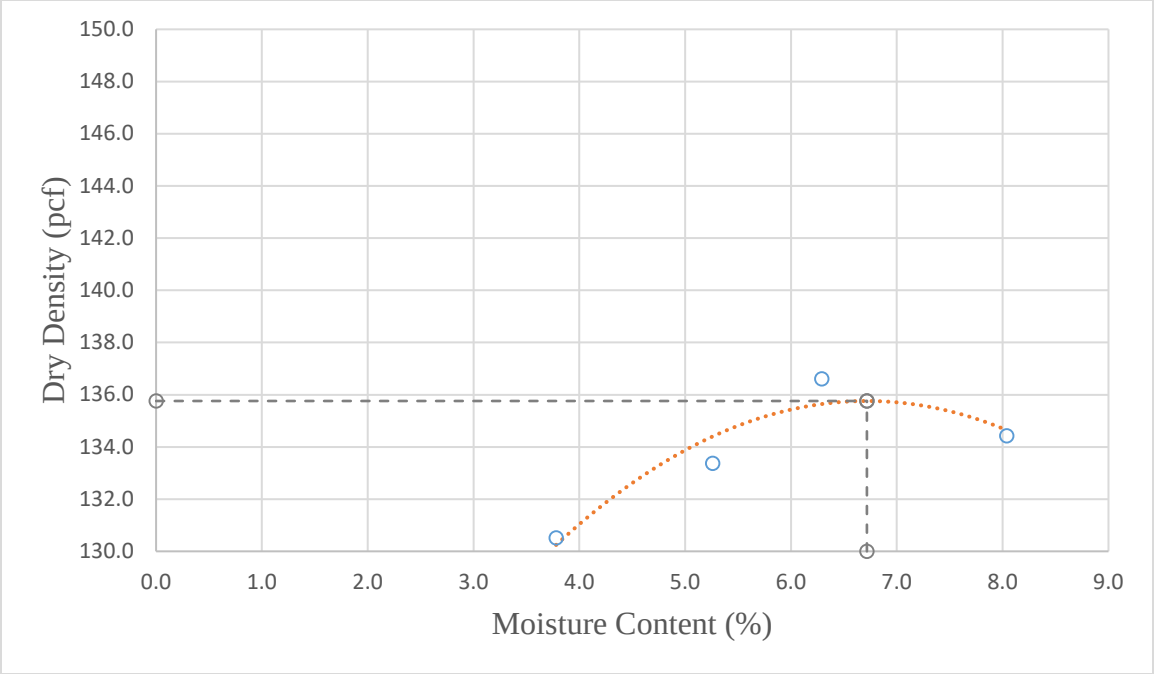

Figure A.5. Moisture-density curve for base material (contract 3607).

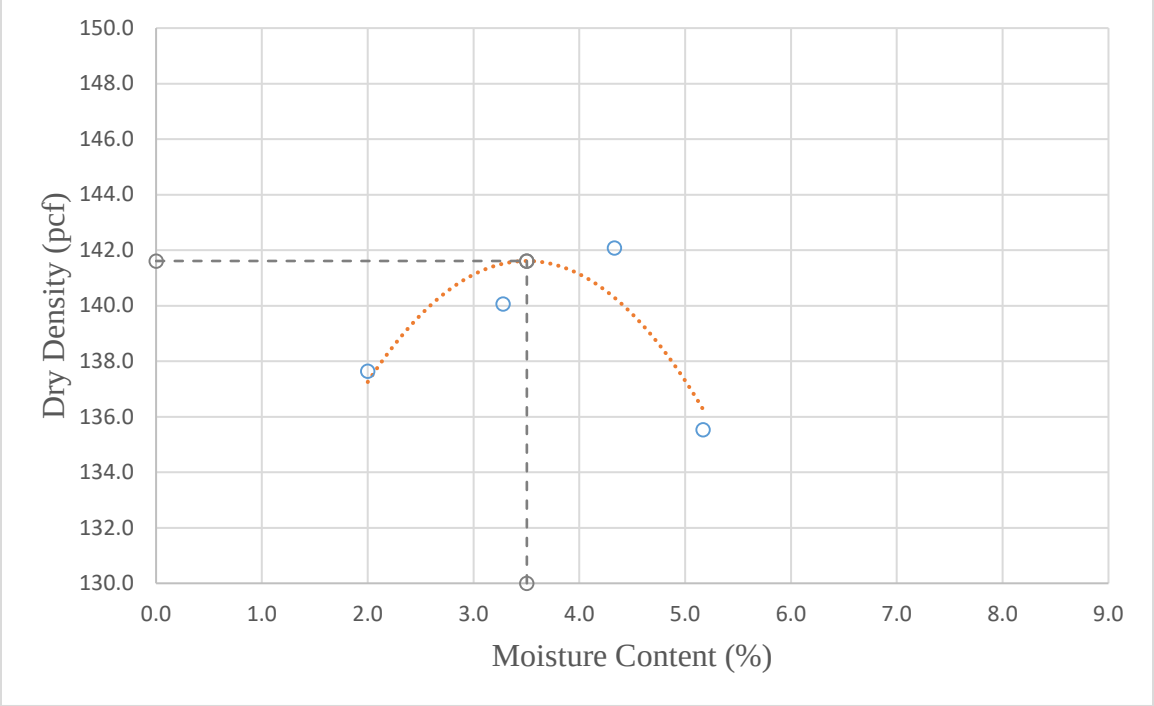

Figure A.6. Moisture-density curve for base material (contract 3613).

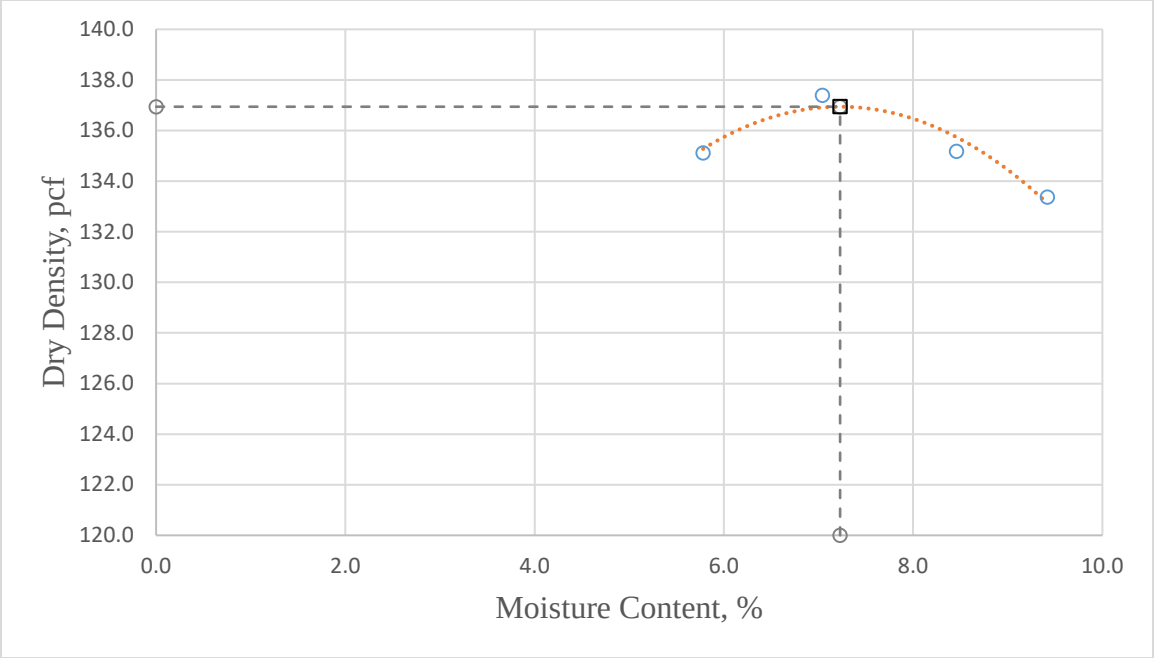

Figure A.7. Moisture-density curve for borrow material (contract 3546).

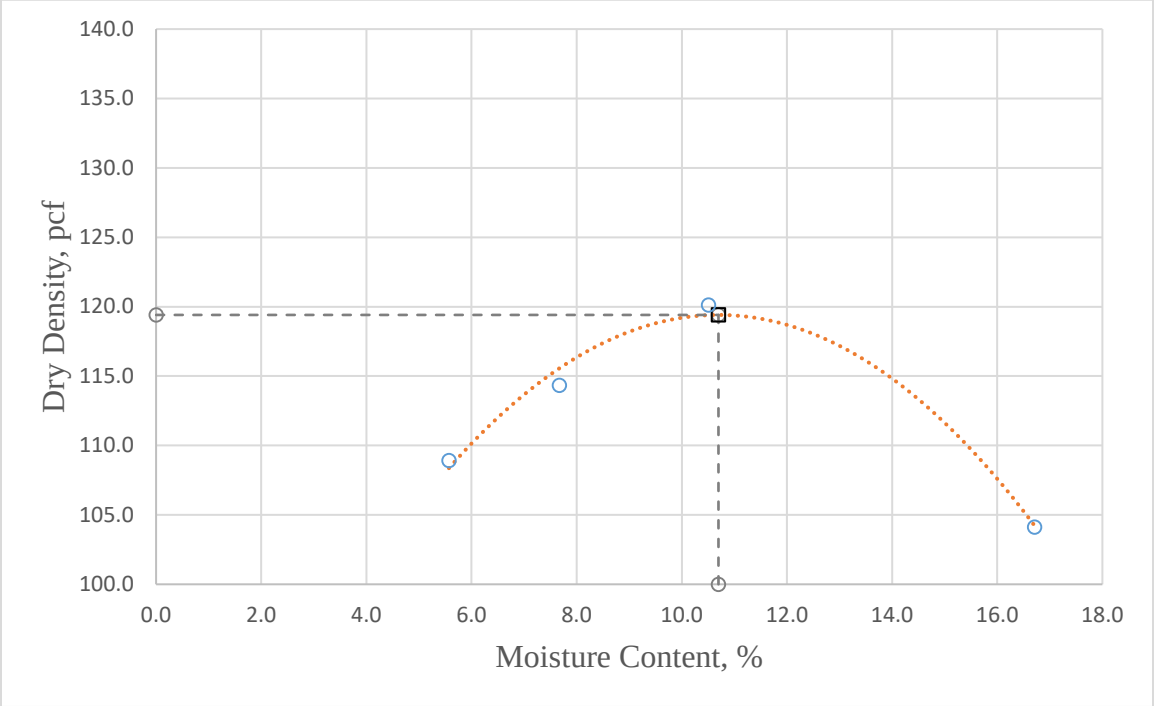

Figure A.8. Moisture-density curve for borrow material (contract 3583).

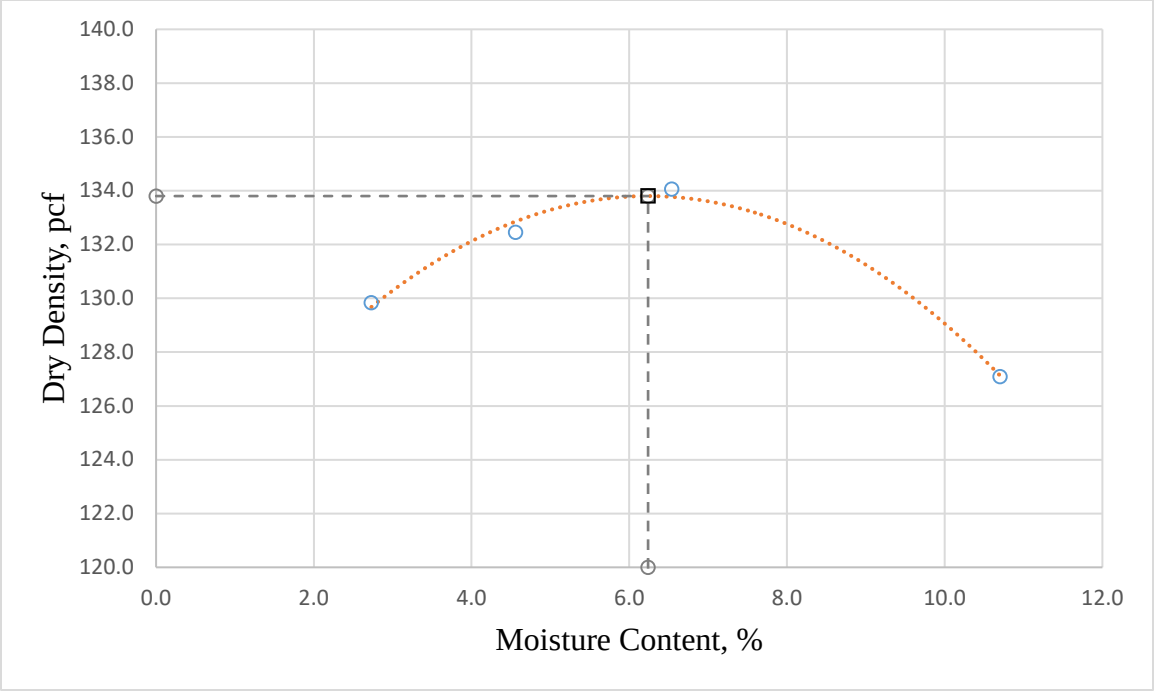

Figure A.9. Moisture-density curve for borrow material (contract 3597).

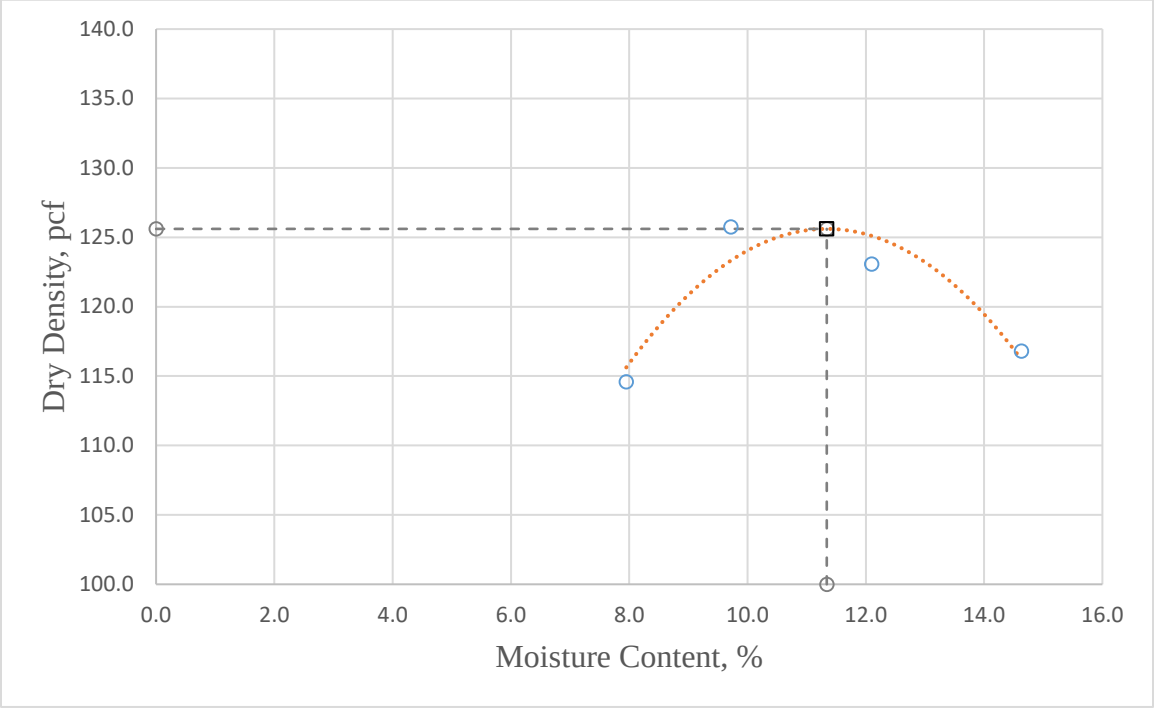

Figure A.10. Moisture-density curve for borrow material (contract 3607).

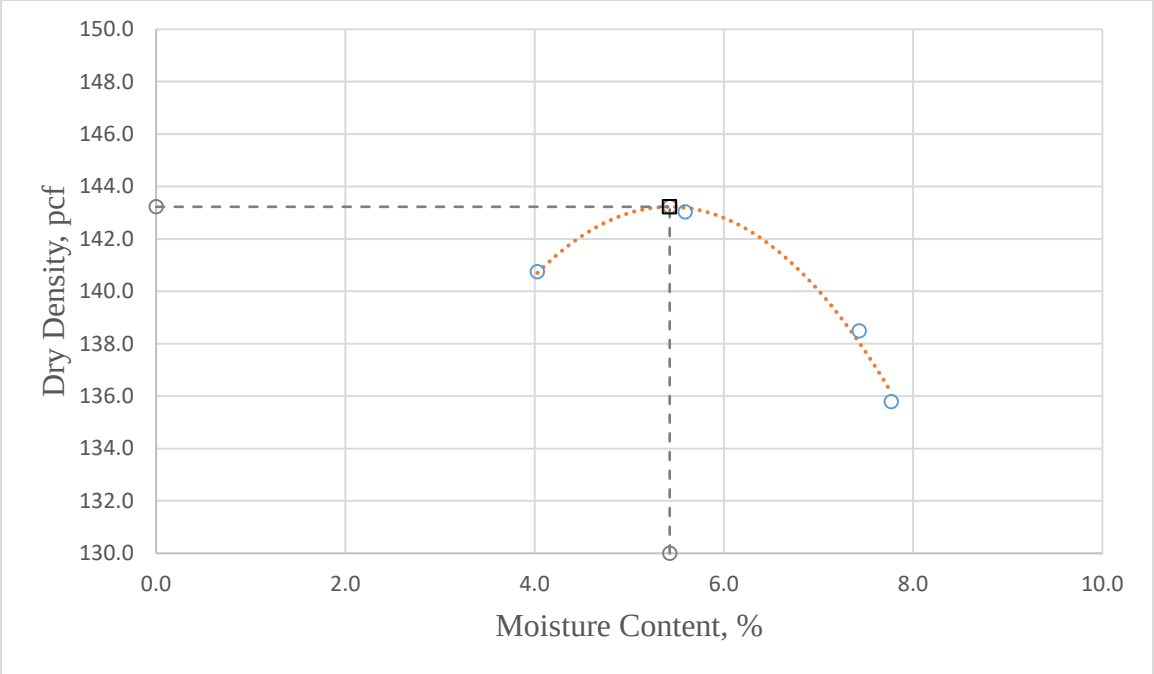

Figure A.11. Moisture-density curve for borrow material (contract 3613).

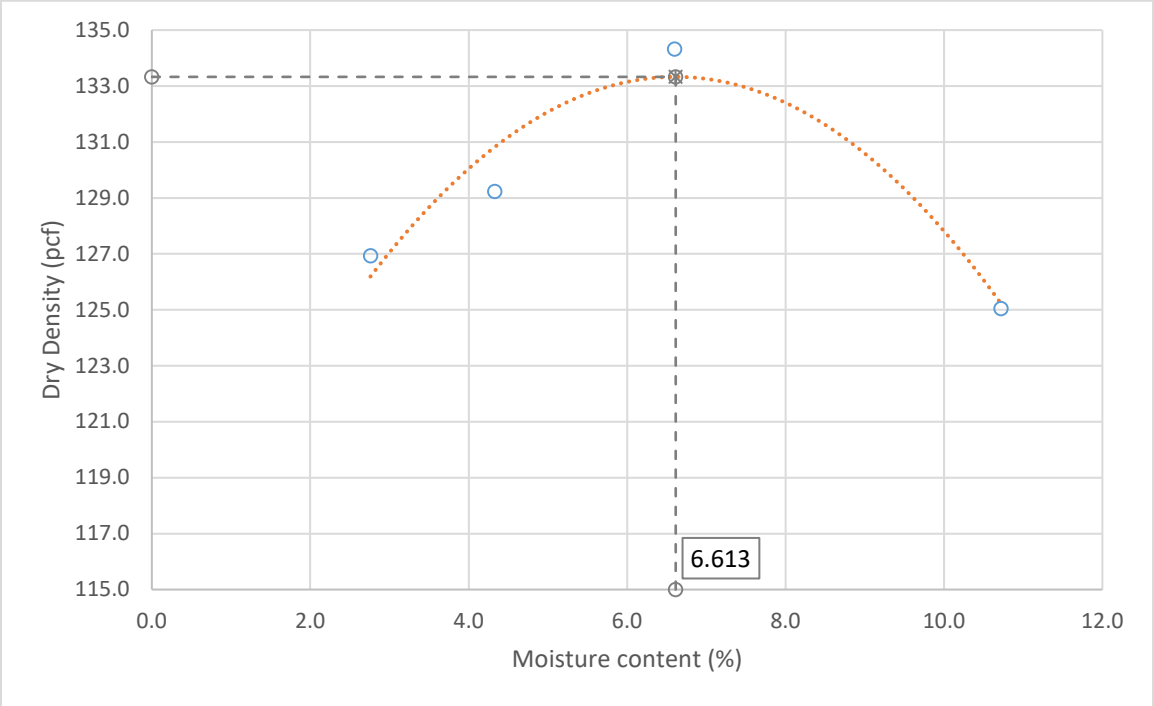

Figure A.12. Moisture-density curve for subgrade material (US-95/Searchlight).

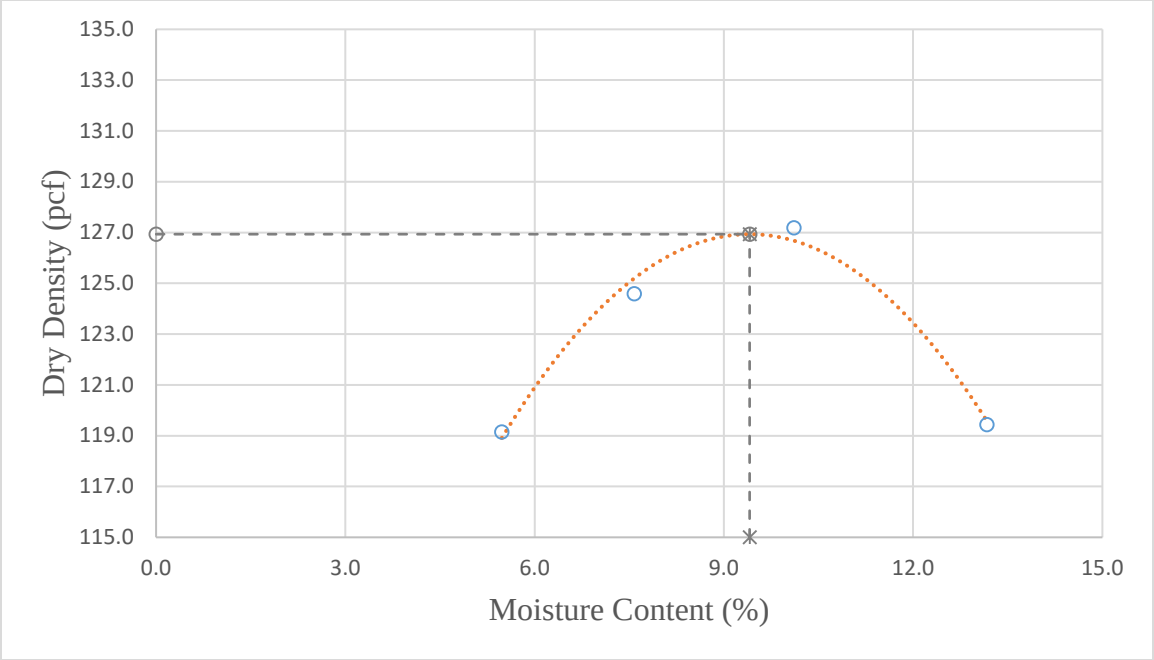

Figure A.13. Moisture-density curve for subgrade material (US-95/Bonnie Claire).

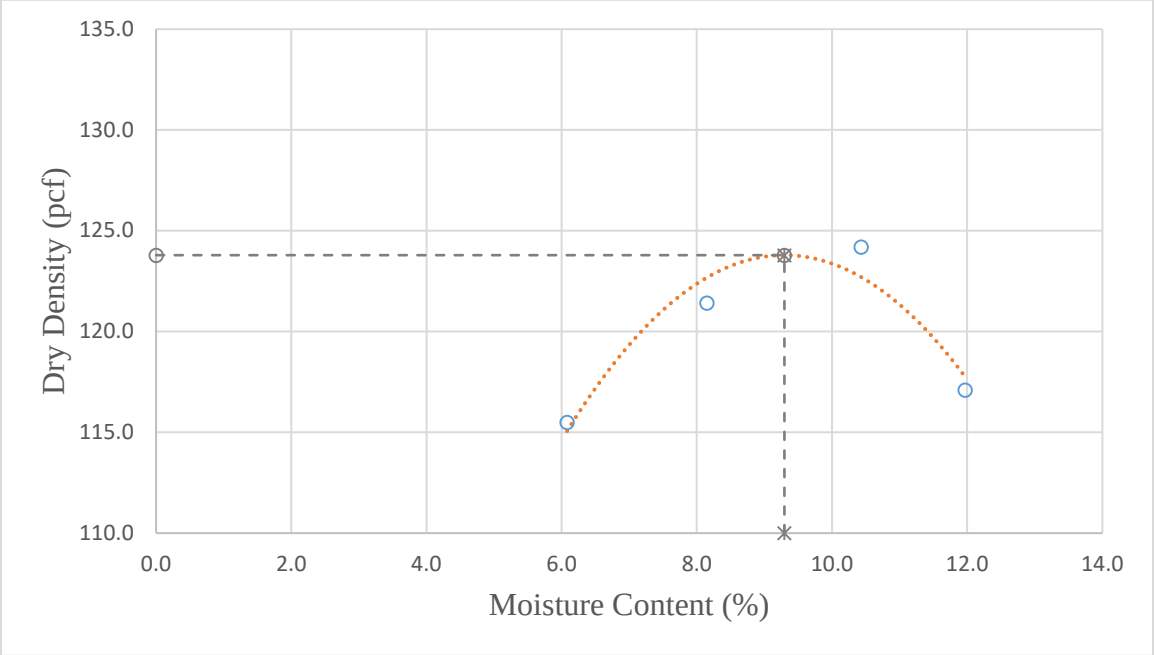

Figure A.14. Moisture-density curve for subgrade material US-93/Crystal Spring MP67).

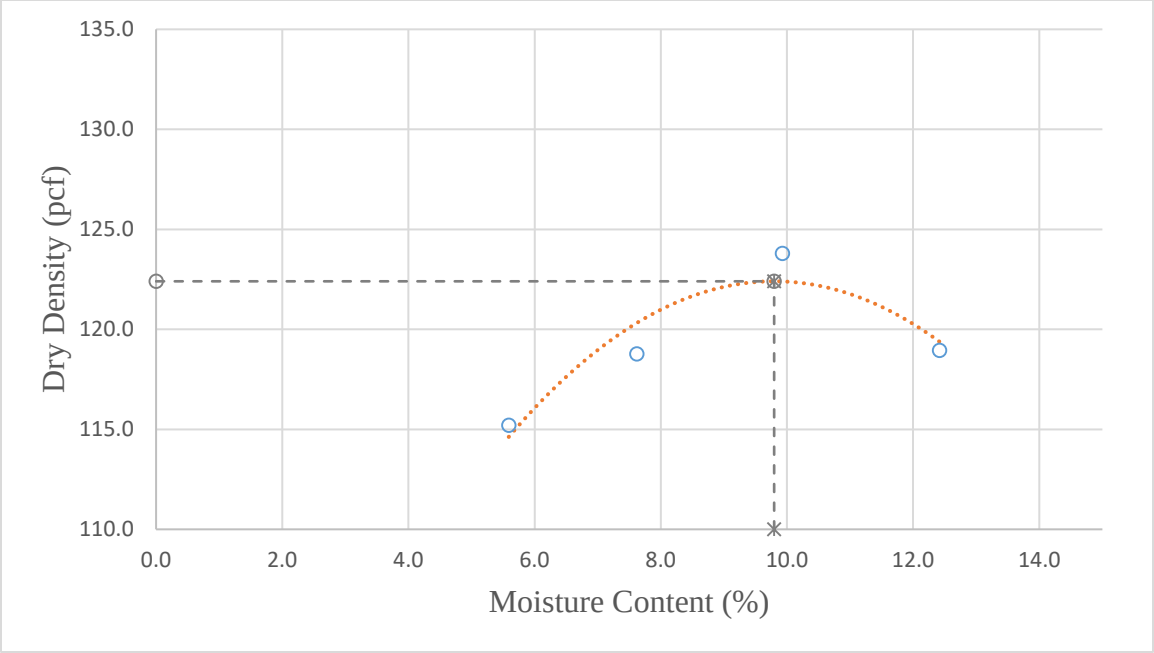

Figure A.15. Moisture-density curve for subgrade material (US-93/Crystal Spring MP62).

Table A.1. Summary of Resilient Modulus Test Results for Base Material (Contract 3546).

Sequence	Cyclic Axial Stress (psi)	Contact Stress (psi)	Confine Stress (psi)	Axial Resilient Modulus (psi)	Deviator Stress, σd (psi)	Sigma 1 (psi)	Sigma 3 (psi)	Bulk Stress,θ (psi)	Octahedral Shear Stress (psi)
1	13.5	1.5	14.8	46,385	15.0	29.8	14.8	59.5	7.1
2	2.7	0.3	2.8	22,854	3.0	5.8	2.8	11.4	1.4
3	5.3	0.6	2.8	23,661	5.9	8.8	2.8	14.4	2.8
4	8.1	0.9	2.8	25,371	9.0	11.8	2.8	17.5	4.2
5	4.5	0.5	4.8	25,231	5.0	9.9	4.8	19.5	2.4
6	9.0	1.0	4.8	28,698	10.0	14.8	4.8	24.4	4.7
7	13.5	1.5	4.8	30,357	15.0	19.9	4.8	29.5	7.1
8	9.0	1.0	9.8	35,372	10.0	19.8	9.8	39.4	4.7
9	18.0	2.0	9.8	41,542	20.0	29.8	9.8	49.5	9.4
10	26.8	3.0	9.8	43,812	29.8	39.7	9.8	59.3	14.1
11	9.0	1.0	14.8	39,750	10.0	24.8	14.8	54.5	4.7
12	13.5	1.5	14.8	43,625	15.0	29.8	14.8	59.4	7.1
13	26.8	3.0	14.8	49,674	29.8	44.6	14.8	74.3	14.0
14	13.7	1.5	19.8	49,374	15.2	35.0	19.8	74.6	7.1
15	18.1	2.0	19.8	53,101	20.1	39.9	19.8	79.6	9.5
16	34.6	4.0	19.8	59,304	38.6	58.4	19.8	98.0	18.2

Table A.2. Summary of Resilient Modulus Test Results for Base Material (Contract 3583).

Sequence	Cyclic Axial Stress (psi)	Contact Stress (psi)	Confine Stress (psi)	Axial Resilient Modulus (psi)	Deviator Stress, σd (psi)	Sigma 1 (psi)	Sigma 3 (psi)	Bulk Stress,θ (psi)	Octahedral Shear Stress (psi)
1	13.4	1.5	14.9	37,900	14.9	29.9	14.9	59.8	7.0
2	2.7	0.3	2.9	17,271	3.0	5.9	2.9	11.8	1.4
3	5.4	0.6	2.9	19,119	6.0	8.9	2.9	14.8	2.8
4	8.0	0.9	3.0	20,614	8.9	11.9	3.0	17.8	4.2
5	4.5	0.5	4.9	21,228	5.0	10.0	4.9	19.9	2.4
6	9.0	1.0	4.9	24,154	10.0	15.0	4.9	24.9	4.7
7	13.4	1.5	5.0	26,025	14.9	19.9	5.0	29.8	7.0
8	9.0	1.0	10.0	30,687	10.0	19.9	10.0	39.9	4.7
9	18.0	2.0	9.9	33,837	20.0	29.9	9.9	49.8	9.4
10	27.0	3.0	9.9	35,517	30.0	40.0	9.9	59.9	14.2
11	9.0	1.0	14.9	32,838	10.0	24.9	14.9	54.8	4.7
12	13.5	1.5	15.0	35,322	15.0	30.0	15.0	59.9	7.1
13	26.9	3.0	15.0	40,462	29.9	44.8	15.0	74.8	14.1
14	13.7	1.5	19.9	39,028	15.2	35.1	19.9	75.0	7.2
15	18.1	2.0	19.9	41,872	20.1	40.0	19.9	79.9	9.5
16	17.4	4.0	19.9	38,051	21.4	41.4	19.9	81.3	10.1

Table A.3. Summary of Resilient Modulus Test Results for Base Material (Contract 3597).

Sequence	Cyclic Axial Stress (psi)	Contact Stress (psi)	Confine Stress (psi)	Axial Resilient Modulus (psi)	Deviator Stress, σd (psi)	Sigma 1 (psi)	Sigma 3 (psi)	Bulk Stress,θ (psi)	Octahedral Shear Stress (psi)
1	13.5	1.5	14.7	43,837	15.0	29.7	14.7	59.2	7.1
2	2.7	0.3	2.7	18,985	3.0	5.7	2.7	11.2	1.4
3	5.4	0.6	2.7	21,208	6.0	8.8	2.7	14.2	2.8
4	8.0	0.9	2.7	22,543	8.9	11.6	2.7	17.1	4.2
5	4.5	0.5	4.7	23,140	5.1	9.8	4.7	19.3	2.4
6	9.0	1.0	4.7	26,244	10.0	14.7	4.7	24.2	4.7
7	13.5	1.5	4.7	28,732	15.0	19.7	4.7	29.2	7.1
8	9.1	1.0	9.7	32,788	10.1	19.9	9.7	39.4	4.8
9	18.0	2.0	9.7	38,023	20.1	29.8	9.7	49.3	9.5
10	26.9	3.0	9.7	40,903	29.9	39.7	9.7	59.1	14.1
11	9.0	1.0	14.7	36,665	10.0	24.8	14.7	54.2	4.7
12	13.5	1.5	14.7	39,178	15.0	29.7	14.7	59.2	7.1
13	26.9	3.0	14.7	47,096	29.9	44.6	14.7	74.1	14.1
14	13.6	1.5	19.7	43,398	15.1	34.8	19.7	74.3	7.1
15	18.2	2.0	19.7	49,003	20.3	40.0	19.7	79.5	9.5
16	34.5	4.0	19.7	56,815	38.5	58.3	19.7	97.7	18.2

Table A.4. Summary of Resilient Modulus Test Results for Base Material (Contract 3605).

Sequence	Cyclic Axial Stress (psi)	Contact Stress (psi)	Confine Stress (psi)	Axial Resilient Modulus (psi)	Deviator Stress, σd (psi)	Sigma 1 (psi)	Sigma 3 (psi)	Bulk Stress,θ (psi)	Octahedral Shear Stress (psi)
1	13.5	1.5	15.0	38,800	15.0	29.9	15.0	59.8	7.1
2	2.7	0.3	3.0	15,056	3.0	6.0	3.0	11.9	1.4
3	5.3	0.6	3.0	16,734	5.9	8.9	3.0	14.8	2.8
4	8.1	0.9	2.9	18,600	9.0	12.0	2.9	17.9	4.3
5	4.4	0.5	5.0	19,680	5.0	9.9	5.0	19.8	2.3
6	9.1	1.0	4.9	22,302	10.1	15.0	4.9	24.9	4.7
7	13.5	1.5	5.0	24,051	15.0	19.9	5.0	29.8	7.1
8	9.0	1.0	10.0	29,860	10.0	20.0	10.0	39.9	4.7
9	18.0	2.0	10.0	33,595	20.0	29.9	10.0	49.9	9.4
10	26.8	3.0	10.0	34,616	29.8	39.8	10.0	59.7	14.1
11	9.1	1.0	15.0	33,620	10.1	25.0	15.0	55.0	4.8
12	13.6	1.5	14.9	36,136	15.1	30.0	14.9	59.9	7.1
13	27.0	3.0	15.0	40,879	30.0	44.9	15.0	74.8	14.1
14	13.6	1.5	20.0	40,414	15.1	35.0	20.0	75.0	7.1
15	18.0	2.0	20.0	42,512	20.0	40.0	20.0	79.9	9.4
16	35.4	4.0	19.9	49,098	39.4	59.3	19.9	99.2	18.6

Table A.5. Summary of Resilient Modulus Test Results for Base Material (Contract 3607).

Sequence	Cyclic Axial Stress (psi)	Contact Stress (psi)	Confine Stress (psi)	Axial Resilient Modulus (psi)	Deviator Stress, σd (psi)	Sigma 1 (psi)	Sigma 3 (psi)	Bulk Stress,θ (psi)	Octahedral Shear Stress (psi)
1	13.5	1.5	14.3	37,768	15.0	29.3	14.3	57.9	7.1
2	2.7	0.3	2.3	14,357	3.0	5.3	2.3	9.9	1.4
3	5.4	0.6	2.3	15,807	6.0	8.3	2.3	12.9	2.8
4	8.1	0.9	2.3	17,012	9.0	11.3	2.3	15.9	4.2
5	4.5	0.5	4.3	17,810	5.0	9.3	4.3	17.9	2.4
6	8.9	1.0	4.3	20,323	9.9	14.2	4.3	22.8	4.7
7	13.6	1.5	4.3	22,873	15.1	19.4	4.3	28.0	7.1
8	9.0	1.0	9.3	27,093	10.0	19.3	9.3	37.9	4.7
9	18.0	2.0	9.3	32,894	20.0	29.3	9.3	47.9	9.4
10	27.0	3.0	9.3	35,618	30.0	39.3	9.3	57.9	14.1
11	9.1	1.0	14.3	32,890	10.1	24.4	14.3	53.0	4.8
12	13.4	1.5	14.3	36,272	14.9	29.2	14.3	57.8	7.0
13	27.0	3.0	14.3	42,799	30.0	44.3	14.3	72.9	14.1
14	14.0	1.5	19.3	41,969	15.5	34.8	19.3	73.4	7.3
15	18.2	2.0	19.3	44,864	20.2	39.5	19.3	78.1	9.5
16	35.2	4.0	19.3	51,748	39.2	58.5	19.3	97.1	18.5

Table A.6. Summary of Resilient Modulus Test Results for Base Material (Contract 3613).

Sequence	Cyclic Axial Stress (psi)	Contact Stress (psi)	Confine Stress (psi)	Axial Resilient Modulus (psi)	Deviator Stress, σd (psi)	Sigma 1 (psi)	Sigma 3 (psi)	Bulk Stress,θ (psi)	Octahedral Shear Stress (psi)
1	13.7	1.5	15.0	38,859	15.1	30.1	15.0	60.1	7.1
2	2.7	0.3	3.0	17,223	3.0	6.0	3.0	11.9	1.4
3	5.3	0.6	3.0	18,871	5.9	8.8	3.0	14.8	2.8
4	8.5	0.9	3.0	21,026	9.4	12.4	3.0	18.3	4.4
5	4.4	0.5	5.0	21,262	4.9	9.9	5.0	19.8	2.3
6	8.9	1.0	5.0	23,960	9.9	14.9	5.0	24.8	4.7
7	13.4	1.5	5.0	25,751	14.9	19.9	5.0	29.9	7.0
8	8.9	1.0	10.0	30,775	9.9	19.9	10.0	39.9	4.7
9	17.9	2.0	10.0	33,889	19.9	29.9	10.0	49.8	9.4
10	27.0	3.0	10.0	35,301	30.0	39.9	10.0	59.9	14.1
11	9.0	1.0	15.0	32,603	10.0	25.0	15.0	55.0	4.7
12	13.5	1.5	15.0	35,350	15.0	30.0	15.0	59.9	7.1
13	27.0	3.0	15.0	40,558	30.0	45.0	15.0	75.0	14.2
14	13.6	1.5	20.0	39,540	15.1	35.1	20.0	75.0	7.1
15	18.2	2.0	20.0	42,611	20.2	40.1	20.0	80.1	9.5
16	35.2	4.0	20.0	48,969	39.2	59.1	20.0	99.1	18.5

Table A.7. Summary of Resilient Modulus Test Results for Borrow Material (Contract 3546).

Sequence	Cyclic Axial Stress (psi)	Contact Stress (psi)	Confine Stress (psi)	Axial Resilient Modulus (psi)	Deviator Stress, σd (psi)	Sigma 1 (psi)	Sigma 3 (psi)	Bulk Stress,θ (psi)	Octahedral Shear Stress (psi)
1	13.5	1.5	14.8	36,969	15.0	29.8	14.8	59.3	7.1
2	2.7	0.3	2.8	15,355	3.0	5.8	2.8	11.4	1.4
3	5.5	0.6	2.8	17,586	6.1	8.9	2.8	14.5	2.9
4	8.2	0.9	2.8	18,860	9.1	11.8	2.8	17.4	4.3
5	4.4	0.5	4.8	19,484	4.9	9.7	4.8	19.3	2.3
6	8.9	1.0	4.8	22,107	9.9	14.7	4.8	24.2	4.7
7	13.4	1.5	4.8	23,425	14.9	19.7	4.8	29.2	7.0
8	9.0	1.0	9.8	28,556	10.0	19.8	9.8	39.3	4.7
9	18.0	2.0	9.8	32,585	20.0	29.8	9.8	49.4	9.4
10	27.0	3.0	9.8	34,008	30.0	39.7	9.8	59.3	14.1
11	9.1	1.0	14.8	32,001	10.1	24.9	14.8	54.4	4.8
12	13.5	1.5	14.8	33,651	15.0	29.7	14.8	59.3	7.1
13	27.0	3.0	14.8	38,956	30.0	44.8	14.8	74.3	14.1
14	13.8	1.5	19.8	37,861	15.3	35.0	19.8	74.5	7.2
15	18.1	2.0	19.8	40,689	20.1	39.8	19.8	79.4	9.5
16	35.1	4.0	19.8	46,956	39.1	58.9	19.8	98.4	18.4

Table A.8. Summary of Resilient Modulus Test Results for Borrow Material (Contract 3583).

Sequence	Cyclic Axial Stress (psi)	Contact Stress (psi)	Confine Stress (psi)	Axial Resilient Modulus (psi)	Deviator Stress, σd (psi)	Sigma 1 (psi)	Sigma 3 (psi)	Bulk Stress,θ (psi)	Octahedral Shear Stress (psi)
1	13.4	1.5	14.7	16,244	14.9	29.6	14.7	59.1	7.0
2	2.7	0.3	2.7	11,167	3.0	5.7	2.7	11.1	1.4
3	5.3	0.6	2.7	10,489	5.9	8.6	2.7	14.0	2.8
4	8.1	0.9	2.7	10,012	9.0	11.7	2.7	17.1	4.2
5	4.5	0.5	4.7	12,149	5.0	9.8	4.7	19.2	2.4
6	9.0	1.0	4.7	11,267	10.0	14.7	4.7	24.1	4.7
7	13.5	1.5	4.7	10,847	15.0	19.7	4.7	29.2	7.1
8	8.9	1.0	9.7	14,029	9.9	19.6	9.7	39.1	4.7
9	17.9	2.0	9.7	12,915	19.9	29.6	9.7	49.1	9.4
10	26.5	3.0	9.7	11,246	29.5	39.2	9.7	58.6	13.9
11	9.0	1.0	14.7	16,039	10.0	24.7	14.7	54.2	4.7
12	13.5	1.5	14.7	15,442	15.0	29.7	14.7	59.2	7.1
13	26.9	3.0	14.7	14,653	29.9	44.6	14.7	74.0	14.1
14	13.7	1.5	19.7	18,521	15.2	34.9	19.7	74.4	7.2
15	18.1	2.0	19.7	18,488	20.1	39.9	19.7	79.3	9.5
16	34.0	4.0	19.7	16,316	38.0	57.7	19.7	97.1	17.9

Table A.9. Summary of Resilient Modulus Test Results for Borrow Material (Contract 3597).

Sequence	Cyclic Axial Stress (psi)	Contact Stress (psi)	Confine Stress (psi)	Axial Resilient Modulus (psi)	Deviator Stress, σd (psi)	Sigma 1 (psi)	Sigma 3 (psi)	Bulk Stress,θ (psi)	Octahedral Shear Stress (psi)
1	13.5	1.5	14.6	35,264	15.0	29.6	14.6	58.8	7.1
2	2.7	0.3	2.6	16,966	3.0	5.6	2.6	10.9	1.4
3	5.4	0.6	2.6	17,628	6.0	8.6	2.6	13.9	2.8
4	8.1	0.9	2.6	18,718	9.0	11.6	2.6	16.8	4.2
5	4.5	0.5	4.6	19,896	5.1	9.7	4.6	18.9	2.4
6	9.1	1.0	4.6	21,766	10.1	14.7	4.6	23.9	4.8
7	13.5	1.5	4.6	23,047	15.0	19.6	4.6	28.8	7.1
8	8.9	1.0	9.6	27,102	9.9	19.5	9.6	38.8	4.7
9	18.0	2.0	9.6	30,128	20.0	29.6	9.6	48.8	9.4
10	26.9	3.0	9.6	31,053	29.9	39.5	9.6	58.7	14.1
11	9.1	1.0	14.6	29,872	10.1	24.7	14.6	53.9	4.8
12	13.6	1.5	14.6	32,406	15.1	29.8	14.6	59.0	7.1
13	27.2	3.0	14.6	37,144	30.2	44.8	14.6	74.0	14.2
14	13.7	1.5	19.6	37,280	15.2	34.8	19.6	74.0	7.2
15	18.0	2.0	19.6	39,087	20.0	39.6	19.6	78.9	9.4
16	35.0	4.0	19.6	44,426	39.0	58.6	19.6	97.8	18.4

Table A.10. Summary of Resilient Modulus Test Results for Borrow Material (Contract 3613).

Sequence	Cyclic Axial Stress (psi)	Contact Stress (psi)	Confine Stress (psi)	Axial Resilient Modulus (psi)	Deviator Stress, σd (psi)	Sigma 1 (psi)	Sigma 3 (psi)	Bulk Stress,θ (psi)	Octahedral Shear Stress (psi)
1	13.5	1.5	14.7	37,085	15.0	29.7	14.7	59.1	7.1
2	2.8	0.3	2.7	15,729	3.1	5.7	2.7	11.0	1.4
3	5.4	0.6	2.7	17,481	6.0	8.6	2.7	14.0	2.8
4	8.0	0.9	2.7	18,980	8.9	11.6	2.7	16.9	4.2
5	4.5	0.5	4.7	19,925	5.0	9.7	4.7	19.0	2.4
6	8.7	1.0	4.7	21,992	9.7	14.3	4.7	23.7	4.6
7	13.5	1.5	4.7	24,546	15.0	19.7	4.7	29.0	7.1
8	8.8	1.0	9.7	27,691	9.8	19.5	9.7	38.8	4.6
9	17.9	2.0	9.7	32,462	19.9	29.6	9.7	48.9	9.4
10	27.1	3.0	9.7	34,900	30.1	39.7	9.7	59.1	14.2
11	9.0	1.0	14.7	30,752	10.0	24.6	14.7	53.9	4.7
12	13.6	1.5	14.7	33,837	15.1	29.8	14.7	59.1	7.1
13	27.2	3.0	14.7	40,414	30.2	44.8	14.7	74.2	14.2
14	13.8	1.5	19.7	38,433	15.2	34.9	19.7	74.3	7.2
15	18.1	2.0	19.7	41,491	20.1	39.7	19.7	79.0	9.5
16	35.4	4.0	19.7	49,656	39.4	59.1	19.7	98.4	18.6

Table A.11. Summary of Resilient Modulus Test Results for Subgrade Material (I-15/Goodsprings).

Sequence	Cyclic Axial Stress (psi)	Contact Stress (psi)	Confine Stress (psi)	Axial Resilient Modulus (psi)	Deviator Stress, σd (psi)	Sigma 1 (psi)	Sigma 3 (psi)	Bulk Stress,θ (psi)	Octahedral Shear Stress (psi)
1	3.5	0.4	5.9	19,538	3.9	9.8	5.9	21.5	1.8
2	1.8	0.2	5.9	18,343	2.0	7.8	5.9	19.6	0.9
3	3.5	0.4	5.9	19,916	3.9	9.8	5.9	21.5	1.8
4	5.4	0.6	5.9	20,171	6.0	11.8	5.9	23.6	2.8
5	7.1	0.8	4.9	18,746	7.9	12.7	4.9	22.5	3.7
6	8.8	1.0	5.9	20,838	9.8	15.7	5.9	27.4	4.6
7	1.8	0.2	3.9	15,251	2.0	5.8	3.9	13.5	0.9
8	3.7	0.4	3.9	15,923	4.1	7.9	3.9	15.7	1.9
9	5.3	0.6	3.9	16,591	5.9	9.7	3.9	17.5	2.8
10	7.1	0.8	3.9	17,308	7.9	11.7	3.9	19.4	3.7
11	8.8	1.0	3.9	18,277	9.8	13.6	3.9	21.4	4.6
12	1.8	0.2	1.9	12,573	2.0	3.8	1.9	7.6	0.9
13	3.4	0.4	1.9	13,075	3.8	5.7	1.9	9.4	1.8
14	5.4	0.6	1.9	14,149	5.9	7.8	1.9	11.5	2.8
15	7.1	0.8	1.9	14,944	7.8	9.7	1.9	13.5	3.7
16	8.9	1.0	1.9	15,758	9.9	11.8	1.9	15.5	4.7

Table A.12. Summary of Resilient Modulus Test Results for Subgrade Material (US-95/Searchlight).

Sequence	Cyclic Axial Stress (psi)	Contact Stress (psi)	Confine Stress (psi)	Axial Resilient Modulus (psi)	Deviator Stress, σd (psi)	Sigma 1 (psi)	Sigma 3 (psi)	Bulk Stress,θ (psi)	Octahedral Shear Stress (psi)
1	3.6	0.4	5.7	16,049	4.0	9.7	5.7	21.1	1.9
2	1.8	0.2	5.7	15,139	2.0	7.7	5.7	19.2	0.9
3	3.6	0.4	5.7	16,294	4.0	9.7	5.7	21.1	1.9
4	5.4	0.6	5.7	16,243	6.0	11.7	5.7	23.2	2.8
5	7.2	0.8	4.7	15,076	8.0	12.7	4.7	22.2	3.8
6	8.9	1.0	5.7	16,137	9.8	15.6	5.7	27.0	4.6
7	1.8	0.2	3.7	12,999	2.0	5.7	3.7	13.1	0.9
8	3.6	0.4	3.7	13,178	4.0	7.7	3.7	15.1	1.9
9	5.4	0.6	3.7	13,627	5.9	9.7	3.7	17.1	2.8
10	7.1	0.8	3.7	13,972	7.9	11.6	3.7	19.0	3.7
11	8.9	1.0	3.7	14,418	9.9	13.7	3.7	21.1	4.7
12	1.8	0.2	1.7	10,602	2.0	3.7	1.7	7.2	0.9
13	3.6	0.4	1.7	10,766	4.0	5.7	1.7	9.2	1.9
14	5.3	0.6	1.7	11,301	5.9	7.6	1.7	11.1	2.8
15	7.2	0.8	1.7	11,938	8.0	9.7	1.7	13.1	3.8
16	8.9	1.0	1.7	12,583	9.8	11.6	1.7	15.0	4.6

Table A.13. Summary of Resilient Modulus Test Results for Subgrade Material (NV-375/Rachel).

Sequence	Cyclic Axial Stress (psi)	Contact Stress (psi)	Confine Stress (psi)	Axial Resilient Modulus (psi)	Deviator Stress, σd (psi)	Sigma 1 (psi)	Sigma 3 (psi)	Bulk Stress,θ (psi)	Octahedral Shear Stress (psi)
1	3.6	0.4	5.7	18,563	4.0	9.7	5.7	21.1	1.9
2	1.8	0.2	5.7	16,968	2.0	7.7	5.7	19.1	0.9
3	3.6	0.4	5.7	18,824	4.0	9.7	5.7	21.1	1.9
4	5.4	0.6	5.7	18,731	6.0	11.7	5.7	23.1	2.8
5	7.2	0.8	4.7	17,317	8.0	12.7	4.7	22.1	3.8
6	9.0	1.0	5.7	19,475	10.0	15.7	5.7	27.1	4.7
7	1.8	0.2	3.7	14,184	2.0	5.7	3.7	13.1	0.9
8	3.6	0.4	3.7	14,300	4.0	7.7	3.7	15.1	1.9
9	5.4	0.6	3.7	15,270	6.0	9.7	3.7	17.1	2.8
10	7.2	0.8	3.7	16,435	8.0	11.7	3.7	19.1	3.8
11	9.0	1.0	3.7	17,200	10.0	13.7	3.7	21.1	4.7
12	1.8	0.2	1.7	10,946	2.0	3.7	1.7	7.2	0.9
13	3.6	0.4	1.7	11,363	4.0	5.7	1.7	9.1	1.9
14	5.4	0.6	1.7	12,765	6.0	7.7	1.7	11.1	2.8
15	7.2	0.8	1.7	13,752	8.0	9.7	1.7	13.1	3.8
16	9.0	1.0	1.7	14,622	10.0	11.7	1.7	15.1	4.7

Table A.14. Summary of Resilient Modulus Test Results for Subgrade Material (US-93/Crystal Spring MP62).

Sequence	Cyclic Axial Stress (psi)	Contact Stress (psi)	Confine Stress (psi)	Axial Resilient Modulus (psi)	Deviator Stress, σd (psi)	Sigma 1 (psi)	Sigma 3 (psi)	Bulk Stress,θ (psi)	Octahedral Shear Stress (psi)
1	3.6	0.4	5.8	13,028	4.0	9.8	5.8	21.3	1.9
2	1.8	0.2	5.8	12,184	2.0	7.8	5.8	19.3	0.9
3	3.6	0.4	5.8	13,115	4.0	9.8	5.8	21.3	1.9
4	5.6	0.6	5.8	13,025	6.2	12.0	5.8	23.5	2.9
5	7.2	0.8	4.8	12,302	8.0	12.8	4.8	22.3	3.8
6	9.0	1.0	5.8	13,420	10.0	15.7	5.8	27.3	4.7
7	1.8	0.2	3.8	9,997	2.0	5.8	3.8	13.3	0.9
8	3.6	0.4	3.8	10,223	4.0	7.8	3.8	15.3	1.9
9	5.4	0.6	3.8	10,567	6.0	9.8	3.8	17.3	2.8
10	7.3	0.8	3.8	11,363	8.1	11.8	3.8	19.4	3.8
11	9.0	1.0	3.8	11,685	10.0	13.8	3.8	21.3	4.7
12	1.8	0.2	1.8	7,710	2.0	3.8	1.8	7.3	0.9
13	3.6	0.4	1.8	8,095	4.0	5.7	1.8	9.3	1.9
14	5.4	0.6	1.8	8,822	6.0	7.7	1.8	11.3	2.8
15	7.2	0.8	1.8	9,648	8.0	9.8	1.8	13.4	3.8
16	8.9	1.0	1.8	9,982	9.9	11.7	1.8	15.2	4.7

Table A.15. Summary of Resilient Modulus Test Results for Subgrade Material (US-93/Crystal Spring MP67).

Sequence	Cyclic Axial Stress (psi)	Contact Stress (psi)	Confine Stress (psi)	Axial Resilient Modulus (psi)	Deviator Stress, σd (psi)	Sigma 1 (psi)	Sigma 3 (psi)	Bulk Stress,θ (psi)	Octahedral Shear Stress (psi)
1	3.6	0.4	5.8	15,555	4.0	9.8	5.8	21.3	1.9
2	1.8	0.2	5.8	14,759	2.0	7.8	5.8	19.4	0.9
3	3.6	0.4	5.8	15,963	4.0	9.8	5.8	21.4	1.9
4	5.4	0.6	5.8	15,526	6.0	11.8	5.8	23.4	2.8
5	7.2	0.8	4.8	14,314	8.0	12.8	4.8	22.3	3.8
6	8.9	1.0	5.8	15,276	9.9	15.7	5.8	27.3	4.7
7	1.8	0.2	3.8	13,366	2.0	5.8	3.8	13.3	0.9
8	3.6	0.4	3.8	13,338	4.0	7.8	3.8	15.4	1.9
9	5.4	0.6	3.8	13,204	6.0	9.8	3.8	17.3	2.8
10	7.2	0.8	3.8	13,367	8.0	11.8	3.8	19.4	3.8
11	9.0	1.0	3.8	13,723	10.0	13.8	3.8	21.4	4.7
12	1.8	0.2	1.8	11,103	2.0	3.8	1.8	7.3	0.9
13	3.6	0.4	1.8	10,789	4.0	5.8	1.8	9.3	1.9
14	5.4	0.6	1.8	11,002	6.0	7.8	1.8	11.3	2.8
15	7.3	0.8	1.8	11,481	8.1	9.8	1.8	13.4	3.8
16	9.0	1.0	1.8	11,940	10.0	11.8	1.8	15.3	4.7

Nevada Department of Transportation
Rudy Malfabon, P.E. Director
Ken Chambers, Research Division Chief
(775) 888-7220
kchambers@dot.nv.gov
1263 South Stewart Street
Carson City, Nevada 89712